INSIGHTS INTO THE ROLE OF THE PAF1 COMPLEX IN PROMOTING H2B MONOUBIQUITYLATION

by

S. Branden Van Oss

B.S. Biology, Wheaton College, 2008

Submitted to the Graduate Faculty of the

Kenneth P. Dietrich School of Arts and Sciences in partial fulfillment

of the requirements for the degree of

Doctor of Philosophy

University of Pittsburgh

2017

UNIVERSITY OF PITTSBURGH

DIETRICH SCHOOL OF ARTS AND SCIENCES

This dissertation was presented

by

S. Branden Van Oss

It was defended on

August 2nd, 2017

and approved by

Donald DeFranco, Ph D, Professor and Vice Chair of Education, Dept. of Pharmacology and Chemical Biology

Anthony Schwacha, Ph.D, Associate Professor, Dept. of Biological Sciences

Andrew Van Demark, Ph.D, Associate Professor, Dept. of Biological Sciences

John Woolford, Ph.D, Professor and Co-director, CNAST, Dept. of Biological Sciences, Carnegie Mellon University

Dissertation Advisor: Karen Arndt, Ph.D, Professor, Dept. of Biological Sciences

INSIGHTS INTO THE ROLE OF THE PAF1 COMPLEX IN PROMOTING H2B MONOUBIQUITYLATION

S. Branden Van Oss, PhD

University of Pittsburgh, 2017

The polymerase-associated factor 1 complex (Paf1C) regulates RNA polymerase II transcription and is required for the monoubiquitylation of histone H2B (H2Bub), a conserved epigenetic modification with broad implications for the regulation of gene expression and human health. This dissertation explores the molecular mechanisms by which Paf1C acts to promote H2Bub. Paf1C regulation of H2Bub is governed largely by the histone modification domain (HMD) of the Rtf1 subunit, which promotes H2Bub even in the absence of all Paf1C subunits and interacts directly with the enzyme that catalyzes H2Bub. The role of the HMD in stimulating H2Bub is direct, and at least partially independent of transcription. My work is part of a collaborative effort to investigate the activity of the HMD through structural, genetic, bioinformatic, and biochemical approaches. As the influence of H2Bub on human health continues to become more clear, interest in this modification will likely continue to expand.

TABLE OF CONTENTS

LIST OF TABLES

LIST OF FIGURES

1.0 INTRODUCTION

Eukaryotic transcription occurs on a chromatin template shaped by the presence of nucleosomes. Comprising approximately 147 base pairs of DNA complexed with an octamer of histone proteins containing two copies each of histones H2A, H2B, H3, and H4, nucleosomes pose a natural barrier to DNA-templated processes such as transcription. Nevertheless, transcription of the eukaryotic genome is now understood to be pervasive, with varied and numerous noncoding RNAs (ncRNAs) continually generated by the cell alongside the better-studied coding transcripts (Jacquier 2009; Tisseur, et al. 2011). The function of and extensive interplay between these many transcripts and the transcription machinery is a subject of intense interest.

RNA polymerase II (Pol II) transcribes all eukaryotic mRNAs as well as several classes of ncRNA, including snRNA, snoRNA, and miRNA. The Pol II transcription cycle is classically divided into the stages of initiation, elongation, and termination. While early work focused largely on the initiation stage, it is now clear that each of these stages is subject to extensive regulation by a wide array of factors (Richard and Manley 2009) (Figure 1). These factors include proteins that directly associate with Pol II to modulate its activity and proteins that alter the chromatin landscape by moving or remodeling nucleosomes and/or by promoting posttranslational modification of the core histone proteins. One such factor is a 5-subunit protein complex known as the polymerase-associated factor 1 complex (Paf1C). The primary

goal of my dissertation was to explore the molecular mechanism by which Paf1C functions to promote a conserved histone modification with broad implications for transcriptional regulation and human health and development.

1.1 EUKARYOTIC TRANSCRIPTION BY RNA POLYMERASE II IS EXTENSIVELY REGULATED AT EACH STAGE

1.1.1 Initiation

The beginning of the initiation stage is characterized by the formation of a preinitiation complex (PIC) at promoters. While the PIC is minimally composed of promoter DNA, Pol II and five "general" (or "basal") transcription factors (TFIIB, TFIIE, TFIIF, TFIID and TFIIH) (Murakami, et al. 2015), most PICs are much larger and include chromatin remodelers and chromatin modifying enzymes as well as various co-activators and co-repressors (Sikorski and Buratowski 2009; Gupta, et al. 2016). The PIC can assemble in a stepwise fashion and is stabilized by the Mediator complex, which activates Pol II and facilitates the response to a number of additional regulatory factors (Sikorski and Buratowski 2009; Allen and Taatjes 2015; Gupta, et al. 2016). This sequential loading of factors leads to the "melting" of double-stranded DNA, followed by loading of the template strand onto the Pol II active site, resulting in a so-called open complex (Liu, et al. 2013). The promoter region is generally maintained in a nucleosome-depleted state, largely through the binding of transcription factors that recruit various ATP-dependent chromatin remodeling enzymes (Ozonov and van Nimwegen 2013).

The transition from initiation to elongation is marked by promoter escape or clearance, in which Pol II exchanges initiation for elongation factors and stably associates with DNA (Luse 2013).

1.1.2 Elongation

In recent years, it has become clear that the elongation stage also involves widespread regulation. At many genes in most metazoa, the early phases of the elongation stage involve promoter-proximal Pol II pausing approximately 20-60 nucleotides from the transcription start site (Jonkers and Lis 2015; Scheidegger and Nechaev 2016; Sharma 2016). Passage of Pol II into productive elongation is largely dependent on the activity of the P-TEFb complex, whose CDK9 subunit phosphorylates Pol II and multiple pausing factors (Jonkers and Lis 2015; Scheidegger and Nechaev 2016). While other eukaryotes such as budding yeast lack canonical Pol II promoter-proximal pausing, the CDK9 ortholog Bur1 is still required for normal levels of Pol II phosphorylation (Bowman and Kelly 2014). Pol II may also "backtrack" during productive elongation, leading to arrest; release from arrest is dependent on the activity of the elongation factor TFIIS (Cheung and Cramer 2011).

Though promoter-proximal pausing in higher eukaryotes is the most intensely studied example of Pol II pausing, the emergence of technologies such as NET-seq, which measures levels of actively transcribing Pol II on chromatin at single nucleotide resolution, has revealed that pausing occurs throughout gene bodies, including in organisms such as yeast and bacteria (Mayer, et al. 2017). In budding yeast, strains lacking Dst1, the TFIIS ortholog, exhibit Pol II enrichment at nucleosomal dyads (Churchman and Weissman 2011), confirming that nucleosomes represent a barrier to Pol II transcription that allows an opportunity for regulation of this stage of transcription.

A further level of transcriptional regulation is mediated by the cotranscriptional modification of the core histone proteins. One example of many is the di- and trimethylation of lysine 36 on histone H3. This modification acts to oppose elongation, and loss of the methyltransferase that specifically catalyzes the mark rescues viability in strains lacking an essential positive elongation factor (Keogh, et al. 2005; Woo, et al. 2017). Histone modifications can exert their effect on elongation in a number of ways: by serving as platforms for the recruitment of various factors, as is common with histone methylation (Flanagan, et al. 2005; Kim and Buratowski 2009); by disrupting contacts between histones and DNA, as has been shown for acetylation (Orphanides and Reinberg 2000); or by governing the structure of local and higher-order chromatin, as in the case of monoubiquitylation (see Section 1.3).

In addition to steric factors such as nucleosomes and DNA-binding factors, Pol II pausing during elongation is dependent on particular residues within Pol II as well as DNA sequence features and the secondary structures of nascent transcripts (Mayer, et al. 2017). Sequences within the nascent RNA transcript can slow elongation directly, such as through the formation of DNA-RNA hybrid structures, also known as R loops, or may promote elongation by acting to recruit various transcription factors, including P-TEFb (Peterlin and Price 2006; Skalska, et al. 2017). Recent evidence also suggests that Pol II elongation rates are both gene-dependent and variable within individual genes, with consequences for the regulation of transciption termination, mRNA splicing, and the deposition of co-transcriptional chromatin modifications (Jonkers and Lis 2015; Alpert, et al. 2017; Fong, et al. 2017). Misregulation of elongation is implicated in many human diseases (Sharma 2016; Mayer, et al. 2017), and therapeutics such as histone deacetylase inhibitors are being developed for conditions such as

Alzheimer's (Yang, et al. 2017) and cancer (Eckschlager, et al. 2017), further underscoring the importance of this stage of gene expression.

1.1.3 Termination

Eukaryotic termination involves two separate but interconnected processes: the dissociation of Pol II from the DNA template, and 3' end formation of the nascent RNA (Mischo and Proudfoot 2013). For mRNAs, the process of 3' end formation is guided by poly(A) signals, which direct the activity of two complexes that engage both Pol II and the nascent RNA, cleavage and polyadenylation factor (CPF) and cleavage factor IA and IB (CF) (Richard and Manley 2009; Mischo and Proudfoot 2013). Release of Pol II from the template occurs downstream of the poly(A) site by as much as several hundred bases, and is dependent on both the speed of the polymerase as well as the relative stability of the RNA:DNA hybrid (Mischo and Proudfoot 2013).

While some noncoding transcripts are processed and terminated by this same method (Marquardt, et al. 2011; Mischo and Proudfoot 2013), other non-polyadenylated transcripts utilize some of the same machinery but are terminated by alternative pathways, such as the Nrd1-Nab3-Sen1 (NNS) pathway in yeast or the cap binding complex (CBC)-ARS pathway in metazoa (Mischo and Proudfoot 2013; Porrua and Libri 2015). It has become evident that eukaryotic transcription is pervasive, both in coding and noncoding regions of the genome (Porrua and Libri 2015). While the function of many ncRNAs is not fully understood, it is thought that many of these transcripts are the result of "leaky" initiation events (Porrua and Libri 2015). The NNS pathway specifically terminates ncRNAs that are destined for degradation by the nuclear exosome, and efficient termination via the NNS pathway serves to

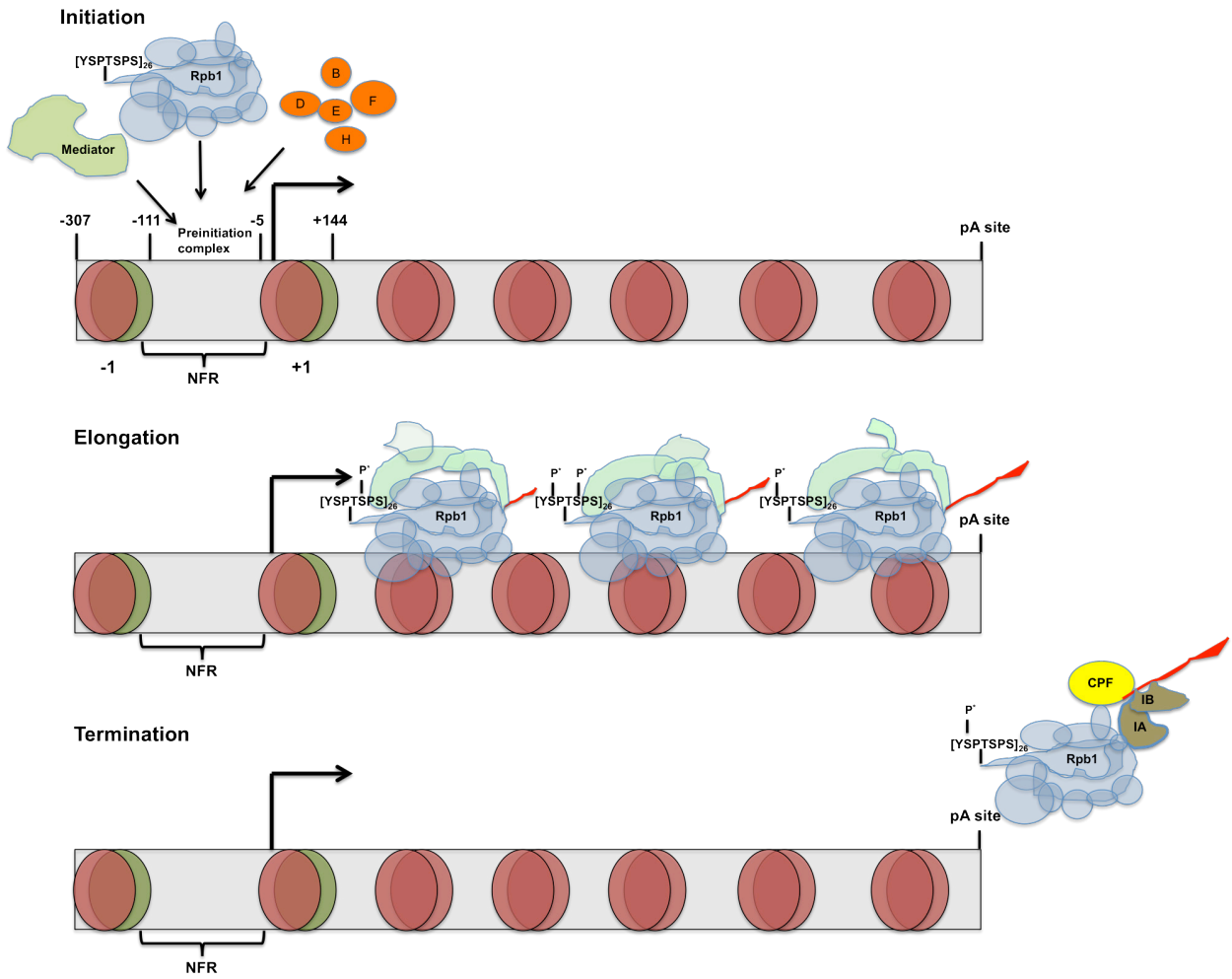

Figure 1: Eukaryotic transcription is a dynamic, highly regulated process.

Diagram showing transcription of a eukaryotic protein-coding gene. The -1 and +1 nucleosomes typically contain the histone variant H2A.Z (olive green) and flank a nucleosome free region (NFR) at the promoter. The boundaries for the consensus positions of the -1 and +1 nucleosomes (Jiang and Pugh 2009) are given as distance in nucleotides from the transcription start site. Initiation (top) is marked by the formation of a pre-initiation complex comprising the 12-subunit RNA polymerase II holoenzyme, general transcription factors (shown in orange), the Mediator complex, and numerous additional gene-specific factors. At this stage, the C-terminal domain (CTD) of the largest Pol II subunit, Rpb1, which in budding yeast contains 26 repeats of the indicated heptapeptide sequence, is unmodified (Buratowski 2009). Elongation (middle) takes place following promoter clearance, at which point various elongation factors (shown in light green) associate with Pol II and regulate its activity. Some factors remain associated throughout elongation, while others associate with the polymerase only transiently. The CTD is first

phosphorylated at serine 5 (Ser5P), and as elongation proceeds, Ser2P accumulates and Ser5P decreases (Buratowski 2009). Termination (bottom) involves dissociation of Pol II from the DNA template downstream of the poly(A) site and release and processing of the nascent RNA (shown in red) through the coordinated activity of termination factors, including cleavage and polyadenylation factor (CPF) and cleavage factor IA and IB.

prevent ncRNA transcription from interfering with the transcription of coding RNAs (Porrua and Libri 2015).

As appreciation of the vast extent to which Pol II transcription can be modulated has grown, there has been increased recognition of the interconnectedness of the various levels of regulation. Correspondingly, factors that were once seen as specific to a particular stage of transcription are now recognized as being involved in multiple co-transcriptional regulatory events. Prominent among these is Paf1C.

1.2 THE PAF1 COMPLEX IS A CONSERVED, MULTIFUNCTIONAL REGULATOR OF RNA POLYMERASE II TRANSCRIPTION

Paf1C has been implicated in regulating all stages of the Pol II transcription cycle as well as events that follow transcript synthesis (Figure 2). Since the discovery of Paf1C as a novel Pol II-interacting complex in *Saccharomyces cerevisiae* over twenty years ago (Wade, et al. 1996; Shi, et al. 1997; Mueller and Jaehning 2002), studies in budding yeast have led the way in elucidating the functions of this highly conserved protein complex. These foundational studies demonstrated that Paf1C regulates transcription elongation (Costa and Arndt 2000; Squazzo, et al. 2002; Rondon, et al. 2004) as well transcription termination and RNA 3'-end formation

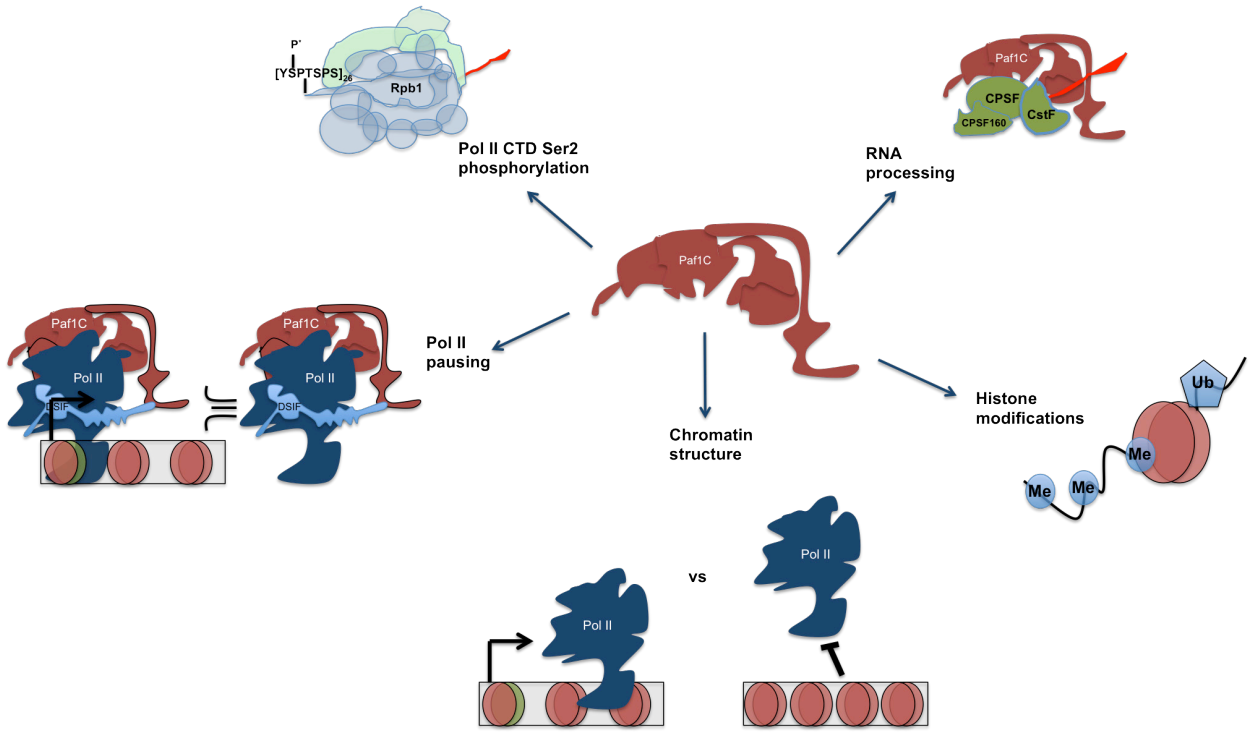

Figure 2: Paf1C regulates numerous cotranscriptional processes.

Paf1C is required for the deposition of cotranscriptional histone modifications, specifically the monoubiquitylation of histone H2B and methylation of H3 K4, K36, and K79 (Krogan, et al. 2003; Ng, Dole, et al. 2003; Ng, Robert, et al. 2003; Wood, Schneider, et al. 2003; Xiao, et al. 2005; Chu, et al. 2007) (bottom right). These chromatin marks play many roles, including roles in the establishment and maintenance of euchromatic and heterochromatic regions of the genome (Verzijlbergen, et al. 2009) (bottom). In higher eukaryotes, Paf1C governs promoter-proximal Pol II pausing (bottom left; see Section 1.2.2 and Figure 4). Paf1C is also required for proper phosphorylation of serine 2 (Ser2) of the Pol II CTD (Mueller, et al. 2004; Nordick, et al. 2008) (top left), a mark that, among other functions, recruits RNA processing factors (Licatalosi, et al. 2002). Paf1C also physically associates with processing factors such as CPSF (Nordick, et al. 2008; Rozenblatt-Rosen, et al. 2009) (top right) and is required for proper processing of the 3' end of the nascent RNA (Mueller, et al. 2004; Nagaike, et al. 2011). Paf1C levels on genes also play a role in determining whether the nascent transcript is shuttled to the cytoplasm or retained in the nucleus (Fischl, et al. 2017) (not shown). Proteins are not drawn to shape or scale, but the shape of Paf1C is loosely modeled on a recently published cryo-EM structure of *S. cerevisiae* Paf1C (Xu, et al. 2017).

(Mueller, et al. 2004; Penheiter, et al. 2005; Nordick, et al. 2008), functions that are mediated at least in part by the ability of Paf1C to promote several critical cotranscriptional histone modifications (Krogan, et al. 2003; Ng, Dole, et al. 2003; Ng, Robert, et al. 2003; Wood, Schneider, et al. 2003; Chu, et al. 2007).

In recent years, new roles for Paf1C have been identified in processes predominantly found in metazoans, particularly in the regulation of promoter-proximal pausing (Chen, et al. 2015; Yu, et al. 2015; Lu, et al. 2016). Studies in metazoans and in fission yeast have also advanced our understanding of previously characterized Paf1C functions, such as the maintenance of heterochromatin and the regulation of alternative cleavage and polyadenylation of mRNAs (Kowalik, et al. 2015; Sadeghi, et al. 2015; Verrier, et al. 2015; Yang, et al. 2016). Furthermore, several new Paf1C-regulated histone modifications have been described that illuminate our understanding of the role that Paf1C plays in modulating chromatin structure (Wu, et al. 2011; Verrier, et al. 2015). Given its fundamental role as a regulator of transcription and its connections to human disease (Moniaux, et al. 2006; Newey, et al. 2009; Hanks, et al. 2014; Zhi, et al. 2015) and development (Ding, et al. 2009; Strikoudis, et al. 2016), interest in the functions of Paf1C in higher organisms will likely continue to expand.

1.2.1 Paf1C is targeted to chromatin by interactions with the Pol II elongation machinery and promoter-associated transcription factors

In budding yeast, Paf1C is composed of five subunits - Paf1, Ctr9, Cdc73, Leo1, and Rtf1. Some organisms, including humans, contain an additional subunit, the multifunctional Ski8/Wdr61 protein (Zhu, et al. 2005)**.** Moreover, in organisms other than budding yeast, ranging from fission yeast to humans, Rtf1 is not strongly associated with Paf1C and has been

shown to function independently of other Paf1C subunits in certain contexts (Mbogning, et al. 2013; Cao, et al. 2015; Yang, et al. 2016) (Figure 3). Although none of the subunits is essential in budding yeast, *paf1Δ* and *ctr9Δ* cells have severe growth defects (Betz, et al. 2002), and Paf1C orthologs are essential in higher organisms (Mosimann, et al. 2006; Bahrampour and Thor 2016). Paf1 and Ctr9 are required for overall complex integrity (Kim, et al. 2010; Chu, et al. 2013); consistent with this, global protein levels of the other subunits are decreased in *S. cerevisiae paf1Δ* and *ctr9Δ* mutants (Mueller, et al. 2004).

In both yeast and human cells, Paf1C localizes to active genes at levels that correlate with transcriptional output (Mayer, et al. 2010; Chen, et al. 2015; Yu, et al. 2015; Van Oss, et al. 2016). Several studies have explored the mechanisms that couple Paf1C and its various activities to Pol II. Early studies of Cdc73 (parafibromin in humans) showed that it interacts directly and stoichiometrically with purified Pol II (Shi, et al. 1997) and is important for Paf1C recruitment (Mueller, et al. 2004). The dynamically modified C-terminal domain (CTD) of Pol II serves as a hub that recruits an array of accessory factors to chromatin (Zaborowska, et al. 2016), and subsequent work showed that a conserved C-terminal domain within Cdc73 preferentially interacts with phosphorylated Pol II CTD peptides *in vitro* (Qiu, et al. 2012). A second attachment point between Paf1C and the Pol II elongation machinery is mediated by the elongation factor Spt5 (Liu, et al. 2009; Qiu, et al. 2012; Mbogning, et al. 2013), which interacts directly with a central region of the Rtf1 subunit (Mayekar, et al. 2013; Wier, et al. 2013) (Figure 3). However, consistent with the weak association between Rtf1 and other Paf1C subunits in metazoans, a recent structure/function analysis of human Rtf1 suggests that Paf1C recruitment in humans may be primarily Rtf1-independent, at least at certain genes (Cao, et al. 2015) (Figure 3). Interestingly, both Spt5 and the Pol II CTD are substrates of the same kinase,

Bur1 (CDK9 in humans), and the activity of this kinase is required for proper Paf1C recruitment in both yeast and human cells (Laribee, et al. 2005; Liu, et al. 2009; Qiu, et al. 2012; Mbogning, et al. 2013; Yu, et al. 2015).

At most genes in *S. cerevisiae*, Paf1C occupancy peaks downstream of the transcription start site near the +2 and +3 nucleosomes (Mayer, et al. 2010; Van Oss, et al. 2016). This enrichment pattern is consistent with an ordered recruitment model in which Paf1C joins the elongation machinery after Spt5 has associated with Pol II. However, in higher eukaryotic systems, the pattern of Paf1C enrichment differs from that observed in budding yeast, possibly reflecting different recruitment strategies predominant in different systems (Figure 3). For example, in some mouse and human cells, Paf1C occupancy was reported to be highest near the transcription start and end sites (TSS and TES) (Chen, et al. 2015; Yu, et al. 2015; Yang, et al. 2016). This is interesting in light of several studies in higher eukaryotes indicating that Paf1C is recruited to promoters and enhancers by transcriptional activators (Figure 3). In one study, a transient complex between Paf1C and the proto-oncogenic transcription factor c-Myc was identified and found to inhibit activation of c-Myc target genes (Jaenicke, et al. 2016). Transactivators of viral genomes have also exploited interactions with Paf1C. For example, the adenovirus E1A protein recruits Paf1C to promoters, leading to the activation of both viral and host genes in a Paf1C-dependent manner (Fonseca, et al. 2013; Fonseca, et al. 2014). Several studies have also identified an important role for parafibromin, the human ortholog of Cdc73, in regulating the transcriptional output of the developmentally critical Wnt, Hedgehog, and Notch signaling pathways through direct interactions with the downstream effectors of these pathways (Mosimann, et al. 2006; Kikuchi, et al. 2016). The interactions between parafibromin and the effectors of the Wnt and Hedgehog pathways (β-catenin and Gli1, respectively) utilize the same

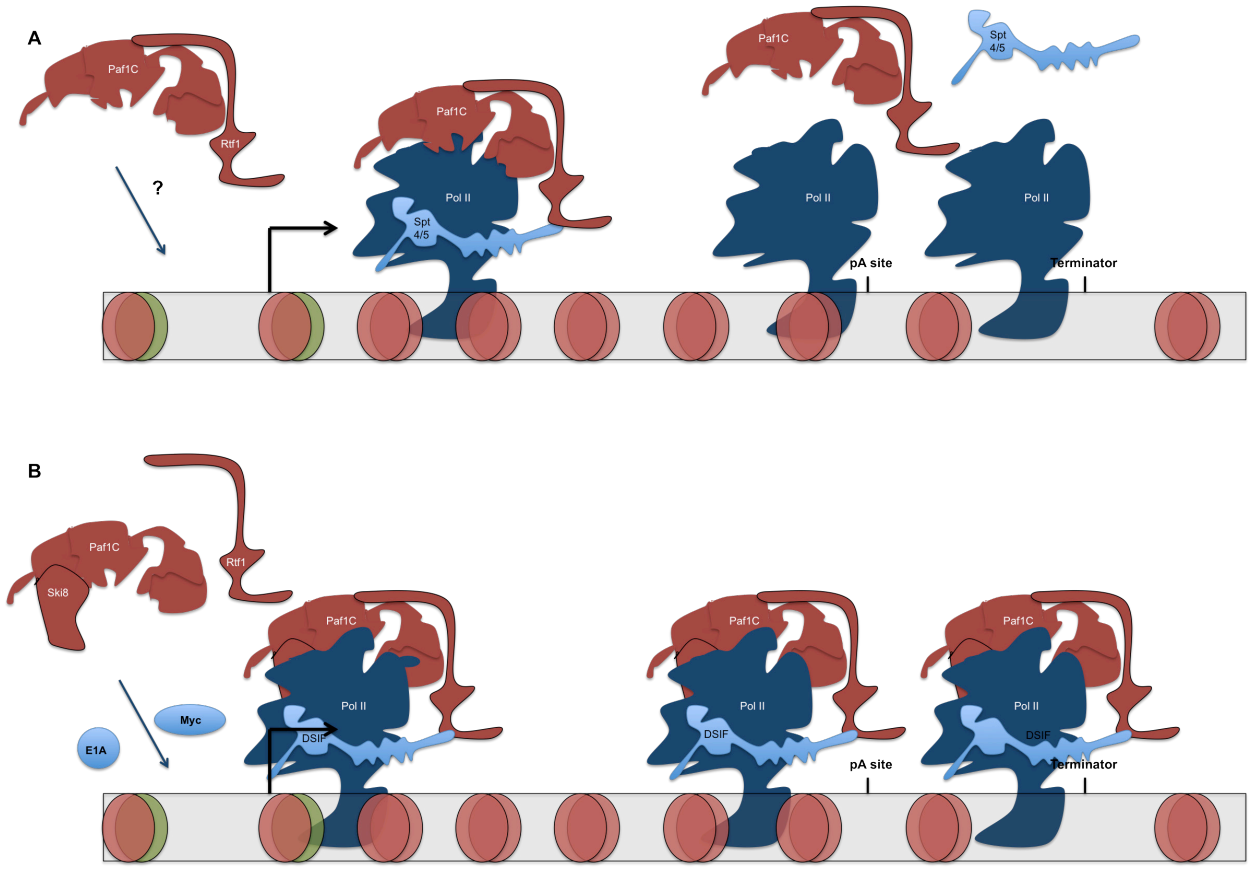

Figure 3: Paf1C recruitment to ORFs in budding yeast vs. metazoa

(A) In *Saccharomyces cerevisiae*, Paf1C is recruited to promoters by unknown mechanisms and is generally depleted in this region. Rtf1 is stably associated with the complex. Paf1C is enriched in the bodies of active genes, where it associates directly with both Pol II and Pol II-associated Spt4/5. Paf1C and Spt4/5 dissociate from Pol II downstream of the polyadenylation (pA) site (Mayer, et al. 2010). (B) In metazoa, Paf1C is recruited to promoters by transcriptional activators such as E1A and Myc. The complex contains an additional subunit, Ski8, while Rtf1 does not stably associate with Paf1C and may function independtly of the Spt4/5 ortholog DSIF (Chen, et al. 2009; Cao, et al. 2015). Paf1C, Pol II and DSIF are enriched at promoter-proximal regions, where Pol II pauses at many genes, and near the pA site. Paf1C and DSIF remain associated with Pol II downstream of the pA site (Rahl, et al. 2010). Proteins are not drawn to shape or scale, but Paf1C shape and interactions with Pol II and Spt4/5 are loosely modeled on a recently published cryo-EM structure of *S. cerevisiae* Paf1C (Xu, et al. 2017).

N-terminal segment of parafibromin and are mutually exclusive (Kikuchi, et al. 2016). In contrast, parafibromin can simultaneously interact with the Wnt and Notch signaling effectors, allowing for coordinate stimulation of these two pathways. Interestingly, parafibromin is capable of stimulating transcription of Wnt target genes even upon depletion of Paf1, which should preclude formation of a stable Paf1C (Takahashi, Tsutsumi, et al. 2011). This is consistent with recent data showing that murine Cdc73 is specifically enriched at promoters under certain conditions (Yang, et al. 2016). While Paf1C recruitment to promoters and enhancers may represent a general mechanism of Paf1C recruitment in higher organisms and may delineate a class of genes as Paf1C-regulated in response to various signals, the means by which Paf1C modulates the expression of any given gene is likely to depend on gene- and cell type-specific factors.

1.2.2 Paf1C regulates gene expression through diverse mechanisms.

Strong support for a role of Paf1C in transcription elongation first came from experiments in budding yeast, which showed that Paf1C is recruited to actively transcribed open reading frames (ORFs) (Pokholok, et al. 2002) and interacts physically and genetically with transcription elongation factors, including the Spt4-Spt5 complex and the FACT histone chaperone complex (Costa and Arndt 2000; Krogan, Kim, et al. 2002; Squazzo, et al. 2002). An early study using yeast extracts and a naked DNA template revealed a direct role for Paf1C as a positive effector of transcription *in vitro* (Rondon, et al. 2004), and a more recent study showed that reconstituted human Paf1C promotes elongation through a chromatinized template both independently and in concert with the elongation factor TFIIS/SII (Kim, et al. 2010). In the cell, deletion or knockdown of Paf1C components alters the expression of many genes, and the results indicate

both positive and negative effects of the complex on transcript levels (Shi, et al. 1996; Penheiter, et al. 2005; Cao, et al. 2015).

In recent years, much attention has been given to the importance of promoter-proximal pausing of Pol II in regulating transcription elongation at many genes in metazoans (Adelman and Lis 2012). The pausing of Pol II 20-60 bp into the transcription unit poises genes for rapid induction in response to external stimuli and maintains promoter-proximal regions in a nucleosome-depleted state (Adelman and Lis 2012). The transcription elongation factor DSIF (human ortholog of the yeast Spt4-Spt5 complex) acts in concert with another protein complex, NELF, to establish promoter-proximal pausing of Pol II (Liu, et al. 2015). Release from pausing is triggered by phosphorylation of NELF and Spt5 by P-TEFb (CDK9-cyclin T complex), upon which NELF dissociates from the polymerase and DSIF becomes a positive elongation factor (Liu, et al. 2015).

Several recent studies have identified Paf1C as a factor that regulates promoter proximal pausing (Wu, et al. 2014; Yu, et al. 2015; Lu, et al. 2016). One genome-wide survey of Pol II and Paf1C occupancy in human monocytic leukemia (THP1) cells indicated that Paf1C promotes release from pausing at > 5,800 genes (Yu, et al. 2015). This study identified a mutual dependence of Paf1C and P-TEFb with respect to their recruitment to/retention on active chromatin (Yu, et al. 2015), an observation consistent with a positive feedback model in which Paf1C promotes pause release by regulating the chromatin association of P-TEFb both directly and via Paf1C-dependent histone modifications (see below) (Wu, et al. 2014). Another recent report postulates the existence of at least four unique P-TEFb-containing super elongation complexes (SECs), each with distinct targets for CDK9 activity (Lu, et al. 2016). Paf1C is critical for the recruitment of two of these SEC subtypes. In this model, Paf1C interacts with

AFF1-SEC to recruit P-TEFb to NELF-A, and subsequently with AFF4-SEC to recruit P-TEFb to the Pol II CTD. It is believed that a direct interaction between the Paf1 subunit and AF9, a component of both of the above SEC subtypes, is responsible for facilitating this recruitment (He, et al. 2011), although others have detected Paf1C binding to CDK9 independently of AF9 (Yu, et al. 2015).

In contrast to studies that implicated Paf1C in pause release, other studies have demonstrated a role for Paf1C in establishing or maintaining the pause. Depletion of Paf1 in human colon cancer cells resulted in a genome-wide increase in the ratio of Pol II in gene bodies relative to promoters, suggesting that Paf1 inhibits release from pausing at a large number of genes in this context (Chen, et al. 2015). Global run-on sequencing (GRO-seq) and nascent RNA-seq in Paf1-depleted cells detected increased transcription of these genes. Furthermore, enhanced enrichment of the CDK9-containing AFF4-SEC complex was observed in Paf1 deficient cells, establishing a model whereby Paf1C promotes pausing by inhibiting the recruitment of P-TEFb in the context of SEC (Chen, et al. 2015). Similar results were seen in another cancer cell line (MCF7) as well as in Drosophila, and interestingly, the same study that found that a majority of genes displayed more pausing upon Paf1C depletion in THP1 cells observed the opposite effect in human acute lymphoblastic leukemia CCRF-CEM cells (Yu, et al. 2015). Also of note is the observation that turnover of c-Myc promotes P-TEFb recruitment (Jaenicke, et al. 2016). When c-Myc turnover is inhibited, a transient c-Myc-Paf1C complex (see above) is stabilized and transcription of Myc targets is downregulated (Jaenicke, et al. 2016). It is possible that cellular environments that stabilize this complex may also inhibit P-TEFb recruitment. Taken together, these observations argue that the role of Paf1C in regulating pausing is complex and may depend on secondary genetic or physiological factors (Figure 4).

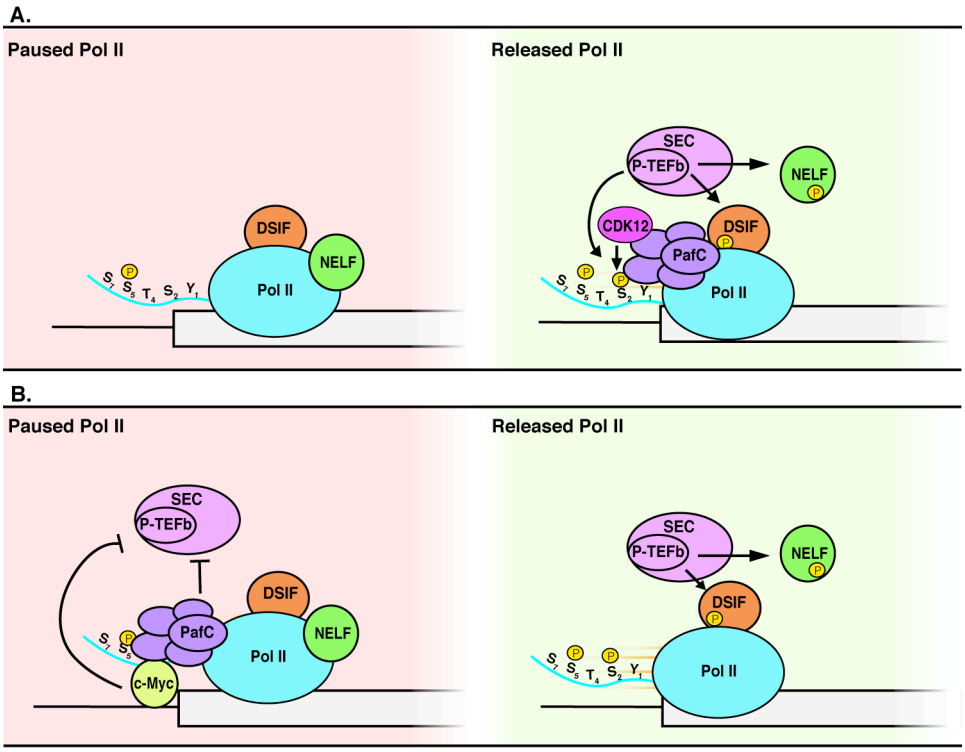

Figure 4: Paf1C regulates promoter-proximal pausing in higher eukaryotes.

(A) In cells where Paf1C promotes pause release, it acts to recruit the P-TEFb-containing super elongation complex (SEC). Subsequently, the CDK9 subunit of P-TEFb phosphorylates DSIF, NELF, and Ser2 of the Pol II CTD. Upon phosphorylation, NELF dissociates from Pol II and DSIF becomes a positive elongation factor, allowing for productive transcription elongation. Paf1C also recruits CDK12, which is thought to be the major Ser2 kinase in mammalian cells. (B) In some cells Paf1C acts to stabilize Pol II pausing. At Myc target genes, for example, Paf1C forms a transient complex with c-Myc that is inhibitory to SEC/P-TEFb recruitment. This figure was made by Christine Cucinotta and is used with permission.

Phosphorylation of the serine 2 residues in the CTD heptad repeats (Ser2P) of Pol II is strongly associated with transcription elongation. While Ser2P is dependent on CDK9, more recent studies indicate that the major Ser2P kinase is CDK12 (Bartkowiak, et al. 2010). Interestingly, Paf1C was recently shown to recruit CDK12 to chromatin (Yu, et al. 2015). Because the interaction between Paf1C and CDK12 is stronger than that between CDK12 and Pol II (Yu, et al. 2015), it is possible that Paf1C not only recruits CDK12, but also stimulates its activity by helping to position it at the site of catalysis on the Pol II CTD. A recent report suggests that Ser2P occurs downstream of pause release (Lu, et al. 2016), suggesting that Paf1C's role in this process may relate more to its interactions with P-TEFb (Yu, et al. 2015; Lu, et al. 2016), which targets numerous pausing factors, than to its involvement in CDK12 recruitment.

While at many genes Paf1C likely impacts transcript levels by direct and chromatin-mediated effects (see below) on Pol II elongation, several studies have implicated Paf1C in co- and post-transcriptional RNA processing events. Polyadenylation of mRNAs takes place cotranscriptionally (Maniatis and Reed 2002; Proudfoot, et al. 2002), and Pol II pausing also occurs upon transcription through the polyadenylation (pA) site and prior to termination (Jonkers and Lis 2015). One known function of Pol II CTD-Ser2P is the recruitment of RNA 3' processing factors to the pA site (Licatalosi, et al. 2002; Ahn, et al. 2004). A role for Paf1C in the regulation of mRNA processing was first suggested by studies in budding yeast, which showed that loss of Paf1C subunits leads to shortened poly(A) tails and alternative pA site selection (Mueller, et al. 2004; Penheiter, et al. 2005). In support of a direct role for Paf1C in this process, physical interactions between Paf1C subunits and multiple cleavage and polyadenylation factors have been detected (Nordick, et al. 2008; Rozenblatt-Rosen, et al.

2009), and Paf1C has also been shown to stimulate transcript cleavage and polyadenylation *in vitro* (Nagaike, et al. 2011).

In contrast to budding yeast, where Paf1C dissociates from chromatin just upstream of the pA site (Mayer, et al. 2010), mammalian Paf1C occupancy persists downstream of the pA site (Yang, et al. 2016) (Figure 3). A recent study showed that depletion of specific Paf1C subunits from mouse myoblasts caused global alterations in pA site selection, with increased use of alternative pA sites in introns and internal exons (Yang, et al. 2016). At genes with upregulation of intronic or exonic pA site usage following Paf1C depletion, transcription is diminished (Yang, et al. 2016). Interestingly, Paf1C is enriched in the bodies of these genes, suggesting a direct role in guarding against alternative pA site selection. (Yang, et al. 2016). Whether Paf1C impacts pA site selection by controlling Pol II elongation rates or by affecting the recruitment/activity of cleavage and polyadenylation factors remains to be clarified.

Recent evidence also suggests that, distinct from its role in promoting elongation, Paf1C controls the fate of nascent transcripts. Global analysis in budding yeast found that Paf1C enrichment at ORFs promotes the nuclear export of nascent transcripts, while Paf1C depletion leads to their retention and degradation (Fischl, et al. 2017). Paf1C enrichment in gene bodies was shown to be governed at least in part by promoter elements (Fischl, et al. 2017), although it is as yet unclear whether Paf1C is recruited to budding yeast promoters by transcription factors, as in higher organisms.

1.2.3 Paf1C has connections to development and human disease

In spite of the diverse and context-dependent functions of Paf1C, its role as a regulator of Pol II transcription is broadly conserved across eukaryotes, and interest in Paf1C has continued to

grow as its role in development and human disease has become more evident. Historically, interest was focused on the parafibromin (Cdc73) subunit, a tumor suppressor that when mutant can lead to hyperparathyroidism-jaw tumor (Wang, et al. 2005). More recently, *CTR9* was also identified as a tumor suppressor gene in humans, with mutations predisposing to Wilms tumor (Hanks, et al. 2014). Additionally, Paf1C is recruited to targets of the p53 tumor suppressor upon transcription stress and is required for their full activation (Albert, et al. 2016). Paf1C can also promote tumorigenesis in several cell types (Moniaux, et al. 2006; Zhi, et al. 2015; Karmakar, et al. 2017). In the case of non-small cell lung cancer, Paf1 protein levels correlate negatively with survival, and interestingly, depletion of both Paf1 and c-Myc synergistically inhibit cell proliferation (Zhi, et al. 2015).

A role in cancer is consistent with Paf1C regulation of development and differentiation. Paf1C mutants display developmental defects in zebrafish and fruit flies (Akanuma, et al. 2007; Nguyen, et al. 2010; Langenbacher, et al. 2011; Bahrampour and Thor 2016), and Paf1C is implicated in the maintenance of pluripotency in mouse and human embryonic stem cells (ESCs) (Ding, et al. 2009; Ponnusamy, et al. 2009; Rigbolt, et al. 2011). Interestingly, a recent report suggests that Paf1C regulation of promoter-proximal pausing may underlie its role in these processes. Like Paf1C, the PHD-finger protein Phf5a acts to maintain pluripotency in mouse ESCs (Strikoudis, et al. 2016). Paf1C binds Phf5a directly, and both Paf1C and Phf5a are downregulated upon differentiation (Strikoudis, et al. 2016). In the context of pluripotent stem cells, Paf1C and Phf5a appear to cooperate to maintain pluripotency by promoting pause release and thereby productive transcription of genes in the self-renewal network (Strikoudis, et al. 2016). Furthermore, and consistent with studies in zebrafish (Nguyen, et al. 2010; Langenbacher, et al. 2011) and *C. elegans* (Trappe, et al. 2002), both Paf1C and Phf5a are also

required for differentiation of myoblasts to myotubules (Strikoudis, et al. 2016), again emphasizing the contextual nature of Paf1C regulation of transcriptional networks.

1.3 H2B MONOUBIQUITYLATION GOVERNS CHROMATIN STRUCTURE AND REGULATES GENE EXPRESSION AND COTRANSCRIPTIONAL PROCESSES

Eukaryotic transcription is regulated by dynamic changes in chromatin, which include conserved post-translational modifications of the core histones that comprise the protein component of the nucleosome. The consequences of these modifications have been the subject of intense study. While many of these modifications are found on the disordered N-terminal tails of the histones, one modification of particular interest is the monoubiquitylation (ub) of a lysine (K) residue on the C-terminal helix of histone H2B: K120 in *H. sapiens* and the orthologous K123 residue in *S. cerevisiae*.

At ~7.5 kDa, the ubiquitin moiety is substantially larger than most other histone modifications, and as such it has a significant impact on the formation of higher-order chromatin structures. Decreased nucleosome occupancy at transcribed genes in a yeast strain lacking H2B K123ub indicates that this modification promotes nucleosome stability *in vivo*, most likely in conjunction with the FACT histone chaperone complex (Fleming, et al. 2008; Batta, et al. 2011), an observation that is supported by histone solubility assays (Chandrasekharan, et al. 2009). H2Bub inhibits chromatin fiber compaction (Fierz, et al. 2011), possibly by precluding internucleosomal contacts between H2B C-termini. This results in an "open" chromatin conformation; consistent with this, deubiquitylation of H2B was shown to promote heterochromatin spreading in Arabidopsis (Sridhar, et al. 2007).

H2B is ubiquitylated co-transcriptionally, and levels of H2Bub correlate with Pol II elongation rates (Kim, et al. 2009; Fuchs, et al. 2014). Though associated with regions of active transcription, the mark regulates transcript levels both positively and negatively for a subset of genes (Zhang, Kolaczkowska, et al. 2005; Mutiu, et al. 2007; Shema, et al. 2008; Batta, et al. 2011), particularly genes where transcription is rapidly induced in response to various stimuli (Shema, et al. 2008). The effect of H2Bub on transcriptional output appears dependent on its genomic context, as transcripts negatively regulated by H2Bub are enriched for the mark in promoter regions, while those positively regulated by H2Bub exhibit higher levels in gene bodies (Batta, et al. 2011). Interestingly, analysis of global H2Bub distribution in HeLa cells found that genes whose expression is repressed by H2Bub exhibited high levels of H2Bub and enrichment of other marks of active transcription but were weakly expressed and had a relatively closed chromatin conformation (Shema, et al. 2008). This suggests that the intrinsic ability of H2Bub to promote open chromatin is likely modulated by other factors in the genomic context.

H2Bub is also implicated in DNA repair pathways. An early report found that H2Bub-deficient cells fail to initiate cell cycle arrest in response to DNA damage (Giannattasio, et al. 2005). More recently, it was shown that the modification recruits factors important for both homologous recombination and non-homologous end joining (Meas and Mao 2015). Deubiquitylation of H2B is also implicated in the DNA damage response (DDR), as ablation of the deubiquitylase machinery inhibited phosphorylation of H2AX, an important step in certain DDR pathways (Ramachandran, et al. 2016).

Although mRNA splicing is not as prevalent in budding yeast as in other organisms, many of the yeast ribosomal protein genes are spliced, and H2Bub is enriched in both the exons

and introns of such genes (Shieh, et al. 2011). Furthermore, in a strain deficient for H2Bub, recruitment of early splicing factors is attenuated (Herissant, et al. 2014). In higher eukaryotes, deubiquitylation of H2B is also required for proper and efficient splicing of many transcripts (Zhang, et al. 2013)

1.4 CROSSTALK BETWEEN H2B MONOUBIQUITYLATION AND OTHER CHROMATIN MODIFICATIONS

Beyond any direct influence that the ubiquitin moiety exerts on chromatin structure and transcriptional regulation, H2Bub is also required for di- and trimethylation (Me^2/Me^3) of H3 K4 and H3 K79, marks associated with active chromatin and required for proper silencing and establishment of heterochromatic regions (Krogan, Dover, et al. 2002; Nguyen and Zhang 2011; Smolle and Workman 2013). H3 K4Me^3 is enriched at or near the promoters of highly transcribed genes, while H3 K79 is found primarily in gene bodies (Smolle and Workman 2013). In budding yeast, deposition of H3 K4Me is catalyzed by the Set1 complex, also known as COMPASS, while in humans there are six orthologous complexes (Soares and Buratowski 2013). In contrast, Dot1, the methyltransferase that catalyzes H3 K79Me (van Leeuwen, et al. 2002), acts as a monomer.

While there remains considerable debate as to the mechanism of this so-called "histone crosstalk," several studies provide hints. One study utilizing a reconstituted *in vitro* system that replicates the *in vivo* dependence of H3 K4Me on H2Bub found that a domain within the catalytic Set1 subunit, termed the n-SET domain, was required for COMPASS activity on a chromatin template (Kim, et al. 2013). Another report using human factors identified a direct

interaction between ubiquitin and Ash2, an ortholog of yeast Bre2 that is common to all six mammalian complexes (Wu, et al. 2013). This interaction was required for H2Bub-dependent H3 K4Me, although interestingly simply tethering ubiquitin directly to Ash2 was sufficient to stimulate H3 K4Me in the absence of ubiquitylation on H2B (Wu, et al. 2013).

With respect to H3 K79Me^{2}/Me^{3}, a study utilizing synthetically ubiquitylated H2B showed that H2Bub stimulated intranucleosomal H3 K79Me directly, likely through an allosteric effect on Dot catalysis (McGinty, et al. 2008). This regulation is specific to the chromatin environment, as H2Bub was required for stimulation of H3 K79Me on nucleosomes but not on naked histone octamers (McGinty, et al. 2008).

Interestingly, attachment of the ~12 kDa small ubiquitin-like modifier (SUMO) moiety to H2B failed to promote either H3 K4Me$^{2/3}$ or H3 K79Me^{3} (Chandrasekharan, et al. 2009). This observation, along with the finding of Ash2 binding to ubiquitin, argues against an early model that hypothesized that H2Bub might function as a "wedge" that opens up chromatin in order to allow access of the methylation machinery, and in favor of a "bridge" model whereby ubiquitin acts as a binding platform (Henry and Berger 2002).

Despite the specific requirement for ubiquitin in promoting these downstream modifications, the specific attachment point of ubiquitin does not appear to be critical for crosstalk, as ubiquitin fused to the H2A N-terminus promotes moderate levels of H3 K4Me and H3 K79Me in the absence of H2Bub (Vlaming, et al. 2014). In humans, H2B can also be monoubiquitylated on K34 (Wu, et al. 2011). H2B K34ub appears to stimulate H3 K4 and H3 K79 methylation directly, similarly to H2B K120ub (Wu, et al. 2011). The two marks appear interdependent, as the H2B K120ub machinery promotes H2B K34ub and vice versa (Wu, et al. 2014).

1.5 H2B MONOUBIQUITYLATION IS A DYNAMIC MODIFICATION REGULATED BY MANY FACTORS

1.5.1 The Rad6 and Bre1 enzymes specifically monoubiquitylate H2B

H2B is monoubiquitylated through the canonical ubiquitin-activating enzyme (E1)→ ubiquitin conjugase (E2)→ ubiquitin ligase (E3) cascade. The E2 Rad6 is required for H2B K123ub in yeast, and Rad6 homologs function similarly in other organisms, including humans (Robzyk, et al. 2000; Kim, et al. 2009). Unlike many E2s, Rad6 is capable of catalyzing ubiquitylation in the absence of an E3, and it promiscuously mono- and polyubiquitylates free histones and nucleosomes *in vitro* (Haas, et al. 1988; Sung, et al. 1988; Kim and Roeder 2009). In the cell, however, the E3 Bre1 (RNF20/40 in humans), as well as the Bre1-associated protein Lge1, are required to monoubiquitylate the target lysine on H2B (Hwang, et al. 2003; Wood, Krogan, et al. 2003; Song and Ahn 2010). In humans, other E3 enzymes have been shown to promote deposition of H2Bub both *in vivo* (e.g. Mdm2) and *in vitro* (e.g. BRCA1) (Weake and Workman 2008). However, in the case of Mdm2, the activity does not appear to be specific to K120, while the ability of BRCA1 to promote H2Bub *in vivo* has yet to be determined (Weake and Workman 2008).

Rad6 has three known E3 partners - Rad18, Ubr1, and Bre1 - all of which are so-called RING E3s (Turco, et al. 2015), which act to guide the direct transfer of ubiquitin from E2s to a specific substrate or substrates, in contrast with HECT-type E3s, which form an intermediate complex with ubiquitin (Zheng and Shabek 2017). Several detailed structural and genetic analyses of Rad6 and Bre1-mediated H2Bub provide clues to the mechanisms that govern catalysis. While binding of the 700 amino acid yeast Bre1 (yBre1) to Rad6 requires only the

first 210 residues of the protein, H2Bub is dependent on Bre1's C-terminal RING domain (Kim and Roeder 2009). The N-terminal Rad6 binding domain of Bre1 interacts with the Rad6 backside (opposite the active site C88 residue) and stimulates catalysis and ubiquitin discharge from Rad6, though the RING domain in conjunction with Rad6 is sufficient to stimulate *in vitro* H2Bub (Turco, et al. 2015). In the case of Rad6-Rad18, Rad18 binding to the Rad6 backside is thought to direct the preference towards mono- over polyubiquitylation (Hibbert, et al. 2011); it is unclear if the binding of Bre1 to the Rad6 backside functions similarly (Turco, et al. 2015).

1.5.2 Regulation of H2Bub by the nucleosome

In addition to the enzymes that deposit the mark, H2Bub is regulated by the nucleosome itself. Multiple groups have shown that a domain within the N-terminal H2A tail, known as the H2A repression domain (HAR), is required for robust H2Bub (Zheng, et al. 2010; Wozniak and Strahl 2014). The HAR also regulates downstream di- and trimethylation of H3K4, and isolation of COMPASS from strains lacking the HAR revealed significantly reduced levels of the COMPASS subunit Cps35 (Zheng, et al. 2010). This finding is in agreement with a model whereby H2Bub is required for the association of Cps35 with COMPASS and subsequent COMPASS activity (Lee, et al. 2007), in contrast to a model that suggests that COMPASS activity is mediated by Rad6 and Bre1-dependent ubiquitylation of Cps35 (Vitaliano-Prunier, et al. 2008), although it remains possible that both mechanisms play a role in COMPASS activation.

More recently, our lab found that specific H2A residues housed within a negatively charged region of the nucleosome known as the nucleosome acidic patch are required for normal levels of H2Bub (Cucinotta, et al. 2015). This is likely due in part to the role these

residues play in the recruitment of the H2Bub machinery, as mutations within the acidic patch dramatically reduced the occupancy of Bre1, Spt16, and other factors involved in promoting H2Bub (Cucinotta, et al. 2015). Furthermore, substitutions within the acidic patch lead to diminished Pol II elongation efficiency (Cucinotta, et al. 2015). Competitive binding of the acidic patch by the herpes virus latency-associated nuclear antigen (LANA) inhibits Bre1-mediated H2Bub *in vitro* (Gallego, et al. 2016), indicating that the role of the acidic patch in promoting H2Bub is direct.

1.5.3 Regulation of H2Bub by deubiquitylating enzymes

H2Bub is a dynamic mark, the removal of which is carried out by the ubiquitin-specific proteases Ubp8 and Ubp10, which target distinct cellular pools of the mark (Schulze, et al. 2011). Deletion of *UBP7* also results in higher global H2Bub levels, though whether this effect is direct or indirect remains unclear (Bohm, et al. 2016). Deletion of *UBP8* reduces expression of a subset of genes (Henry, et al. 2003), and deubiquitylation carried out by Ubp8 is required for the recruitment of the CDK12 ortholog Ctk1 (Wyce, et al. 2007), which phosphorylates Ser2 of the Pol II CTD as in metazoa, thus linking deubiquitylation of H2B to transcriptional activation and suggesting that a complete cycle of ubiquitylation and deubiquitylation is required for optimal gene expression.

Ubp8 is a member of the SAGA complex and is housed within the SAGA DUB module, comprising Ubp8, Sgf11, Sus1, and Sgf73 (Morgan and Wolberger 2017). The loading of the DUB module onto ubiquitylated nucleosomes is dependent on an interaction between the nucleosome acidic patch and an "arginine anchor" on the Sgf11 subunit (Morgan, et al. 2016). Furthermore, phosphorylation by the CK2 kinase of an essential acidic patch residue, H2A Y58,

promotes H2Bub by inhibiting the deubiquitylation activity of SAGA (Basnet, et al. 2014). Interestingly, a recent report found that Bre1 also contacts the acidic patch through a similar arginine motif, competing with Sgf11 (Gallego, et al. 2016).

1.5.4 Regulation of H2Bub by transcription elongation factors

Another well-studied factor known to promote H2B ubiquitylation is the histone chaperone complex FACT. In higher eukaryotes, FACT is composed of Spt16 and SSRP1, while in budding yeast, the functions of SSRP1 are carried out by two proteins, Pob3 and Nhp6 (Winkler and Luger 2011). FACT binds and chaperones both H2A-H2B dimers and H3-H4 tetramers, and binds nucleosomes with high affinity, reorganizing them so as to render the DNA template more accessible (Formosa 2012). The complex has roles in DNA repair and DNA replication, in addition to regulating gene expression by promoting transcription elongation (Formosa 2012). Inactivation of the essential Spt16 subunit in yeast leads to a dramatic reduction in global H2Bub levels (Fleming, et al. 2008), and a study making use of an *in vitro* chromatin template also observed a requirement for FACT in promoting H2Bub (Pavri, et al. 2006). Deletion of the Spt16 N-terminal domain is not lethal but causes sensitivity to hydroxyurea (VanDemark, et al. 2008), which induces DNA replication stress, a phenotype shared with mutants lacking H2Bub due to an H2B K123R substitution (Trujillo and Osley 2012).

Of note, several groups, including our lab, have found that Spt16 and components of Paf1C copurify (Squazzo, et al. 2002; Mayekar, et al. 2013), and depletion of the Paf1 subunit leads to reduced SSRP1 recruitment in *Drosophila* (Adelman, et al. 2006). Also of interest is the observation that CK2 copurifies with FACT, and that, in addition to its role in phosphorylating the nucleosome acidic patch, CK2 extensively phosphorylates Paf1C (Bedard, et al. 2016).

Finally, a recent report showed that H2Bub in mouse embryonic fibroblasts is dependent on the Mediator subunit MED23 (Yao, et al. 2015). Although early studies of Mediator focused on its role in initiation, many recent reports show roles for Mediator in transcription elongation and in various cotranscriptional processes (Conaway and Conaway 2013). MED23 directly associates with RNF20/40 and promotes its recruitment to chromatin (Yao, et al. 2015). Intriguingly, Paf1C functioned cooperatively with Mediator to stimulate H2Bub in an *in vitro* system using purified factors (Yao, et al. 2015).

1.6 THE PAF1 COMPLEX IS REQUIRED FOR H2B MONOUBIQUITYLATION

A role for Paf1C in promoting H2Bub *in vivo* was first suggested by studies showing that certain Paf1C subunits are required for H3 K4 and H3 K79 methylation (Krogan, et al. 2003; Ng, Robert, et al. 2003), and shortly thereafter it was demonstrated independently by several groups that Paf1C is required for H2Bub (Ng, Dole, et al. 2003; Wood, Schneider, et al. 2003; Xiao, et al. 2005). Consistent with this, Bur1, which promotes Pa1C recruitment to chromatin, is also required for H2Bub (Wood, et al. 2005).

While there is some disagreement in the literature concerning the role of individual Paf1C subunits in promoting H2Bub (see Section 2.3.1), our lab and others have shown that this function is dependent on a small, conserved domain within the Rtf1 subunit, both in yeast (Warner, et al. 2007; Tomson, et al. 2011; Piro, et al. 2012) and in higher eukaryotes (Cao, et al. 2015). This domain, termed the Rtf1 histone modification domain (hereafter, HMD), was first identified by screening a series of Rtf1 internal deletion mutants for defects in H3 K4 Me^3 and H3 K79 $Me^{2/3}$ (Warner, et al. 2007). Subsequently, it was found that overexpression of the

HMD is sufficient to restore global H2B K123ub in a yeast strain deleted of the endogenous *RTF1* gene (Piro, et al. 2012). Another study showed that the HMD and other factors that promote catalysis of H2Bub stabilize Bre1 at the protein level (Wozniak and Strahl 2014). Despite these advances and studies showing a role for Paf1C in recruiting various histone modifiers to genes (Krogan, et al. 2003; Ng, Robert, et al. 2003; Xiao, et al. 2005; Chu, et al. 2007), the precise mechanism by which Paf1C facilitates H2Bub has remained unclear. While Bre1 was shown to recruit Rad6 to promoter regions via transcriptional activators (Wood, Krogan, et al. 2003; Kao, et al. 2004), Rtf1 is required for full levels of Rad6 and Bre1 in the coding regions of highly transcribed genes (Xiao, et al. 2005; Van Oss, et al. 2016). However, this relatively modest effect of Rtf1 on Rad6 and Bre1 levels does not fully explain the fact that H2Bub is undetectable in the absence of Rtf1, suggesting a more active role for the Rtf1 HMD in promoting H2Bub. Understanding the molecular details of this mechanism is the central question that this thesis seeks to address.

1.7 RELEVANCE OF H2B MONOUBIQUITYLATION IN HUMAN DEVELOPMENT AND DISEASE

There is evidence suggesting that Paf1C regulation of H2Bub underpins its role in governing development and differentiation in higher eukaryotes. Mutant clones of the Bre1 ortholog in fruit flies exhibit defective Notch signaling (Bray, et al. 2005), and knockdown of the Drosophila Rtf1 ortholog results in similar phenotypes (Tenney, et al. 2006). RNF20/40-mediated H2Bub is also required for proper differentiation in both human and mouse stem cells (Fuchs, et al. 2012; Karpiuk, et al. 2012).

H2Bub is also important for preventing changes in transcription that are associated with tumorigenesis (Shema, et al. 2008), and several recent studies have linked changes in H2Bub with specific cancers (Dickson, et al. 2016; Melling, et al. 2016; Tarcic, et al. 2016). Despite the fact that loss of H2Bub leads to increased apoptosis in *S. cerevisiae*, (Walter, et al. 2010), depletion of RNF20 from human cells led to a dramatic reduction in p53 expression and decreased p53-mediated apoptosis (Shema, et al. 2008). In other cellular contexts RNF20 can function as an oncogene, possibly through regulation of HOX gene expression (Wright, et al. 2011).

The extent to which H2Bub contributes to Paf1C regulation of promoter-proximal pausing in higher eukaryotes is unclear. In HeLa cells, CDK9 both promotes H2B K120ub and is dependent on it marks for its chromatin association (Wu, et al. 2014). In contrast, in cells where Paf1C promotes pausing, H2Bub does not appear linked to this regulation (Chen, et al. 2015). Interestingly, a recent report suggests that Paf1C regulation of promoter-proximal pausing may explain its effects on differentiation and development. In the context of pluripotent stem cells, Paf1C and the PHD-finger protein Phf5a appear to cooperate to maintain pluripotency by promoting pause release and thereby productive transcription of genes in the self-renewal network (Strikoudis, et al. 2016). Paradoxically, H2B K120ub at Paf1C targets increases upon Paf1 depletion in ESCs, while H3 K79Me increases (Strikoudis, et al. 2017).

Since the discovery of H2Bub nearly four decades ago (West and Bonner 1980), interest in this modification and the molecular factors that regulate it has continued to grow. Given its broad implications for regulating chromatin structure and function and its relevance to human health, such studies will likely continue to proliferate.

2.0 THE PAF1 COMPLEX REGULATES GLOBAL H2B MONOUBIQUITYLATION IN SACCHAROMYCES CEREVISIAE

2.1 INTRODUCTION

The Rtf1 HMD was first identified by examining a series of Rtf1 internal deletion mutants for defects in H3 K4 and H3 K79Me$^{2/3}$ (Warner, et al. 2007). Deletion of Rtf1 residues 62-109 or of residues 111-152 resulted in a nearly complete loss of these methylation marks, and H2Bub is undetectable in these mutants; thus, the HMD was initially defined as comprising residues 62-152 (Warner, et al. 2007). Subsequent work showed that overexpression of residues 63-152 (HMD_{63-152}) was sufficient to restore wild-type levels of H2Bub in an *rtf1Δ* strain (Piro, et al. 2012).

In addition to identifying the HMD, the genetic structure/function study of Rtf1 found that a small C-terminal region of Rtf1, comprising residues 536-558 and known as the Paf1C interacting domain (PID), is required for Rtf1 association with Paf1C (Warner, et al. 2007). A recent study that presented a cryo-electron microscopy structure of Paf1C complexed to Pol II confirmed this observation, as crosslinking followed by mass spectrometry analysis found that the vast majority of Rtf1's intracomplex contacts were mediated by the PID (Xu, et al. 2017). This function is conserved in human cells (Cao, et al. 2015), in spite of the weaker association of Rtf1 with Paf1C in higher eukaryotes. Given that the HMD_{63-152} lacks the PID, its ability to

promote H2Bub in an *rtf1Δ* strain suggests that it is able to function independently of Paf1C. Consistent with this, HMD_{63-152} largely restores H2Bub in *rtf1Δ paf1Δ* and *rtf1Δ ctr9Δ* backgrounds (Piro, et al. 2012). However, it is possible that the established roles of the Paf1 and Ctr9 subunits (see Section 2.3.1) are redundant, and the ability of the HMD to function in the complete absence of other Paf1C subunits is yet to be determined.

Several groups have described connections between Paf1C and the ubiquitylation machinery. Reconstituted yPaf1C was shown to interact directly with yBre1, but not with yRad6 or hE1 (Kim and Roeder 2009). When added to an *in vitro* ubiquitylation reaction using HeLa nucleosomes as a substrate, yPaf1C surprisingly inhibited H2Bub (Kim and Roeder 2009). Based on this result and an early report that showed decreased Rad6 association with the *GAL1* ORF upon deletion of *RTF1*, Kim and Roeder argued that Paf1C stimulated H2Bub by recruiting the ubiquitylation machinery to coding regions. However, a global analysis performed by our lab observed a more modest reduction in Rad6 and Bre1 ORF occupancy in an *rtf1Δ* strain, detectable only at the most highly expressed genes (Van Oss, et al. 2016). Given that catalysis of H2Bub stabilizes Bre1 at the protein level (Wozniak and Strahl 2014), it is possible that the diminished Rad6 and Bre1 occupancy in an *rtf1Δ* strain are an indirect effect of reduced catalysis and that the HMD plays a more direct role in stimulating H2Bub.

2.2 MATERIALS AND METHODS

2.2.1 Plasmid construction

The HMD mutants shown or described in Figures 8-11 were made by site-directed mutagenesis using the QuikChangeII kit (Agilent Technologies) and either pLS21-5 or pAP39 as the template. To construct Rtf1 and HMD derivatives for use in BPA crosslinking experiments, Dr. Shirra created a smaller template for mutagenesis by subcloning an EcoRI-SmaI fragment from pLS21-5 into the same sites in pUC18 (Yanisch-Perron, et al. 1985). Following site-directed mutagenesis using the QuikChange II kit, DNA fragments containing the amber codons mutations were subcloned back into pLS21-5, using either *Eco*RI-*Bgl*II fragments or *Bgl*II-*Sma*I fragments. These plasmids were then used as templates for PCR amplification in order to clone either full-length Rtf1 or HMD sequences into KB1140 using the *Nde*I and *Eco*RI restriction sites. Note that the stop codon in the full-length Rtf1 derivatives was changed from TAG to TGATGA in the oligonucleotides used for amplification. All other plasmids used in this chapter are described in the above Table 2.

2.2.2 Protein purification

Expression of Rad6 as well as wild-type and mutant HMD proteins was performed in *E.coli* Codon+ (RIPL) or (RIL) cells (Stratagene). Cells expressing HMD proteins were grown in ZY auto-induction media (Studier 2005) at room temperature for 16-24 hr; cells expressing Rad6 were grown in LB media to an OD of 0.6, induced with 100 μM IPTG, and grown overnight at 18 °C.

Cells were harvested by centrifugation, then resuspended in lysis buffer (25 mM Tris-Cl pH 8.0, 500 mM NaCl, 10% glycerol, 5 mM imidazole, 1 mM β-mercaptoethanol, and 1X protease inhibitors (167μg/mL PMSF, 0.7μg/mL pepstatin, 0.5μg/mL leupeptin; 0.5μg/mL aprotinin was also included in most preps)) and lysed with an EmulsiFlex-C3 homogenizer (Avestin). Lysates were cleared by centrifugation at 30,000 x g. All proteins were purified by nickel affinity chromatography (Ni-NTA agarose; Qiagen) at 4°C followed by digestion with TEV protease, during dialysis into TEV cleavage buffer (20mM Tris-Cl pH 8.0, 400mM NaCl, 8% glycerol, 1 mM β-mercaptoethanol), for 90 minutes at room temperature and then overnight at 4°C. The amount of TEV protease added was based on the amount of protein present as determined by Coomassie staining but was generally 1.5-3mg. Uncleaved protein and His-tagged TEV protease were removed by a second round of nickel affinity chromatography followed by ion exchange chromatography using HiTrap-SP and/or HiTrap-Q FF columns; proteins were kept at 4°C throughout the purification process. Following binding to the HiTrap columns, protein was washed in low-salt buffer (8% glycerol, 20mM Tris-Cl pH 8.0, 1 mM β-mercaptoethanol, 60-100mM NaCl) and then eluted with an increasing salt gradient. Proteins were then dialyzed into storage buffer and concentrated when necessary using a Vivaspin concentrator (Millipore).

Rock, Shroom, and His-Shroom proteins were generous gifts from Jenna Zalewski from Dr. Arndrew VanDemark's lab. His-Rad6 protein was a generous gift from Dr. Jaehoon Kim (Korea Advanced Institute of Science and Technology).

2.2.3 Western blot analysis

For whole cell extracts used in Figures 5, 6A, 8B, 8D, 11, 12, 13, and 14A, cells were grown to mid- to late-log phase as determined by OD_{600} and mixed with a buffered solution (Tris-Cl pH 7.5) containing 10mM sodium azide. An equivalent number of OD units was harvested for each sample. Pellets were resuspended in 75 µL of SUTEB buffer (10 mM Tris-Cl pH 8.0, 1% SDS, 8 M Urea, 10 mM EDTA pH 8.0, and 0.01% bromophenol blue) and boiled for three minutes. Cells were then lysed by bead beating, and extracts were diluted by adding 150 µL of additional SUTEB buffer, then boiled again for one minute followed by a clarifying spin (10 minutes/14,000 rpm/4 °C). For some samples, SDS loading buffer was added to a final concentration of 2X, which tended to improve band resolution on western blots. For extracts used in Figures 9A and 9B, cells were grown to mid-log phase (3-4X10^7 cells/mL) and resuspended in RIPA buffer (50 mM HEPES-KOH pH 7.9, 2 mM EDTA pH 8.0, 0.1% SDS, 0.1% sodium deoxycholate, 1% Triton X-100, and 1X HALT protease inhibitor cocktail (ThermoFisher)). Extracts were made by bead beating, and concentrations determined by Bradford assay, essentially as described previously (Shirra, et al. 2005). Extracts used in Figure 16 were prepared by Dr. Shirra using a modification of the trichloroacetic acid (TCA) precipitation method (Cox, et al. 1997). Briefly, cells were lysed using glass beads in the presence of 20% TCA. Proteins were precipitated by a 3,400 x g centrifugation and pellets were washed with 0.5 M Tris-Cl pH 8.0. The pellets were then resuspended in 0.5 M Tris-Cl pH 8.0, boiled in the presence of SDS loading buffer, and extracts were collected from the supernatant following an 18,000 x g centrifugation for 10 minutes. For chromatin samples in Figure 13, chromatin was prepared by Dr. Shirra as previously described (Van Oss, et al. 2016).

All samples were resolved on SDS-PAGE gels, blotted to a nitrocellulose membrane (with the exception of α-Flag gels, which were blotted to PVDF membranes), and probed with the indicated antibodies following blocking with 5% powdered milk. The antibodies used in this chapter were α-H2Bub (Cell Signaling #5546; 1:1000 dilution), α-H2B (Active Motif #39237; 1:3000), α-Rtf1 (1:2500) (Squazzo, et al. 2002), α-G6PDH (Sigma #A9521; 1:20000), α-Flag (Clone M2) (Sigma #F3165; 1:1000), α-H3 K4Me^2 (Millipore #07-030; 1:2000), α-H3 K4Me^3 (Active Motif #39159; 1:2000), α-H3 K79Me$^{2/3}$ (Abcam #ab2621; 1:1000; note that this antibody recognizes both di- and trimethylated H3 K79), α-H3 (1:30000) (Tomson, et al. 2011), α-HA (Santa Cruz #sc-7392; 1:3000), α-c-Myc (9E10) (Covance #MMS-150P; 1:1000), α-His (Abcam #18184;1:2500), and α-HSV (Sigma #H6030; 1:500). Blots were then probed with a 1:5000 dilution of the appropriate horseradish peroxidase-conjugated secondary antibody (either donkey anti-rabbit, or sheep anti-mouse; GE Healthcare), and visualized via enhanced chemiluminescence. For some blots, particularly α-H2Bub, α-H2B, α-Flag, and α-c-Myc blots, milk was added to the secondary antibody in order to increase specificity, at concentrations of 3%, 5%, 2.5%, and 2%, respectively. Blots were visualized on either a Kodak Image Station (440CF) or a Bio-Rad ChemiDoc XRS+ imager. Signal was quantitated using the ImageJ (NIH) and Image Gauge (Fujifilm) software packages.

2.2.4 Silver staining

Samples used in Figure 15 were resolved on a 7-20% SDP-PAGE gradient gel. The gel was placed in fixative (50% EtOH, 12% acetic acid, 0.1% formaldehyde) for ~30 minutes, washed with 0.01% $Na_2S_2O_3$ and then twice with ddH_2O, and then stained with 0.1% $AgNO_3$ for ~20 minutes. Developer (~280mM Na_2Co_3, 0.1% formaldehyde, 0.002% $Na_2S_2O_3$) was added, and

the staining reaction was stopped by washing the gel in 10mM EDTA. The gel was then stored in a 20%EtOH, 10% glycerol solution prior to imaging.

2.2.5 Serial dilution assays

The indicated plasmids were transformed into KY817 (Figure 6B, synthetic complete minus uracil medium (SC-U), synthetic defined minus uracil medium (SD-U), synthetic defined minus uracil minus histidine medium (SD-U-H), synthetic complete minus uracil plus 6-azauracil medium (SC-U+6AU)), KY1290 (Figure 6B, SC-U, SC-U +Caffeine, and SC-U-H+Galactose media), or KY1370 (Figure 10) and grown to saturation, then harvested, washed with sterile water, and resuspended such that the concentration of each sample was equal to 1 X 10^8 cells/ml. For Figure 6B, tenfold serial dilutions were plated on all media. For Figure 10, twofold or threefold dilutions were then plated either to a growth control or to media containing the drug 5-fluoroorotic acid (5-FOA). For Figure 6B, 6AU was at a concentration of 50μg/mL, caffeine was at a concentration of 15mM, and galactose was at a concentration of 2% (w/v).

2.2.6 Coimmunoprecipitation analysis

Plasmids pAP39, pAP46, and pJB01 were transformed into KY1759 and cells were grown to a density of ~1.5X10^7 cells/mL. For samples that were analyzed by mass spectrometry, formaldehyde was added to a final concentration of either 3% (first experiment/no RNAse treatment) or 1% (second experiment/RNAse treatment), and cells were incubated with swirling for two minutes at room temperature, followed by quenching for five minutes with swirling at room temperature with either 375mM glycine (first experiment) or 125mM glycine (second

experiment). Cells were pelleted, washed, and resuspended in SUME buffer (first experiment; 10mM MOPS pH 6.8, 1% SDS, 8M Urea, 10mM EDTA) or RIPA-like buffer (second experiment; 50mM HEPES-KOH pH 7.5, 150mM NaCl, 1mM EDTA, 1% Triton X-100, 0.1% sodium deoxycholate) with 1X HALT protease inhibitor cocktail. Whole cell extracts were made by bead beating. For the second experiment, lysates in RIPA-like buffer were also sonicated (1X20 seconds on setting 2, 4X20 seconds on setting 3, with one minute on ice in between each pulse). For the first experiment, an equivalent volume of SUME extract was used for each sample, while for the second experiment, volumes were normalized to concentration as determined by Bradford assay. For the second experiment, 15μL of RNAse cocktail (Invitrogen, #AM2286) was added to the appropriate samples and incubated with lysates for 20 minutes with rotation at room temperature. Lysates were diluted in IP buffer (150mM NaCl, 15mM Na_2HPO_4, 2% Triton X-100, 0.1% SDS, 0.5% sodium deoxycholate) with 1X HALT, and TAP-tagged proteins were purified by incubation with equilibrated Rabbit IgG-Agarose beads (Sigma #A2909) for 2 hours with rotation at room temperature. Beads were washed once with IP buffer with 1X HALT and three times with wash buffer (50mM NaCl, 10mM Tris-Cl pH 7.5) with 1X HALT. Samples were eluted by boiling beads for three minutes in SUME plus bromophenol blue and analyzed by western blotting as described above. Remaining sample was run ~1 cm into an 8% SDS-PAGE gel, excised, destained, and sent for mass spectrometry analysis.

For affinity purifications shown in Figure 15, the same three plasmids were transformed into KY2421 and cells were grown to a density of ~$1.5X10^7$ cells/mL. No formaldehyde was added to these samples. Extracts were made as described above using RNP buffer (100mM NaCl, 20mM HEPES-KOH pH 7.4, 0.1% NP-40) with 1X HALT and a sonication step, and the volumes used were normalized to concentration as determined by Bradford assay. Extracts were

pre-cleared by incubation with Sepharose CL-4B beads for 1.5 hours at 4°C. Pre-cleared lysates were then incubated with Rabbit IgG-Agarose beads for two hours with rotation at 4°C, and beads were washed five times with RNP buffer with 1X HALT. Samples were eluted by boiling beads for three minutes in 1X SDS loading buffer and analyzed by western blotting and silver staining as described above.

For affinity purifications shown in Figure 17, plasmids pKB1140, pKB1191, pKB1247, and pKB1309 into KY2507, and cells were grown to a density of ~1.5X10^7 cells/mL. No formaldehyde was added to these samples. Extracts were made using RNP buffer and 1X HALT as described above except that no sonication step was performed, and the volumes used were normalized to concentration as determined by Bradford assay. Lysates were incubated with IgG Sepharose 6 Fast Flow beads for two hours with rotation at 4°C, and beads were washed four times with RNP buffer with 1X HALT. Samples were eluted by boiling beads for three minutes in 1X SDS loading buffer and analyzed by western blotting as described above.

2.2.7 Mass spectrometry

Tandem mass spectrometry analysis was conducted by the lab of Dr. Richard Gardner at the Fred Hutchinson Cancer Research Center Proteomics Facility.

2.2.8 *In vitro* crosslinking with recombinant proteins

All proteins were stored in HEPES-KOH pH 7.9 and added as indicated at a concentration of 100μM to 5mM BS^3 in a final reaction volume of 10.5μL. Reactions were incubated at 30°C for

30 minutes, followed by addition of 40mM Tris-Cl pH 7.5 and incubation at room temperature for 15 minutes. Samples were analyzed by western blotting as described above.

2.2.9 Far western analysis

One μg of each prey protein was resolved on an SDS-PAGE gel, and blotted to a nitrocellulose membrane overnight at 4°C using prechilled transfer buffer. Following Ponceau staining, membranes were washed with AC buffer (10% glycerol, 100mM NaCl, 20mM Tris-Cl pH 7.5, 1mM EDTA, 0.1% Tween-20, 1mM DTT, and 2% powdered milk) containing gradually decreasing concentrations of guanidine-HCl. Membranes were washed in AC buffer containing 6M guanidine-HCl for 30 minutes at room temperature, then in AC buffer containing 3M guanidine-HCl for 30 minutes at room temperature, then in AC buffer containing 1M guanidine-HCl for 30 minutes at room temperature, then in AC buffer containing 0.1M guanidine-HCl for 30 minutes at 4°C for 30 minutes at room temperature, then in AC buffer containing no guanidine-HCl for 105 minutes at 4°C. Membranes were then blocked with 5% milk for 50 minutes at room temperature, then for 15 minutes at 4°C , and then incubated overnight at 4°C with 10 μg of bait protein diluted in binding buffer (150mM NaCl, 20mM Tris-Cl pH 7.6, 0.5 mM EDTA, 10% glycerol, 0.1% Tween-20, 1mM DTT, and 2% powdered milk). Membranes were then probed with the indicated antibodies (α-Rtf1 (1:2500 dilution) (Squazzo, et al. 2002) or α-His (Abcam #18184;1:2500)) for two hours at room temperature, then probed with a 1:5000 dilution of the appropriate horseradish peroxidase-conjugated secondary antibody (either donkey anti-rabbit, or sheep anti-mouse; GE Healthcare), and visualized via enhanced chemiluminescence.

Table 1. *Saccharomyces cerevisiae* strains used in Chapter 2

Strain	Genotype	Used in Figure(s)
KY404	*MAT***a** *rtf1Δ101::LEU2 his4-912δ lys2-128δ leu2Δ1 ura3-52 trp1Δ63*	13
KY524	*MAT*α *ppr2Δ::HISG-URA3 his4-912δ lys2-128δ leu2Δ1 ura3-52*	14A
KY817	*MAT***a** *ctr9Δ::KanMX his4-912δ lys2-128δ leu2Δ1 ura3-52*	6
KY903	*MAT***a** *dot1Δ::HIS3 his4-912δ lys2-128δ his3Δ200 leu2Δ1 ura3-52*	9A, 9B
KY907	*MAT***a** *set1Δ::HIS3 lys2-128δ his3Δ200 leu2Δ1 ura3-52*	9A, 9B
KY1021	*MAT***a** *his4-912δ lys2-128δ leu2Δ1 trp1Δ63*	5, 14A
KY1290	*MAT*α *ctr9Δ::KanMX GAL1pr-FLO8-HIS3::KanMX his3Δ200 lys2-128δ leu2Δ1 ura3-52 trp1Δ63*	6
KY1370	*MAT*α *rtf1Δ::ARG4 GAL1pr-FLO8-HIS3::KanMX TELVR::URA3 his3Δ200 arg4-12 ura3-52 trp1Δ63*	9A-C, 10
KY1419	*MAT*α *3HA-RTF1 his3Δ200 lys2-128δ leu2Δ1 ura3-52 trp1Δ63*	13
KY1759	*MAT***a** *rtf1Δ101::LEU2 his4-912δ lys2-128δ leu2Δ1 trp1Δ63*	9A-C; Tables 3 and 4
KY2124	*MAT***a** *rtf1Δ::KanMX hta1-htb1Δ::LEU2 hta2-htb2Δ::KanMX his3Δ200 lys2-128δ leu2Δ1 ura3-52 trp1Δ63 pJH23-WT [HTA1-HTB1/HIS3/CEN/ARS/ Amp^r]*	8B, 8C
KY2125	*MAT***a** *rtf1Δ::KanMX hta1-htb1Δ::LEU2 hta2-htb2Δ::KanMX lys2-128δ his3Δ200 leu2Δ1 ura3-52 trp1Δ63 pJH23-FL [HTA1-FLAG-HTB1/HIS3/CEN/ ARS/Amp^r]*	8B, 8C, 9C
KY2167	*MAT*α *HTA1-htb1-K123R (hta2-htb2)Δ::KanMX ura3Δ0*	5, 8D, 12A, 12B, 13, 14A
KY2239	*MAT*α *ctr9Δ::KanMX his4-912δ lys2-128δ trp1Δ63*	5
KY2241	*MAT***a** *cdc73Δ::KanMX his4-912δ lys2-128δ trp1Δ63*	5
KY2243	*MAT*α *rtf1Δ::KanMX his4-912δ lys2-128δ leu2Δ1 trp1Δ63*	5
KY2244	*MAT***a** *leo1Δ::URA3 his4-912δ lys2-128δ ura3-52 trp1Δ63*	5

KY2271	*MAT*α *paf1Δ::KanMX his4-912δ lys2-128δ leu2Δ1 trp1Δ63*	5
KY2277	*MAT*α *rtf1Δ::KanMX his3Δ200 leu2Δ1 trp1Δ63*	16A
KY2421	*MAT*a *rtf1Δ::ARG4 GAL1pr-FLO8-HIS3::KanMX TELVR::URA3 his3Δ200 leu2Δ1 ura3-52 trp1Δ63*	8D, 11, 12A, 12B, 15
KY2466	*MAT*a *rtf1Δ::LEU2 paf1Δ::URA3 ctr9Δ::KanMX cdc73Δ::KanMX leo1Δ::URA3 leu2Δ1 ura3-52 trp1Δ63*	12B
KY2507	*MAT*a *rtf1Δ::KanMX RAD6-13xMyc::KanMX his3Δ200 leu2Δ1 ura3-52 trp1Δ63*	16A-D, 17
KY2566	*MAT*a *rtf1Δ::KanMX hta1-htb1Δ::LEU2 hta2-htb2Δ::KanMX lys2-128δ his3Δ200 leu2Δ1 ura3-52 trp1Δ63 pCD2 [HTA1-FLAG-htb1-K123R/HIS3/ CEN/ARS/Amp^r]*	8B, 8C
KY2600	*MAT*α *rtf1Δ::KanMX 3xHA-BRE1 his3Δ200 leu2Δ1 ura3-52 trp1Δ63*	16B
KY2713	*MAT*a *rtf1Δ::KanMX bre1Δ::KanMX RAD6-13xMyc::KanMX his3Δ200 leu2Δ1 ura3-52 trp1Δ63*	16C, 16D

Table 2. Plasmids used in Chapter 2

Plasmid	Construction	Yeast Origin	Promoter	Gene Product	Markers
pAP39	(Piro, et al. 2012)	2μ	*ADH1*	NLS-Myc-HMD$_{63-152}$	*TRP1*; Kan^R
pAP45	(Piro, et al. 2012)	2μ	*ADH1*	NLS-Myc-Rtf1	*TRP1*; Kan^R
pAP46	TAP tag was amplified from pBS1539 and introduced into pAP39 by homologous recombination	2μ	*ADH1*	NLS-Myc-HMD$_{63-152}$-TAP	*URA3; TRP1*; Kan^R
pAP48	(Van Oss, et al. 2016)	2μ	*ADH1*	NLS-Myc-HMD$_{74-139}$	*TRP1*; Kan^R
pAP54	(Piro, et al. 2012)	2μ	*ADH1*	NLS-Myc-HMD$_{63-152}$-E104K	*TRP1*; Kan^R
pJB01	E104K substitution was made in pAP46 by site-directed mutagenesis	2μ	*ADH1*	NLS-Myc-HMD$_{63-152}$-E104K-TAP	*URA3; TRP1*; Kan^R
pKB747	*In vivo* homologous recombination using PCR product made from AP025/26 and pAP10	*CEN/ARS*	*CTR9*	Ctr9-13XMyc	*URA3; TRP1*; Amp^R
pKB748	*In vivo* homologous recombination using PCR product made from AP025/27 and pAP10	*CEN/ARS*	*CTR9*	Ctr9Δ975-1077-13XMyc	*URA3; TRP1*; Amp^R
pKB749	*In vivo* homologous recombination using PCR product made from AP025/28 and pAP10	*CEN/ARS*	*CTR9*	Ctr9Δ871-1077-13XMyc	*URA3; TRP1*; Amp^R
pKB814	(Van Oss, et al. 2016)		T7	6XHis-V5-TEV-HMD $_{74-184}$	Amp^R
pKB993	(Van Oss, et al. 2016)		T7	6XHis-V5-TEV-HMD $_{74-184}$-E104K	Amp^R
pKB1140	(Van Oss, et al. 2016)	2μ	*ADH1*	NLS-3XHSV-HMD$_{63-152}$	*TRP1*; Kan^R
pKB1164	E104K substitution was made in pTOPO yHMD $_{74-139}$ by site-directed mutagenesis		T7	6XHis-V5-TEV-HMD $_{74-139}$-E104K	Amp^R
pKB1191	*In vivo* homologous recombination using PCR product made from	2μ	*ADH1*	NLS-HSV-HMD$_{63-152}$-TAP	*URA3; TRP1*; Kan^R

	AP080/81 and pAP46				
pKB1228	(Van Oss, et al. 2016).	2μ	*ADH1*	NLS-3XHSV-Rtf1	*TRP1*; Kan^R
pKB1247	*Sma*1 fragment from pPC59 cloned into *Sma*1 sites of pKB1228	2μ	*ADH1*	NLS-3XHSV-Rtf1-TAP	*TRP1*; Kan^R
pKB1309	PCR stitching used to delete sequence for residues 63-152 from pKB1247	2μ	*ADH1*	NLS-3XHSV-Rtf1 Δ63-152-TAP	*TRP1*; Kan^R
pLH157/ *HIS3*	(Van Oss, et al. 2016)	2μ	*ADH1*; N(GTT)PR	*E. coli* Tyr tRNA synthetase; *E. coli* $tRNA^{Tyr}$ amber suppressor tRNA	*HIS3*; Amp^R
pLS21-5	(Stolinski, et al. 1997)	*CEN/ARS*	*RTF1*	3XHA-Rtf1	*TRP1*; Amp^R
pRS314	(Sikorski and Hieter 1989)	*CEN/ARS*	n/a	n/a	*TRP1*; Amp^R
pRS316	(Sikorski and Hieter 1989)	*CEN/ARS*	n/a	n/a	*URA3*; Amp^R
pTOPO-yHMD $_{74-139}$	(Van Oss, et al. 2016)		T7	6XHis-V5-TEV-HMD $_{74-139}$	Amp^R

2.3 RESULTS

2.3.1 Paf1, Ctr9, and Rtf1 regulate H2B K123ub

Though the requirement for the Rtf1 HMD in promoting H2Bub is well established in both yeast and higher eukaryotes (see Section 1.6), data concerning the role of other Paf1C members are more equivocal. While most reports have found that H2Bub is nearly undetectable in strains lacking Paf1 (Wood, Schneider, et al. 2003; Xiao, et al. 2005; Wozniak and Strahl 2014), the reported effects of *CTR9* and *CDC73* deletion on H2Bub levels range from moderate (Xiao, et

al. 2005) to severe (Wozniak and Strahl 2014). Interestingly, in human cells, depletion of Cdc73 leads to a reduction in H2Bub without a corresponding loss of H3 K4 Me^3 (Hahn, et al. 2012). Furthermore, while several groups have reported a modest effect of *LEO1* deletion on H2Bub levels (Xiao, et al. 2005; Wozniak and Strahl 2014), another study showed that H2Bub was undetectable in a *leo1Δ* strain, while H3 K4 and K79 Me were unaffected (Thornton, et al. 2014).

I therefore examined the contribution of each Paf1C subunit to global H2Bub in our strain background, making use of deletion strains that were otherwise wild-type except for marker genes, and a recently developed antibody which recognizes the modification directly (see Section 2.3.2.2). I found that, while H2Bub was greatly diminished in *ctr9Δ* and *paf1Δ* strains, Rtf1 is the only Paf1C subunit strictly required for detection of this modification *in vivo*. Deletion of *LEO1* or *CDC73* did not significantly affect H2Bub levels (Figure 5). Due to the discrepancy with the result published by Thornton et al., PCR genotyping was performed on the *leo1Δ* strain used (KY2244), which revealed that *LEO1* was only partially deleted in this strain. I therefore examined several independently constructed *leo1Δ* strains with confirmed complete deletions, including the deletion collection strain used by Thornton et al.; all strains tested showed wild-type levels of H2Bub (data not shown). An early report suggested that Paf1, Ctr9, and Cdc73 regulation of H2Bub may be an indirect effect of their role in stabilizing Rtf1, as Rtf1 was barely detectable by western blot upon deletion of any of these three subunits (Mueller, et al. 2004). However, I observed a much more modest effect on Rtf1 levels in these strains (Figure 5).

As part of a larger collaboration with the VanDemark lab, I sought to characterize the activity of mutant proteins that may be used for structural studies. I further examined the role of

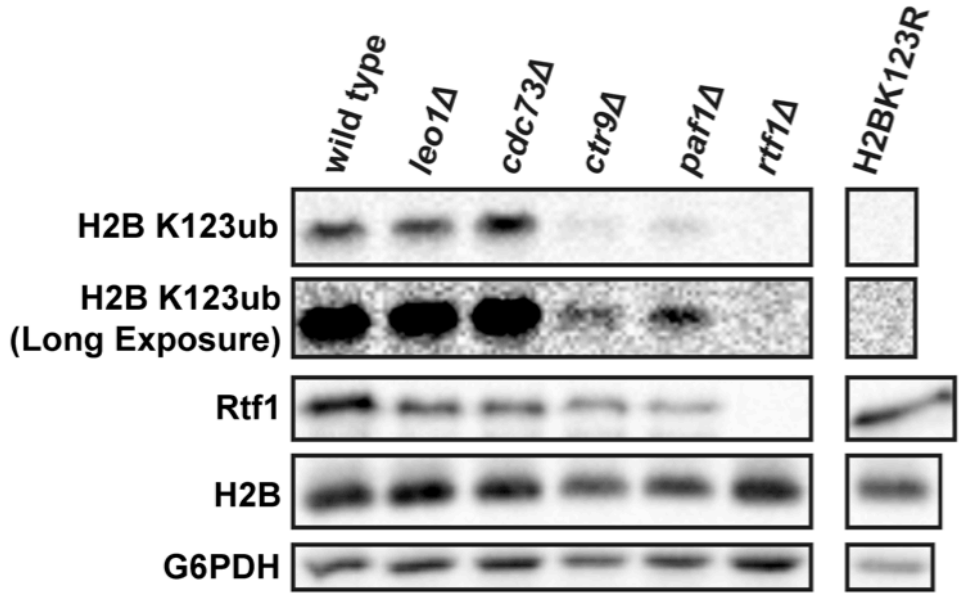

Figure 5: Ctr9, Paf1, and Rtf1 regulate global H2B ubiquitylation in *S. cerevisiae*.

Western blot analysis was performed on the indicated strains. The H2B K123R control was run on the same gel as the other samples. A long exposure permits visualization of H2B K123ub signal in the *ctr9Δ* and *paf1Δ* strains. The experiment was conducted using biological triplicates and technical duplicates.

Ctr9 in promoting H2Bub, performing western blot analysis on strains expressing Ctr9 C-terminal deletion mutants. Deletion of the residues 975-1077, representing the most C-terminal portion of the protein, had no detectable effect on global H2Bub (Figure 6A). In contrast, deletion of residues 871-1077 dramatically reduced H2Bub (Figure 6A), indicating that residues 871-974 are required to establish normal levels of the modification *in vivo*. Despite the large reduction in H2Bub in the Ctr9Δ871-1077 mutant, the very subtle decrease in Rtf1 levels was statistically insignificant, suggesting a function for this region of Ctr9 that is separate from promoting Rtf1 stability (Figure 6A). Ctr9 protein levels were also examined and both mutant proteins were expressed at levels similar to the wild-type protein, although proteolysis evident in all three constructs made accurate quantitation difficult (data not shown).

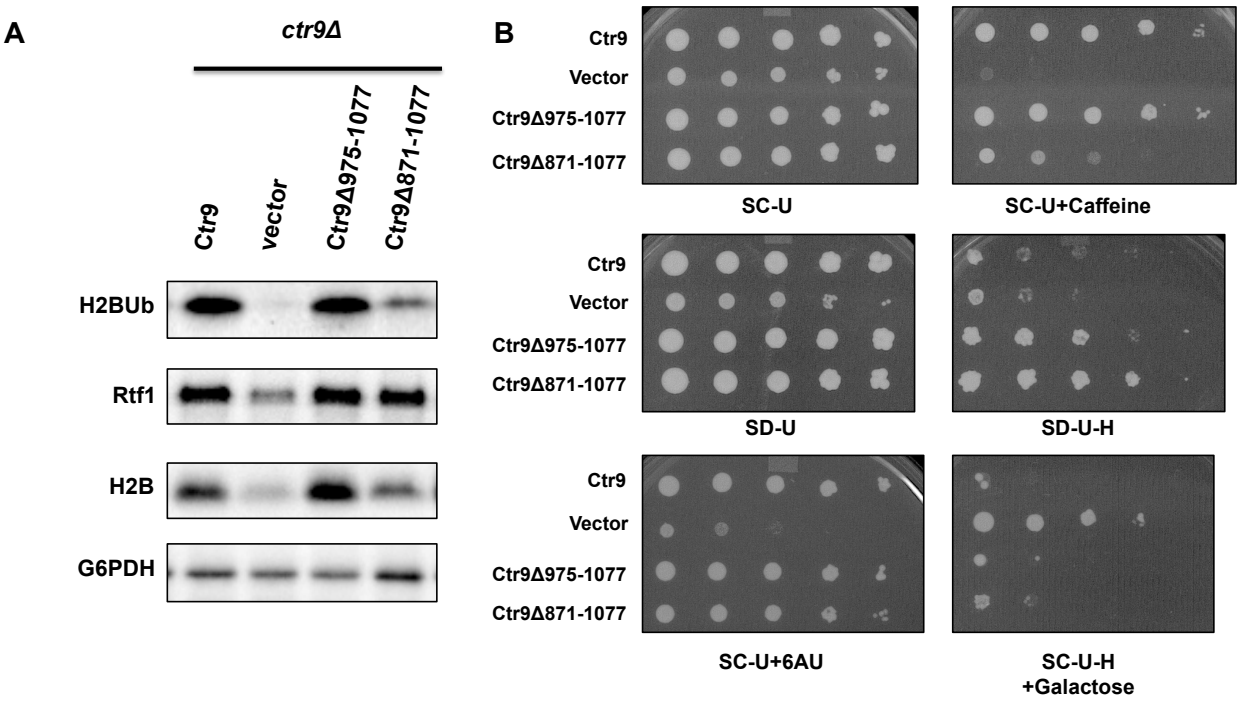

Figure 6: Ctr9 residues 871-974 are required for normal H2B ubiquitylation and resistance to caffeine.

(A) Western blot analysis was performed on a *ctr9Δ* strain transformed with *URA3*-marked plasmids expressing wild type, full-length Ctr9 or the indicated deletion mutants. The experiment was conducted using biological triplicates derived from independent transformants. (B) Two *ctr9Δ* strains were transformed with wild-type Ctr9, empty vector, or the indicated mutants, and tenfold serial dilutions were plated to growth control medium (SC-U or SD-U) or various test media to look for phenotypes indicative of transcriptional defects. Cells plated to SD-U-H are from a strain harboring the *his4-912δ* allele; growth on this medium is indicative of an Spt^- phenotype. Cells plated to SC-U-H+Galactose medium are from a strain in which the *FLO8* is under the control of a galactose-inducible promoter and is fused to the *HIS3* gene such that *HIS3* is in frame with a naturally occurring cryptic promoter within *FLO8* (Cheung, et al. 2008). The experiment was conducted using biological duplicates derived from independent transformants.

To further explore the function of the Ctr9 C-terminus, serial dilution assays were performed in order to assess transcription-related phenotypes in these mutants. Deletion of *CTR9* results in yeast cells that are unable to grow on medium containing caffeine, and interestingly, the same Ctr9 residues required for normal H2Bub are necessary for normal growth in the presence of caffeine (Figure 6B). Both mutants exhibited the Supressor of Ty (Spt^-) phenotype, as indicated by their ability to grow on medium lacking histidine in a strain where *HIS4* expression is disrupted by the insertion of the Ty-derived δ element in the 5' noncoding region of the gene (Winston, et al. 1984), even though cells lacking Ctr9 entirely show very little growth (Figure 6B, SD-U-H medium); however, the lack of a phenotype in the *ctr9Δ* strain is likely due at least in part to the fact that these cells are much sicker than either C-terminal mutant (data not shown). In contrast, neither mutant displayed sensitivity to the base analog 6-azauracil (6AU), nor was either mutant capable of growth on medium lacking histidine in a strain where the *HIS3* gene is transcribed from a galactose-inducible cryptic promoter (Figure 6B, SC-U-H+Galactose medium).

The Spt^- phenotype and defects leading to cryptic transcription within genes such as *FLO8* often result from the same mutations and can be indicative of changes in overall Pol II function (Cui, et al. 2016), while sensitivity to 6AU suggests a defect in transcription elongation (Shaw and Reines 2000). This indicates that the H2Bub defect specifically observed in the Ctr9Δ871-1077 mutant is likely not the result of a general defect in transcription. In contrast, the specific sensitivity of the Ctr9Δ871-1077 to caffeine mirrors the H2Bub defect observed in this mutant. The mechanisms underlying caffeine sensitivity in budding yeast are not fully understood but are thought to be the result of changes to certain signaling pathways, and mutants with defects in cell wall integrity are generally caffeine sensitive (Kuranda, et al. 2006).

It seems likely, then, that the role of Ctr9 residues 871-974 in regulating H2Bub represents a unique function of this region of the protein that is distinct from the well-characterized role of Ctr9 in regulating Pol II transcription.

2.3.2 Genetic analysis of the Rtf1 HMD

Several residues within the HMD are known to be required for H2Bub in budding yeast. An unbiased genetic screen identified the E104 residue as critical for HMD function, and subsequent analysis found that substitutions of E104 eliminated both H2Bub as well as its dependent methylation marks on H3 (Tomson, et al. 2011). Furthermore, these substitutions resulted in phenotypes indicative of transcriptional defects, including impaired silencing of a telomeric reporter, enhanced transcription from a normally cryptic promoter, and sensitivity to 6AU (Tomson, et al. 2011). This screen also revealed that substitutions of F123 largely phenocopy substitutions of E104, although the reduction in H3 K4 and K79 methylation is only partial, compared to the complete loss observed in E104 mutants (Tomson, et al. 2011). Additionally, three sets of alanine scanning mutations were made based on sequence conservation. Of these mutants, *rtf1-108-110A* and *rtf1-102-104A*, in which the critical E104 residue is mutated, are impaired in their ability to promote H2Bub and its dependentmodifications (Tomson, et al. 2011). In order to better understand the specific roles played by residues within the HMD, and to develop tools for *in vivo* and *in vitro* experiments, I set out to construct and characterize a larger collection of HMD mutants.

2.3.2.1 Multiple sequence alignment of Rtf1 orthologs reveals highly conserved residues within the HMD

In order to identify highly conserved residues within the HMD that are likely to be functionally important, I performed a multiple sequence alignment of 73 fungal Rtf1 species. Although our lab has previously published Rtf1 alignments examining a handful of model organisms (Warner, et al. 2007; Tomson, et al. 2011), no large alignment examining fungal Rtf1 proteins had previously been conducted. I focused my analysis on residues 74-184, as this larger HMD-containing domain was identified in an earlier bioinformatic analysis conducted by the VanDemark lab (Van Oss, et al. 2016).

Within these boundaries, there are three regions of high conservation, two of which fall within the boundaries of the minimal functional HMD (residues 63-152). The region spanning F80 to R110 contains many highly conserved residues; strikingly, R103, E104, and R110 are invariant among the species examined (Figure 7). There is also a small pocket of conservation spanning residues R147 to R151; R147 is found in 68/73 species, while R151 is present in 72/73 species. Finally, there is another region of moderately high conservation, roughly spanning residues L166 to K176; R173 is present in 70/73 species examined. While this region lies outside of the minimally functional HMD as defined by Piro et al., it remains possible that this region of Rtf1 modulates HMD function in the context of the full-length protein.

2.3.2.2 Analysis of H2B K123ub in HMD mutants

Dr. Adam Wier, a former member of the VanDemark lab, has solved the crystal structure of the minimal HMD_{74-139} construct. Mapping the degree of sequence identity among Rtf1 orthologs onto a surface representation of the HMD structure showed that many of the most conserved residues are surface exposed (Figure 8A). Guided by this evolutionary and structural data, I

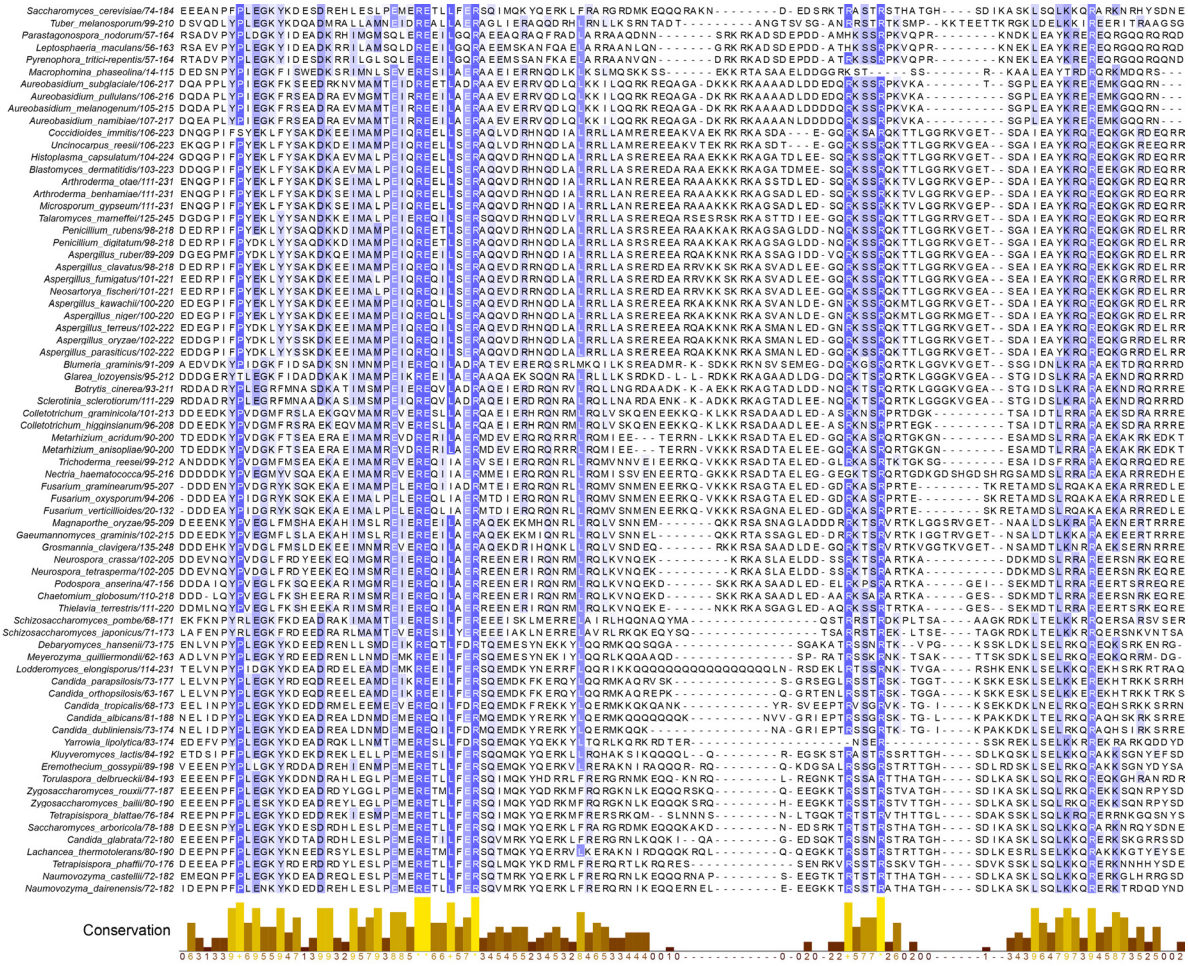

Figure 7: Multiple sequence alignment of Rtf1 orthologs reveals highly conserved residues within the HMD.

Multiple sequence alignment of 73 Rtf1 proteins from the *Ascomycota* phylum generated using Clustal Omega (Sievers, et al. 2011) and visualized via Jalview (Waterhouse, et al. 2009). The region of the protein corresponding to residues 74-184 in *S. cerevisiae* is shown; the amino acid boundaries for all other species are included with the species label. Darker blue indicates more highly conserved positions, which is also presented as a histogram (bottom).

performed extensive mutagenesis of *RTF1* and assessed the effects of substitutions within $HMD_{74\text{-}139}$ on bulk H2B K123ub levels. Substitutions E104A and R110E, as well as the previously identified E104K substitution, eliminated detectable H2B K123ub while substitutions D91A, E100A, L107A, F108A, R110A, Q115A, and R126A greatly reduced the mark ($p<0.05$) (Figures 8B-D). Initially, this analysis was performed on strains in which H2B bears a FLAG epitope; this strategy has conventionally been used to detect the modification by western blot due to the lack of a commercially available antibody that detects the mark in yeast. This analysis identified several substitutions that resulted in hyperubiquitylation of H2B (Figures 8B and 8C). However, our lab recently obtained an antibody that recognizes the modification directly and found that hyperubiquitylation as detected by the FLAG system was generally artifactual (Cucinotta, et al. 2015). I therefore repeated my analysis on a subset of mutants using a strain with untagged H2B and the commercial α-H2Bub antibody. Mutants with reduced H2Bub levels as identified by the FLAG system were also deficient as measured by the new antibody; however, those identified as hyperubiquitylated were generally indistinguishable from wild-type (Figure 8D and data not shown).

2.3.2.3 Analysis of H3 K4 and H3 K79 methylation in HMD mutants

In addition to examining H2Bub levels in these mutants, I also measured H3 $K4Me^2$, H3 $K4Me^3$ and H3 $K79Me^{2/3}$ levels in all mutants except for the S90 mutants (Figures 9A and 9B). Importantly, I observed that all HMD mutant proteins are normally expressed, with the exception of the E104K protein, which is expressed at about ~50% of wild-type levels, and the E100A and E102A proteins, which showed small (~20%) but statistically significant reductions in expression (Figures 9A and 9B). I observed a strong correlation between relative H2B

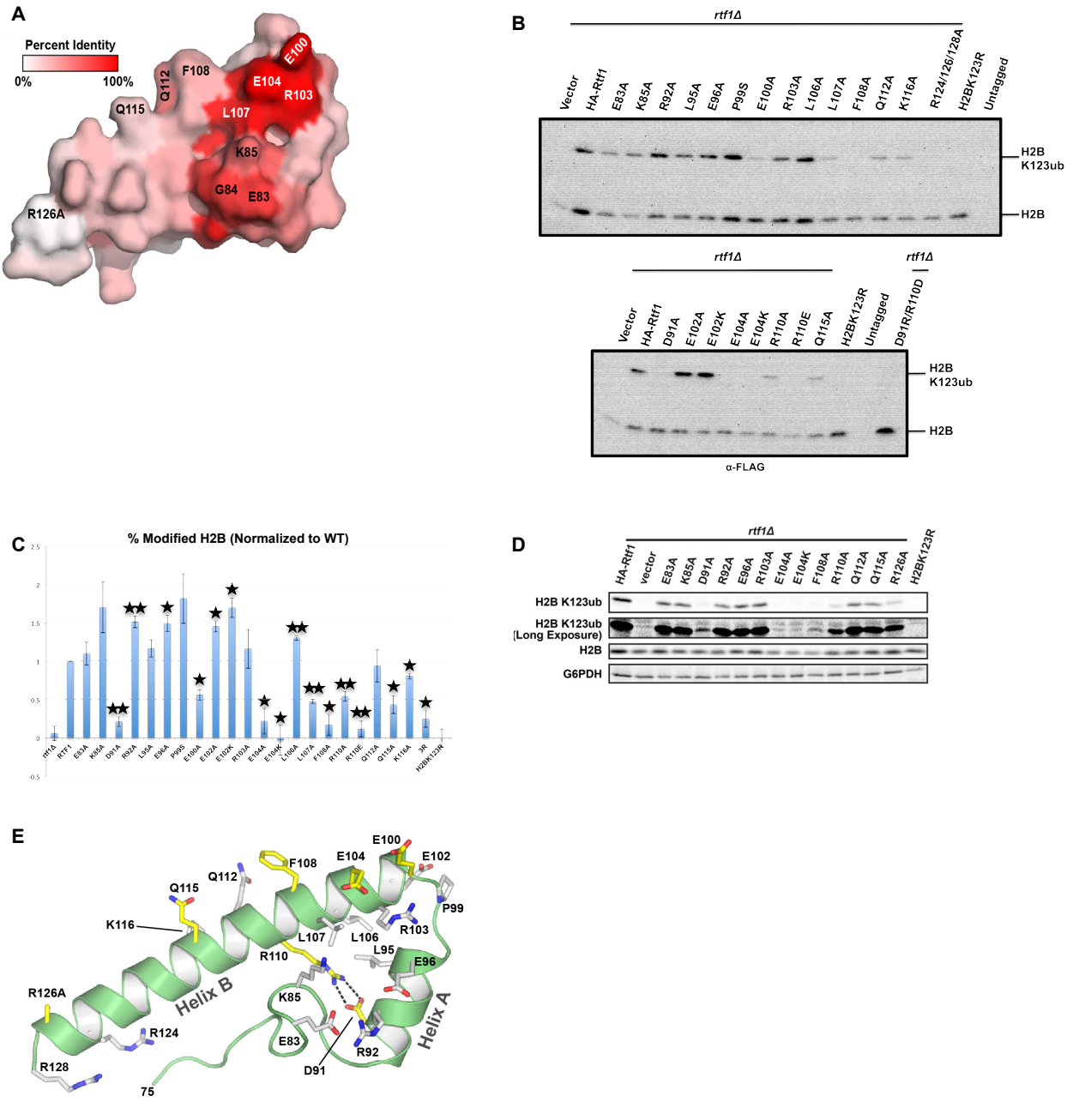

Figure 8: Identification of HMD residues required for H2B K123ub.

(A) Surface view of HMD_{74-139} with sequence identity among 74 fungal Rtf1 orthologs mapped onto the surface. Red indicates highest conservation. See Figure 7 for the associated alignment. This figure was made by Dr. Andrew VanDemark and is used with permission. (B) Anti-FLAG western blots were performed on an *rtf1Δ* strain in which both genomic copies of the genes encoding H2A and H2B have been deleted and a single copy of FLAG-tagged *HTA1-HTB1* is expressed on a plasmid. This strain was transformed with empty vector or plasmids

expressing wild-type, full-length HA-Rtf1 or full-length Rtf1 derivatives with the indicated substitutions in the HMD. Strains transformed with HA-Rtf1 in which the plasmid borne copy of *HTA1-HTB1* is untagged or carries the H2B K123R substitution serve as negative controls. Both unmodified H2B and the more slowly migrating H2B K123ub are detected by the antibody. (C) Quantitation of western blots shown in Panel B. Values represent the mean of 3-4 biological replicates. Error bars represent standard error of the mean. One star indicates a significant ($p<.05$) difference from wild type, and two stars indicates a highly significant ($p<.002$) difference. (D) Western blot analysis was performed on an *rtf1Δ* strain transformed with plasmids expressing wild type, full-length HA-Rtf1 or derivatives with the indicated substitutions within the HMD. The experiment was conducted using biological duplicates derived from independent transformants. (E) Ribbon diagram of HMD_{74-139}. Residues at which substitutions diminished (yellow) or did not diminish (white) H2B K123ub are indicated. Dashes indicate hydrogen bonds. This figure was made by Dr. Andrew VanDemark and is used with permission.

K123ub and both H3 K4Me^3 and H3 K79Me$^{2/3}$ levels, while H2B K123ub was less well correlated with H3 K4Me^2 (Figure 9C). In addition to the previously identified E104 residue, residues D91 and R110 seem to be most important for HMD function; in particular, the D91A and R110E mutants have very little detectable H3 K79Me$^{2/3}$, consistent with the fact that these mutants are the most severely impaired for H2Bub.

Five of the substitutions tested were also made in plasmids expressing HMD_{63-152} rather than full-length Rtf1 (Figure 9B). As with full-length Rtf1, the E104K substitution eliminated all detectable H3 K4 and H3 K79Me$^{2/3}$. Though the D91A substitution does not greatly affect expression of full-length Rtf1, making this substitution in HMD_{63-152} dramatically reduced expression and, consequently, both H3 K4 and H3 K79Me$^{2/3}$ were nearly undetectable.

Interestingly, in the context of the crystal structure, the D91 and R110 residues form a salt bridge. To investigate if these two residues are important for HMD function due to a role in maintaining its active conformation, as opposed to a role in mediating interactions with other

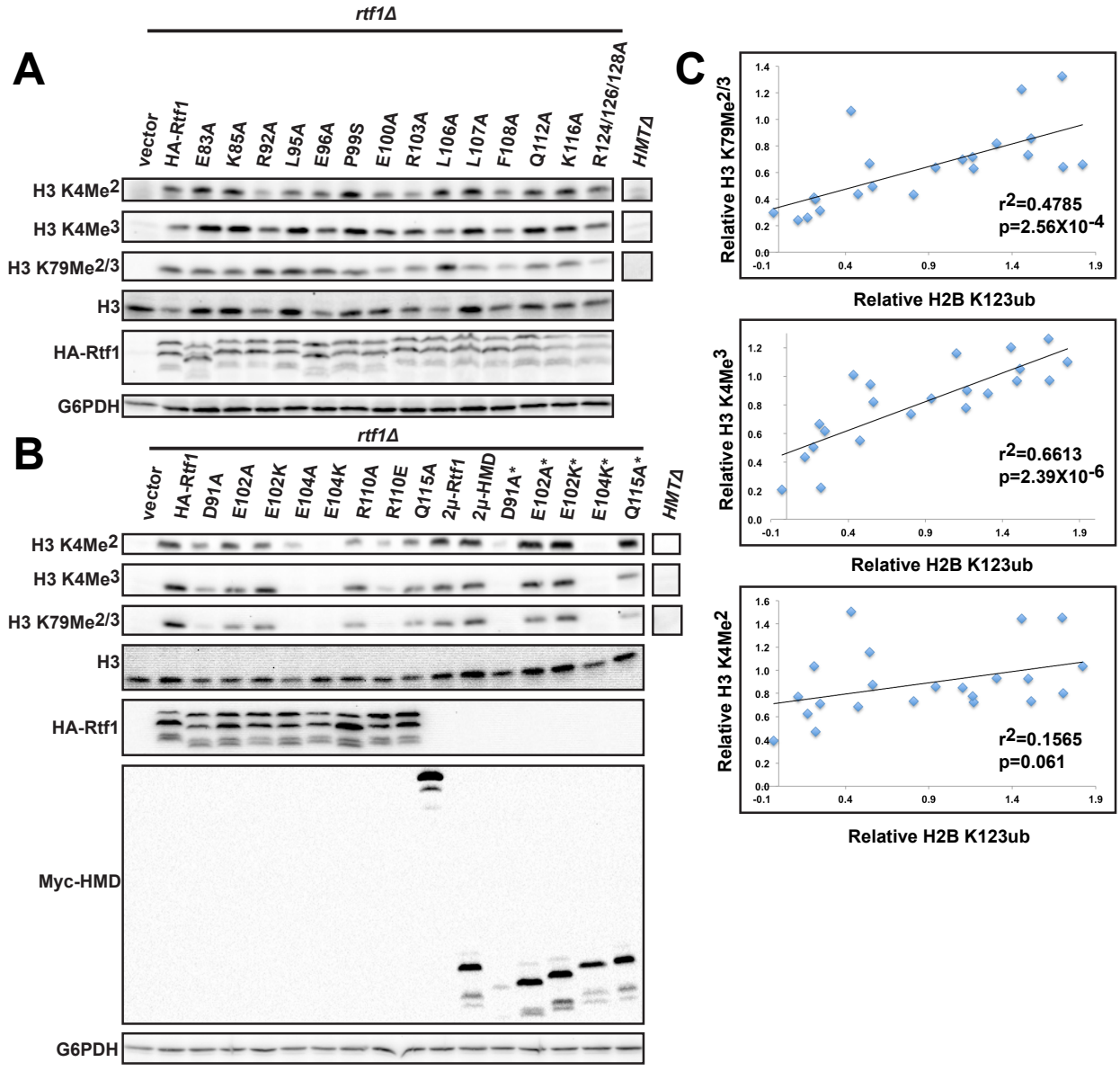

Figure 9: H2Bub defects in HMD mutants are correlated to defects in H3 K4 and H3 K79Me.

(A, B) Western blot analysis was performed on an *rtf1Δ* strain transformed with empty vector, or plasmids expressing wild type, full-length HA-Rtf1 or derivatives with the indicated substitutions within the HMD. In Panel B, an *rtf1Δ* strain was also transformed with a 2-micron plasmid overexpressing full-length Myc-Rtf1 or plasmids overexpressing wild type Myc-HMD$_{63\text{-}152}$ or derivatives with the indicated substitution (denoted with an asterisk). Strains in which the H3 K4 and K79 methyltransferases have been deleted (*HMTΔ; set1Δ* (H3 K4Me^2 and H3 K4Me^3 strips) and *dot1Δ* (H3 K79Me$^{2/3}$ strip)) serve as negative controls for the modifications tested and were run on the same gel. (C) Scatter plots showing correlation between relative H3 K79Me$^{2/3}$ (top), H3 K4Me^3 (middle), or

H3K4Me^2 (bottom) and H2B K123ub levels in *rtf1Δ* strains transformed with plasmids expressing 22 full-length HA-Rtf1 derivatives with amino acid substitutions in the HMD. H3 K79Me$^{2/3}$ and H3 K4Me^2 levels are normalized to total H3, and H2B K123ub levels represent percent H2B modified (H2B K123ub/total H2B), as determined by western blotting (see Figure 8C). Values are reported relative to wild type, which was set to one, and represent the mean of three biological replicates. Trendlines were generated by performing a standard linear regression.

molecules, I sought to reconstitute the salt bridge by making a D91R/R110D double mutant. This double mutant remained incapable of stimulating H2Bub, however (Figure 8B), and analysis of H3 K4 and H3 K79Me$^{2/3}$ showed that the double mutant was less active than either of the single mutants (data not shown).

2.3.2.4 Analysis of telomeric silencing in HMD mutants

H2Bub and its dependent H3 K4 and H3 K79Me marks are required for the silencing of a telomeric reporter gene, and an early report demonstrated that Rtf1 is also required for this silencing (Ng, Dole, et al. 2003). Subsequently, it was shown that overexpression of the HMD in *rtf1Δ* cells largely rescues this silencing defect (Wozniak and Strahl 2014). I therefore examined silencing in my HMD mutants, making use of a well-characterized reporter system (Singer, et al. 1998) in which *URA3* is expressed from a telomeric locus (note that our reporter is slightly different then that described by Singer et al. in that *URA3* is at a different telomeric locus). I found that the telomeric silencing phenotype is highly sensitive to H2Bub levels, as mutants defective for H2Bub are also defective for silencing (Figure 10). This phenotype is therefore a useful tool for genetic screens that seek to identify suppressors of mutations within the HMD. I also tested these mutants for sensitivity to 6AU, as well as for cryptic initiation and the Spt$^-$ phenotype, but saw little correlation to ubiquitylation defects observed in the HMD

mutants (data not shown). With respect to the cryptic initiation and Spt$^-$ phenotypes, however, this is likely due at least in part to technical issues related to expressing these mutants from plasmids, as integrated Rtf1-E104K and H2BK123R strains exhibit these phenotypes.

It should be noted that the general applicability of the reporter used to assess telomeric silencing in these studies was called into question by a study which found that deletion of the gene encoding Dot1, the H3 K79 methyltransferase, disrupted silencing at a relatively small number of telomeric loci (Takahashi, Schulze, et al. 2011). However, telomeric silencing is also dependent on H3 K4 methylation (Krogan, Dover, et al. 2002). Interestingly, a more recent study found that silencing of the reporter gene was also disrupted when both Bre1 and the HMD were overexpressed, a finding validated at two naturally silenced telomeric loci (Wozniak and Strahl 2014). Given that H2Bub is mislocalized to telomeric regions when the HMD is overexpressed outside of the context of Paf1C (Piro, et al. 2012; Van Oss, et al. 2016), this suggests that normal telomeric silencing may depend on both the presence of H2Bub at actively transcribed genes, and its absence at telomeres.

2.3.2.5 HMD function does not appear to be regulated by phosphorylation of S90

The *Saccharomyces* Genome Database (www.yeastgenome.org) contains data, derived primarily from high-throughput studies, which indicate sites of post-translational modifications. One residue within the HMD, S90, has been identified as a phosphorylation site. Although this site was identified in a study that used quantitative mass spectrometry to identify Cdk1 substrates (Holt, et al. 2009), the phosphoGRID database (https://phosphogrid.org/) identifies residues 90-93 as a Casein Kinase II motif. To examine whether phosphorylation of S90 might regulate the ubiquitylation activity of the HMD, I made an alanine substitution mutant at S90 as well as the phosphomimetic S90E substitution, and examined the ability of these mutant HMD

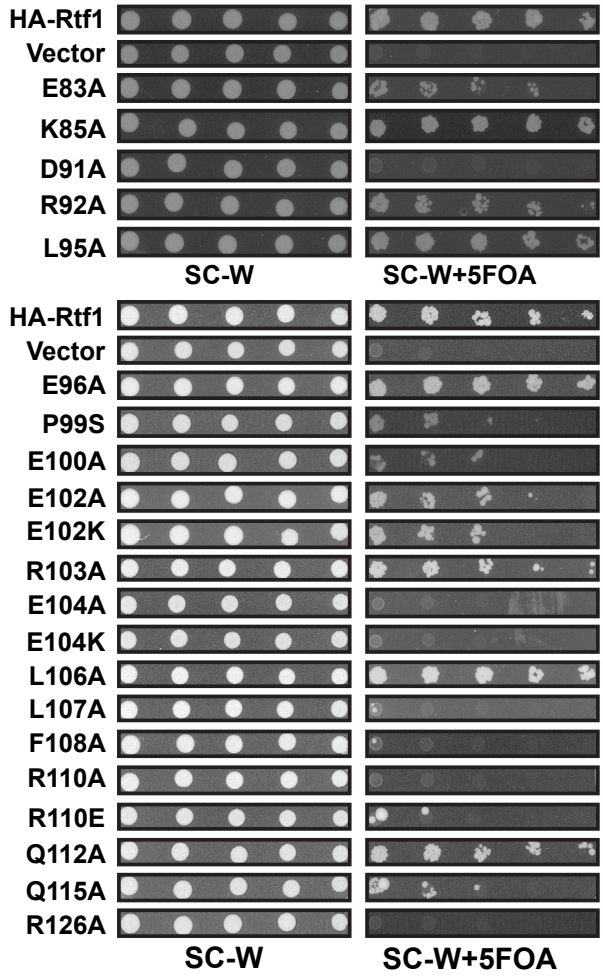

Figure 10: HMD residues required for normal H2Bub are also required for silencing of a telomeric reporter gene.

An *rtf1Δ* strain that contains the *URA3* gene at a telomeric locus (near *TEL-VR*) was transformed with empty vector or *TRP1*-marked plasmids expressing wild type, full-length HA-Rtf1 or full-length HA-Rtf1 derivatives with the indicated substitutions in the HMD. Twofold (top) or threefold (bottom) serial dilutions (leftmost spot: $1X10^8$ cells/mL) were plated to control medium (SC-tryptophan (W)) or to medium containing 5-fluoroorotic acid (5-FOA), which causes toxicity in strains expressing *URA3*, indicating a defect in telomeric silencing (Warner, et al. 2007). The experiment was conducted using a minimum of two biological replicates derived from independent transformants.

proteins to promote H2Bub. Both the S90A and the S90E mutants exhibited a ~50% reduction in H2Bub (Figure 11), indicating that, while this residue is important for HMD function, this function may not be regulated by phosphorylation.

2.3.3 A minimal HMD fragment promotes H2B K123ub in the absence of all Paf1C members

Based on sequence conservation (Figure 7) and domain mapping performed by Dr. Adam Wier (Van Oss, et al. 2016), and as a first step in obtaining structural data on the HMD, Dr. In-Ja Byeon in Dr. Angela Gronenborn's lab performed NMR on a larger HMD fragment containing residues 57-184. Preliminary assignments of this domain indicated the presence of a structured region containing residues 74-139, while residues 140-184 appeared poorly ordered (Van Oss, et al. 2016). I therefore asked whether a minimal 66-amino acid HMD construct, consisting only of residues 74-139 tagged with a Myc epitope and a nuclear localization sequence, was capable of promoting H2B K123ub. When expressed in an *rtf1Δ* background, both Myc-HMD_{63-152} and Myc-HMD_{74-139} restored global H2B K123ub to wild-type levels (Figure 12A). Remarkably, expression of either Myc-HMD_{74-139} or Myc-HMD_{63-152} in a quintuple deletion strain lacking all endogenous Paf1C genes also strongly rescued H2B K123ub levels (Figure 12B, compare lanes 4 and 6 with lane 1). Interestingly, full-length Myc-Rtf1 only weakly stimulated H2B K123ub in this context.

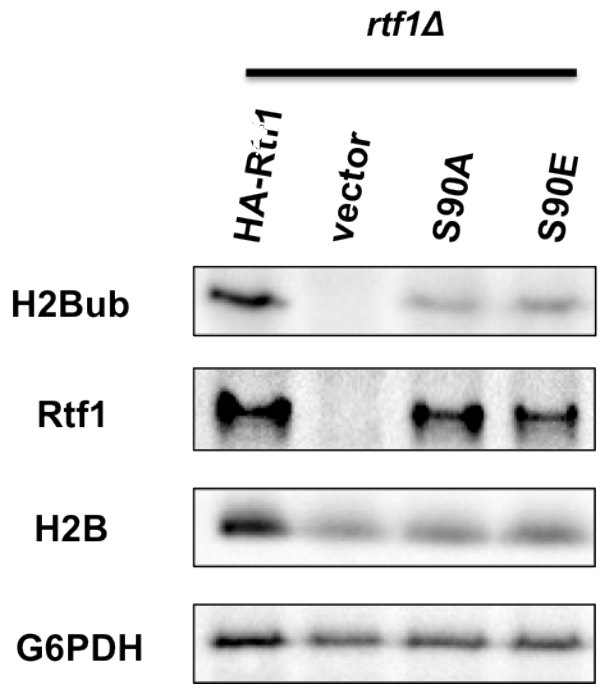

Figure 11: HMD function does not appear to be regulated by phosphorylation of S90.

Western blot analysis was performed on an *rtf1Δ* strain transformed with plasmids expressing wild-type, full-length HA-Rtf1 or derivatives with the indicated substitutions within the HMD. The experiment was conducted using biological triplicates derived from independent transformants.

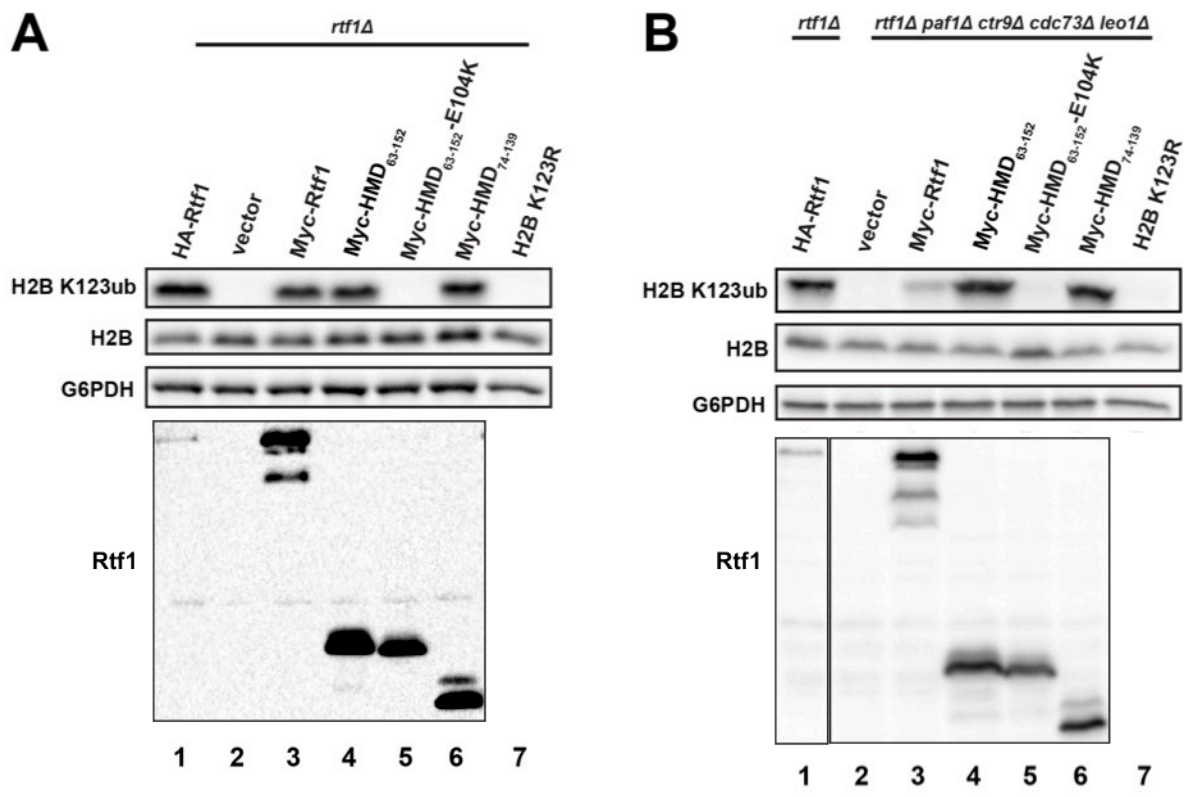

Figure 12: The HMD promotes H2Bub in the absence of all Paf1C subunits.

(A, B) Western blot analysis to detect the indicated proteins was performed on *rtf1Δ* (Panel A) and *rtf1Δ paf1Δ ctr9Δ cdc73Δ leo1Δ* strains (Panel B) transformed with empty vector, a low-copy plasmid expressing full-length HA-Rtf1, or high-copy plasmids expressing full-length Myc-Rtf1, wild type or mutant Myc-HMD_{63-152}, or Myc-HMD_{74-139}. An H2BK123R strain serves as a negative control. For Panel B, HA-Rtf1 transformed into an *rtf1Δ* strain was run on the same gel as the other samples. Both experiments were conducted using a minimum of three biological replicates derived from independent transformants.

2.3.4 The HMD stimulates H2Bub on chromatin

Previous studies in our lab indicated that a domain outside of the HMD, known as the open reading frame association region (OAR) and consisting of Rtf1 residues 201-395, directly interacts with the phosphorylated form of the Pol II-associated elongation factor Spt5 and is primarily responsible for the association of full-length Rtf1 with active chromatin (Warner, et al. 2007; Mayekar, et al. 2013; Wier, et al. 2013). Accordingly, an Rtf1ΔOAR mutant exhibits a dramatic reduction in H2Bub (Mayekar, et al. 2013). Nevertheless, when overexpressed and tethered to a nuclear localization signal, the HMD is able to associate with chromatin (Piro, et al. 2012). However, as the ability of the HMD to promote H2Bub had only been observed in the context of whole cell extracts, and given that the HMD likely does not associate with other Paf1C members, it remained possible that the HMD acted to ubiquitylate the pool of H2B that is not integrated into chromatin as part of the nucleosome. I therefore examined H2Bub levels from the chromatin fraction isolated by Dr. Margaret Shirra from *rtf1Δ* strains overexpressing HSV-HMD or HSV-Rtf1 from plasmids, as well as a strain endogenously expressing HA-Rtf1. I found that the ability of the HMD to restore H2Bub on chromatin was comparable to its ability to restore the mark globally (Figure 13). However, in contrast to Myc-HMD, the ability of HSV-HMD to promote H2Bub is substantially less than that of full-length HSV-Rtf1, both on chromatin and globally. This is likely an artifact of the epitope tag and explains the lack of robustness in ChIP signal from these strains (Van Oss, et al. 2016). Moving forward, it would be preferable to use Myc-HMD whenever possible.

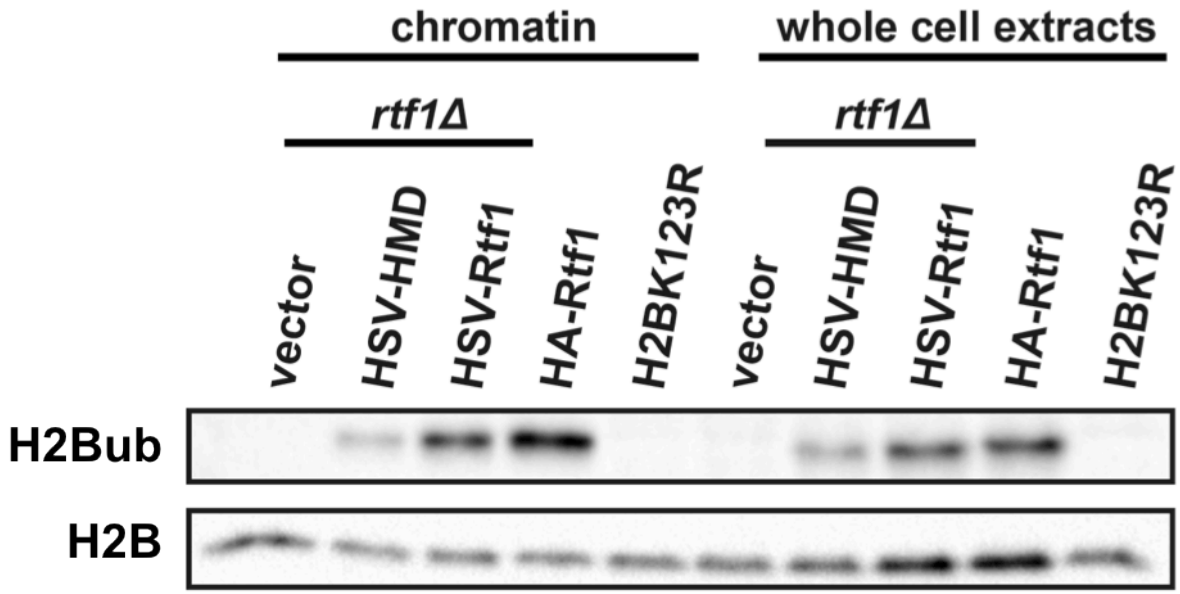

Figure 13: The HMD stimulates H2Bub on chromatin.

Western blot analysis was performed on chromatin fractions or whole cell extracts from an *rtf1Δ* strain expressing the indicated plasmids. A strain endogenously expressing HA-Rtf1 and an H2BK123R strain serve as positive and negative controls, respectively. The experiment was conducted using biological duplicates derived from independent transformants and two technical replicates.

2.3.5 Identification of HMD-associated proteins

To test the hypothesis that the HMD promotes H2Bub through a direct interaction with another protein, I used affinity purification followed by mass spectrometry analysis to identify proteins associated with the HMD *in vivo*. A TAP-tagged HMD_{63-152} derivative was used as the bait. In addition to an untagged control, I also purified the inactive HMD_{63-152} E104K mutant. A previous lab member, Anthony Piro, had conducted a similar experiment under native conditions; however, no copurifying proteins specific to the active HMD were detected. Because the relevant protein-protein interaction might be transient or low affinity, formaldehyde was added to the cells to crosslink associated proteins prior to immunoprecipitation. Purifications were conducted in biological triplicate, and following confirmation of specific and efficient immunoprecipitation of TAP-tagged constructs, samples were sent to Dr. Richard Gardner at the University of Washington for mass spectrometry analysis.

A filtering criteria based on peptide counts, the ratio of peptides for a given protein in the untagged samples to that in HMD-TAP samples, and *p*-value as determined by a Student's T-test resulted in a list of 27 "top hits." Gene Ontology (GO) analysis was performed on these 27 proteins. GO analysis by process revealed a highly significant ($p<.00005$) enrichment for genes involved in RNA processing, DNA-dependent transcription termination, and RNA metabolism. GO analysis by function revealed a highly significant enrichment for two related functions, RNA-dependent ATPase activity and RNA helicase activity. To enrich for genuine protein-protein interactions and reduce crosslinking mediated by RNA, the experiment was repeated with extracts treated with RNAse. There was considerable overlap between the two datasets. Using the same filtering criteria, 12 of the 27 proteins identified as top hits in the first

Table 3. Proteins associated with HMD_{63-152} *in vivo*.

Peptides were identified by tandem mass spectrometry of samples purified from an *rtf1Δ* strain expressing wild-type or mutant TAP-tagged HMD_{63-152} derivatives or an untagged control. The numbers shown for untagged, HMD-TAP, and E104K-TAP represent total peptide counts from three biological replicates. Data are shown for Rtf1 (bold) and the 12 proteins identified with high confidence in two independent experiments (values given are from the first experiment). No peptides were detected for the E2 and E3 enzymes Rad6 and Bre1 (red). Protein functions for most proteins are taken from the *Saccharomyces* genome database (www.yeastgenome.org).

Protein	Function	Untagged	HMD-TAP	HMD-E104K-TAP	Untagged/HMD-TAP	*p*-value
Rtf1	**Paf1C subunit, elongation factor, required for H2Bub**	**9**	**84**	**53**	**0.11**	**0.000**
Spt6	Histone chaperone	0	13	21	0.00	0.003
Dbp3	DExD/H-box RNA-dependent ATPase	0	9	5	0.00	0.040
Zpr1	Essential protein, involved in DNA replication stress response	0	8	14	0.00	0.016
Cbc1	Large subunit of nuclear mRNA cap-binding protein complex	0	7	4	0.00	0.002
Dst1	Elongation factor (TFIIS in higher organisms)	0	5	7	0.00	0.007
Sub2	DEAD-box RNA helicase, member of TREX mRNA export complex	1	26	27	0.04	0.012
Prp43	DEAH-box RNA helicase	1	11	17	0.09	0.002
Rfa1	DNA-binding protein involved in DNA replication, repair, recombination	1	11	8	0.09	0.011
Spt16	Essential subunit of FACT histone chaperone complex, promotes H2Bub	1	10	25	0.10	0.016
Has1	ATP-dependent RNA helicase, involved in ribosome biogenesis	1	9	13	0.11	0.016
Pus1	tRNA:pseudouridine synthase	1	9	12	0.11	0.001
Kap123	Member of nuclear pore complex, required for import of histones H3 and H4	1	8	9	0.13	0.035

Rad6	Ubiquitin conjugase (E2), partners with Bre1 to specifically monoubiquitylate H2B	0	0	0	N/A	N/A
Bre1	Ubiquitin ligase (E3), partners with Rad6 to specifically monoubiquitylate H2B	0	0	0	N/A	N/A`

Table 4: RNAse treatment reduces association of proteins with HMD_{63-152}

Peptides were identified by tandem mass spectrometry of samples purified from an *rtf1Δ* strain expressing a wild-type, TAP-tagged HMD_{63-152} derivative or an untagged control. The numbers shown represent total peptide counts from three biological replicates. Data are shown for Rtf1 (bold) and the 12 proteins identified with high confidence in two independent experiments (values given are for the second experiment), and the E2 and E3 enzymes Rad6 and Bre1 (red).

Protein	Untagged	HMD-TAP	Untagged + RNase	HMD-TAP + RNase
Rtf1	**7**	**53**	**4**	**35**
Spt6	2	59	0	23
Dbp3	0	53	0	23
Zpr1	1	33	1	16
Cbc1	0	30	1	8
Dst1	0	22	0	12
Sub2	11	80	7	51
Prp43	1	48	1	23
Rfa1	0	44	0	22
Spt16	7	104	12	57
Has1	0	40	0	18
Pus1	0	23	1	26
Kap123	4	39	2	9
Rad6	0	0	0	0
Bre1	0	6	0	8

experiment were detected in the second experiment (Tables 3 and 4). The total number of peptides detected for most proteins decreased substantially upon RNAse treatment (Table 4). Furthermore, the majority of peptides detected in RNAse-treated samples were found in a single sample (data not shown), suggesting that RNAse treatment in this sample may have been inefficient and that the reduction in peptides observed upon RNAse treatment may be an underestimate.

Although the data from these experiments were robust and largely reproducible, none of the top hits identified in the first experiment exhibited reduced association with the inactive HMD-E104K mutant. In the first experiment, no peptides were detected for the E2 and E3 proteins Rad6 and Bre1 (Table 3). In the second experiment, no Rad6 peptides were detected, while six Bre1 peptides were detected in the TAP-tagged, untreated sample and eight Bre1 peptides were detected in the TAP-tagged, RNAse-treated sample, compared to none in the untagged samples (Table 4). Though top hits Spt6, Spt16, and Dst1 (TFIIS in mammals) have known connections to Paf1C (Squazzo, et al. 2002; Kim, et al. 2010; Mayekar, et al. 2013; Dronamraju and Strahl 2014), only Spt16 mutants are known to have an H2Bub defect (Fleming, et al. 2008). Given the cooperative relationship between human Paf1C and TFIIS in promoting transcription elongation (Kim, et al. 2010), I examined global H2Bub levels in yeast in a *dst1Δ* strain and found that they were indistinguishable from wild type (Figure 14A). To ask whether any of the other proteins identified as HMD-associated might be functionally connected to Rtf1 and/or Paf1C, I made use of a measurement known as evolutionary rate covariation (ERC). ERC utilizes the observation that proteins that experience a similar acceleration or deceleration to the rate of changes in their primary sequence over a given evolutionary timeframe are more likely to be physically interacting and/or functionally related (Clark, et al.

2012). ERC values between two proteins are reported as a correlation coefficient, with +1 indicating the maximum possible correlation between two proteins.

I therefore examined ERC values between Rtf1 and the 12 proteins I identified with high confidence as Rtf1-associated. Rtf1 showed high ERC values with Spt6, Spt16, and Dst1, consistent with previously identified physical and functional interactions between these proteins and Paf1C. Amongst the 9 other proteins identified for which no functional relationship to Rtf1 is known, two proteins, Sub2 and Kap123, stood out as having particularly high ERC values (Figure 14B). I therefore examined ERC between these two proteins and each Paf1C member, and found high ERC between both proteins and each Paf1C subunit (Figures 9C and 9D). Thus, while the fact that these two proteins still associate with the inactive HMD-E104K mutant suggests that they may not be important for HMD-mediated H2Bub, it is nevertheless possible that there are functional connections between these proteins and Paf1C that are yet to be elucidated (see Section 2.4).

Because of the large number of proteins that copurified with the HMD, I decided to repeat the experiment without formaldehyde crosslinking. Although a similar experiment had been conducted previously by Anthony Piro, the efficiency of the immunoprecipitation, as measured by the number of Rtf1 peptides detected, was low. I was able to immunoprecipitate the HMD_{63-152}-TAP and HMD_{63-152}-E104K-TAP proteins efficiently under native conditions (data not shown). However, silver staining of the eluate revealed a large number of copurifying proteins, despite the fact that no crosslinker was used (Figure 15). We therefore turned to other methods to identify protein-protein interactions with the HMD.

A

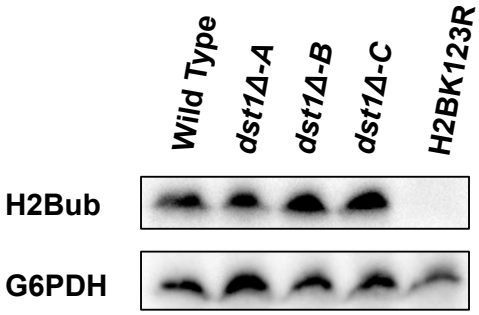

B

	RTF1	SPT16	SPT6	DBP3	ZPR1	DST1	SUB2	PRP43	RFA1	HAS1	PUS1	KAP123
RTF1	N/A	0.575	0.810	-0.268	-0.143	0.442	0.592	0.308	0.326	-0.182	0.226	0.759
SPT16	0.575	N/A	0.796	-0.197	-0.333	0.339	0.401	0.271	0.186	-0.030	-0.053	0.612
SPT6	0.810	0.796	N/A	-0.432	-0.262	0.620	0.609	0.121	0.239	-0.150	0.106	0.739
DBP3	-0.268	-0.197	-0.432	N/A	-0.016	-0.748	-0.469	0.509	-0.005	0.473	0.074	-0.300
ZPR1	-0.143	-0.333	-0.262	-0.016	N/A	0.069	0.083	-0.034	0.108	0.041	0.254	-0.147
DST1	0.442	0.339	0.620	-0.748	0.069	N/A	0.613	-0.417	-0.008	-0.356	0.031	0.409
SUB2	0.592	0.401	0.609	-0.469	0.083	0.613	N/A	-0.047	-0.025	-0.308	-0.038	0.408
PRP43	0.308	0.271	0.121	0.509	-0.034	-0.417	-0.047	N/A	0.060	0.092	0.012	0.086
RFA1	0.326	0.186	0.239	-0.005	0.108	-0.008	-0.025	0.060	N/A	0.306	0.636	0.651
HAS1	-0.182	-0.030	-0.150	0.473	0.041	-0.356	-0.308	0.092	0.306	N/A	0.137	-0.020
PUS1	0.226	-0.053	0.106	0.074	0.254	0.031	-0.038	0.012	0.636	0.137	N/A	0.427
KAP123	0.759	0.612	0.739	-0.300	-0.147	0.409	0.408	0.086	0.651	-0.020	0.427	N/A

C

	RTF1	PAF1	CTR9	LEO1	CDC73	KAP123
RTF1	N/A	0.550	0.349	0.413	0.485	0.759
PAF1	0.550	N/A	0.407	0.631	0.668	0.536
CTR9	0.349	0.407	N/A	0.272	0.428	0.386
LEO1	0.413	0.631	0.272	N/A	0.659	0.409
CDC73	0.485	0.668	0.428	0.659	N/A	0.473
KAP123	0.759	0.536	0.386	0.409	0.473	N/A

D

	RTF1	PAF1	CTR9	LEO1	CDC73	SUB2
RTF1	N/A	0.550	0.349	0.413	0.485	0.592
PAF1	0.550	N/A	0.407	0.631	0.668	0.471
CTR9	0.349	0.407	N/A	0.272	0.428	0.637
LEO1	0.413	0.631	0.272	N/A	0.659	0.292
CDC73	0.485	0.668	0.428	0.659	N/A	0.476
SUB2	0.592	0.471	0.637	0.292	0.476	N/A

Figure 14: *In vivo* and bioinformatic analysis of HMD-associated proteins

(A) Western blot analysis of global H2Bub levels in 3 biological replicates of a *dst1Δ* strain. (B) Evolutionary rate covariation (ERC) group analysis of *RTF1* and high-confidence Rtf1-associated proteins. Proteins that exhibit high ERC are shown in red. (C-D) ERC group analysis of Paf1C and *KAP123* (C) and *SUB2* (D). The web tool used to generate these data was designed by Dr. Nathan Clark and colleagues (Wolfe and Clark 2015).

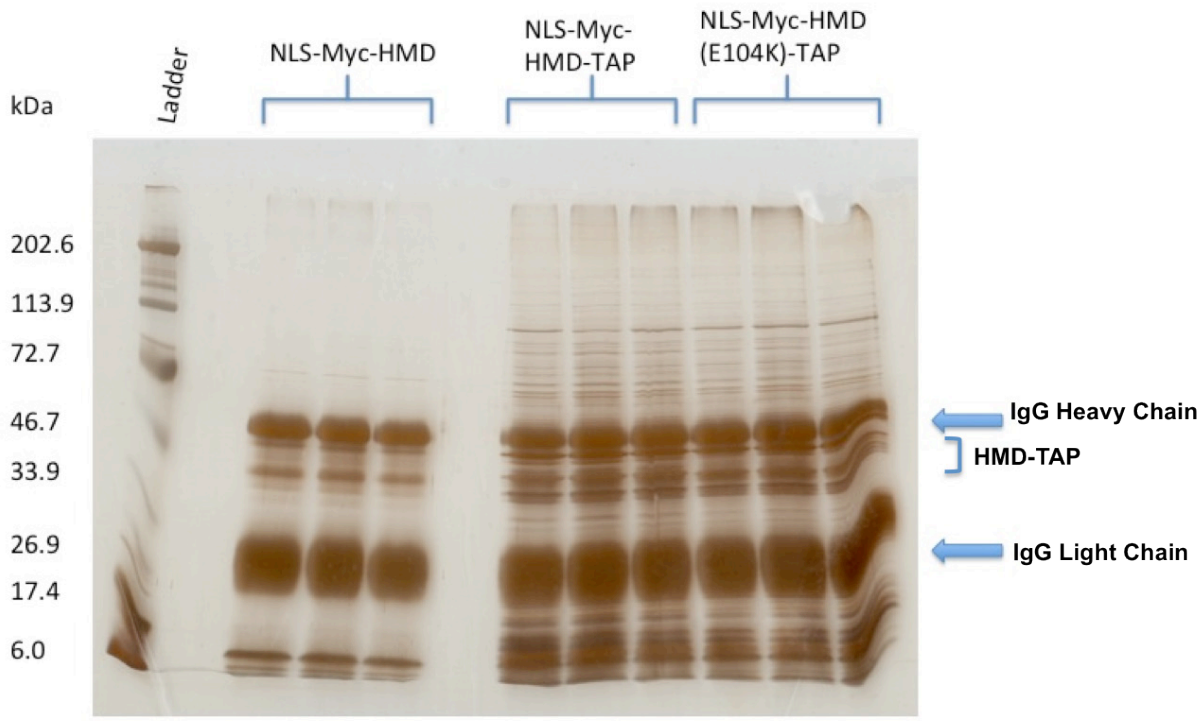

Figure 15: Many proteins copurfiy with the HMD even under native conditions

Silver stained gel showing the eluate from affinity purifications of the indicated constructs, conducted in biological triplicate. IgG heavy and light chain are released from the agarose beads during the elution step. Samples represent biological triplicates derived from three independent transformants.

2.3.6 Rtf1 directly interacts with the ubiquitin conjugase Rad6 through the HMD

Informed by the results of my genetic analysis, Dr. Margaret Shirra employed an *in vivo* crosslinking strategy that makes use of the non-natural, photo-reactive phenylalanine analog *p*-benzoyl-L-phenylalanine (BPA). When grown in the presence of BPA, cells carrying a plasmid expressing an engineered aminoacyl-tRNA synthetase and a tRNA that recognizes the amber (UAG) codon will incorporate BPA into the elongating polypeptide chain by amber suppression (Chin, et al. 2003). Dr. Shirra mutagenized plasmids expressing either full-length HSV-Rtf1 or HSV-HMD$_{63\text{-}152}$, changing a single codon within the HMD to an amber codon at sites that, when mutated, did not impair the HMD's ability to promote H2Bub but were near residues that were critical for this function. One exception was F108. Although the F108A substitution nearly abolishes H2B K123ub, we reasoned that incorporation of a phenylalanine analog at this location might restore function. Indeed, Dr. Shirra found that these BPA-containing proteins, including the F108 derivative, are able to promote H2B K123ub-dependent histone modifications (Van Oss, et al. 2016).

When exposed to long-wave UV light, proteins containing BPA form crosslinks with a short linker distance to the side chains of nearby amino acids (Dormán and Prestwich 1994), leading to the identification of proteins that are in direct physical contact. To determine the identity of proteins crosslinked to the HMD, Dr. Shirra focused on components of the H2B K123ub pathway. One enticing candidate was Rad6, the E2 that catalyzes H2B K123ub in cooperation with the E3 Bre1. Dr. Shirra therefore asked if the HMD interacts directly with Rad6 by performing *in vivo* BPA crosslinking experiments with all 14 of our plasmid-encoded HSV-Rtf1 and HSV-HMD$_{63\text{-}152}$ derivatives in an *rtf1Δ RAD6-13xMyc* genetic background.

Probing for Myc revealed a slower migrating band that was present exclusively in HSV-Rtf1 and HSV-HMD_{63-152} derivatives where BPA was incorporated in place of T105, F108, or Q112 (Figures 16A and 16B). This band was not detected when Rad6 was untagged or when the inactivating E104K substitution was introduced into the HSV-Rtf1 derivatives that contained BPA at positions 108 or 112 (Figure 16A). The specific detection of this band in both the full-length and HMD-only constructs under conditions of BPA crosslinking at the same three residues, and not in the E104K mutant context, strongly suggests that Rtf1 directly contacts Rad6 through the HMD and that this interaction is required for the establishment of H2Bub.

To test if the Rtf1-Rad6 interaction is dependent on Bre1, Dr. Shirra performed BPA crosslinking experiments with an *rtf1Δ bre1Δ RAD6-13xMyc* strain and the same HSV-Rtf1 and HSV-HMD_{63-152} BPA derivatives where crosslinking to Rad6 was observed. Interestingly, for the HMD_{63-152} BPA derivatives, we found that the extent of crosslinking to Rad6 was unaffected by the absence of Bre1 (Figure 16C). For the full-length Rtf1 BPA derivatives, we observed a substantial reduction in the level of the crosslinked species, which may suggest that regions in Rtf1 outside the HMD impose a requirement for Bre1 in facilitating the interaction with Rad6, although this interpretation is somewhat complicated by the partial reduction in Rtf1 levels in strains lacking Bre1 (Figure 16D).

2.3.7 Attempts to detect the HMD-Rad6 interaction by alternative methods

The HMD-Rad6 interaction as detected by Dr. Shirra's BPA experiments is quite convincing, given the dependence on both BPA and the E104 residue, and the fact that the interaction was detected at the same locations in both the full-length and HMD-only BPA derivatives. Nevertheless, I did not detect any Rad6 or Bre1 peptides for any of the samples in either mass

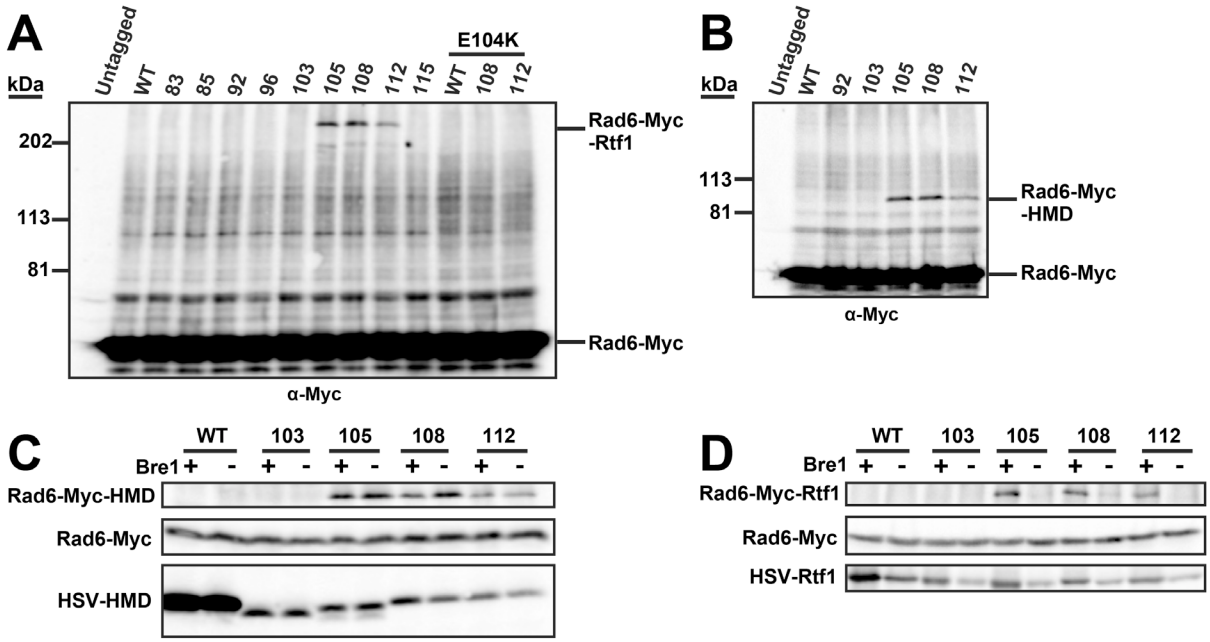

Figure 16: The HMD directly interacts with the ubiquitin conjugase Rad6.

(A-D) These experiments were performed by Dr. Margaret Shirra. All experiments were conducted using a minimum of two biological replicates derived from independent transformants. (A,B) Western blot analysis of an *rtf1Δ RAD6-13XMyc* strain transformed with pLH157/HIS3 and plasmids expressing WT HSV-Rtf1 (Panel A) or HSV-$HMD_{63\text{-}152}$ (Panel B), or their respective derivatives in which BPA is incorporated at the indicated position. In Panel A, indicated plasmids also contain the inactivating E104K substitution. All samples were grown in the presence of BPA and exposed to UV light. (C,D) Western blot analysis was performed with samples processed as in (A) and (B), with the indicated HSV-$HMD_{63\text{-}152}$ (Panel C) or HSV-Rtf1 (Panel D) derivatives expressed in an *rtf1Δ RAD6-13XMyc* strain or an *rtf1Δ bre1Δ RAD6-13XMyc* strain. Top row shows crosslinked species.

spectrometry experiment that I conducted (Tables 3 and 4). Given the high sensitivity of western blot analysis, I asked whether the interaction could be detected by a directed coimmunoprecipitation under native conditions. As an alternative approach to my mass spectrometry experiments, which used HMD_{63-152} as the "bait" protein, I also used full-length Rtf1 as the bait, and designed a plasmid expressing Rtf1 with sequence encoding residues 63-152 deleted. This approach thus asked whether the HMD was necessary for the interaction between Rtf1 and Rad6. However, although I successfully and efficiently immunoprecipitated all three TAP-tagged proteins, no Rad6 was detected in the bound fraction of any sample (Figure 17).

I next sought to determine if I could detect the HMD-Rad6 interaction *in vitro*, using purified components and the BS^3 crosslinker. However, upon the addition of BS^3, HMD_{74-139} formed multimers (Figure 18, reaction 1), and no unique species indicative of an HMD-Rad6 heterodimer were observed upon addition of Rad6 (Figure 18, reactions 2 and 3). After observing *in vitro* activity for a larger, HMD_{74-184} construct, and not for HMD_{74-139} (see Section 3.3.1), I sought to detect the HMD-Rad6 interaction by far western, using wild-type and mutant HMD_{74-184} as the "bait" protein. However, although I was able to detect the well-characterized Rock-Shroom interaction, which served as a positive control, no interaction between HMD_{74-184} and Rad6 was detected by this method (Figure 19).

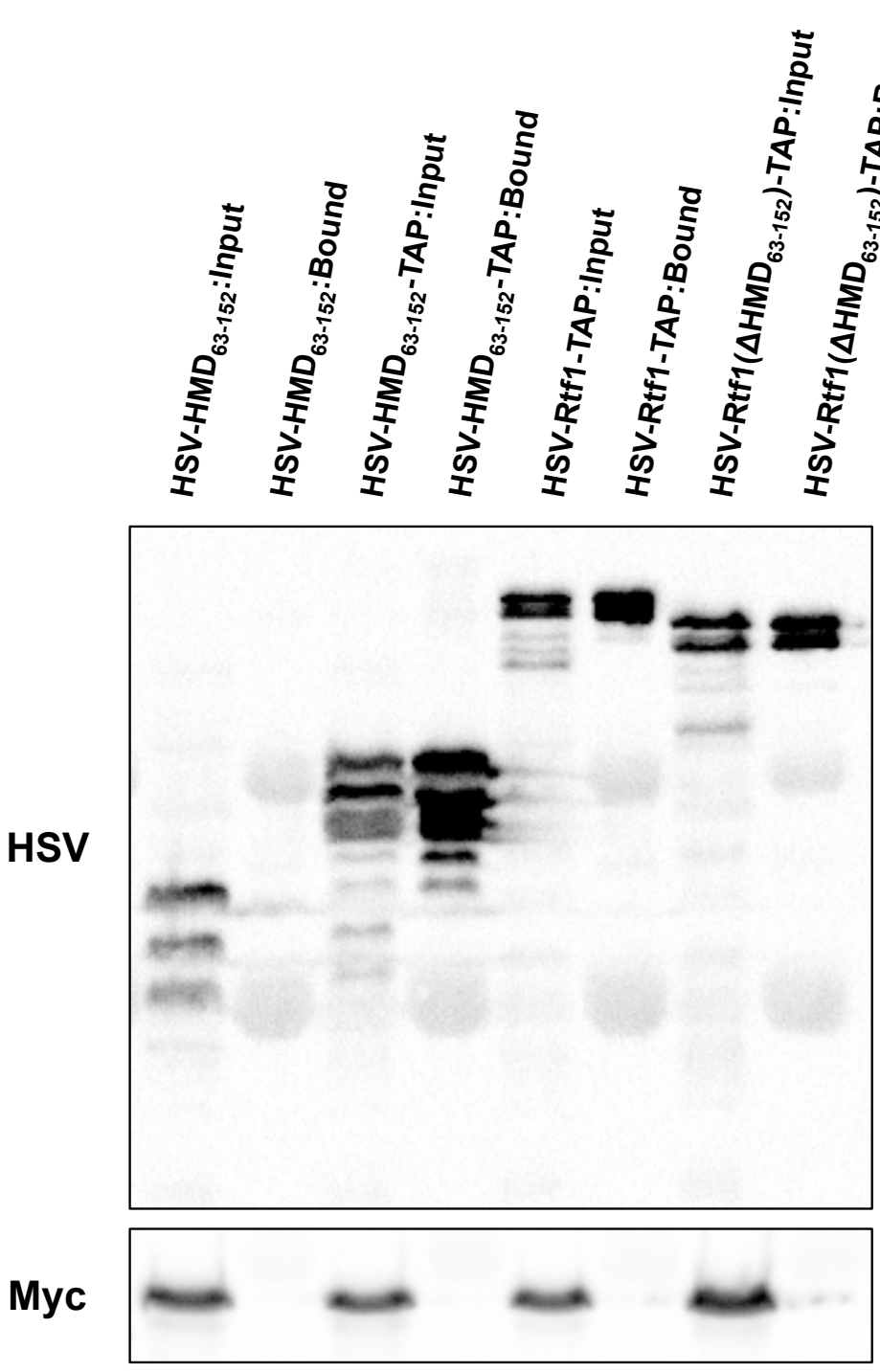

Figure 17: The HMD-Rad6 interaction cannot be detected by *in vivo* coimmunoprecipitation.

Western blot analysis of input and bound fractions following affinity purification with IgG agarose beads. Samples are from an *rtf1Δ* strain, transformed with the indicated plasmids, in which Rad6 is tagged with the Myc epitope. Probing for HSV shows the specificity and efficiency of the purification.

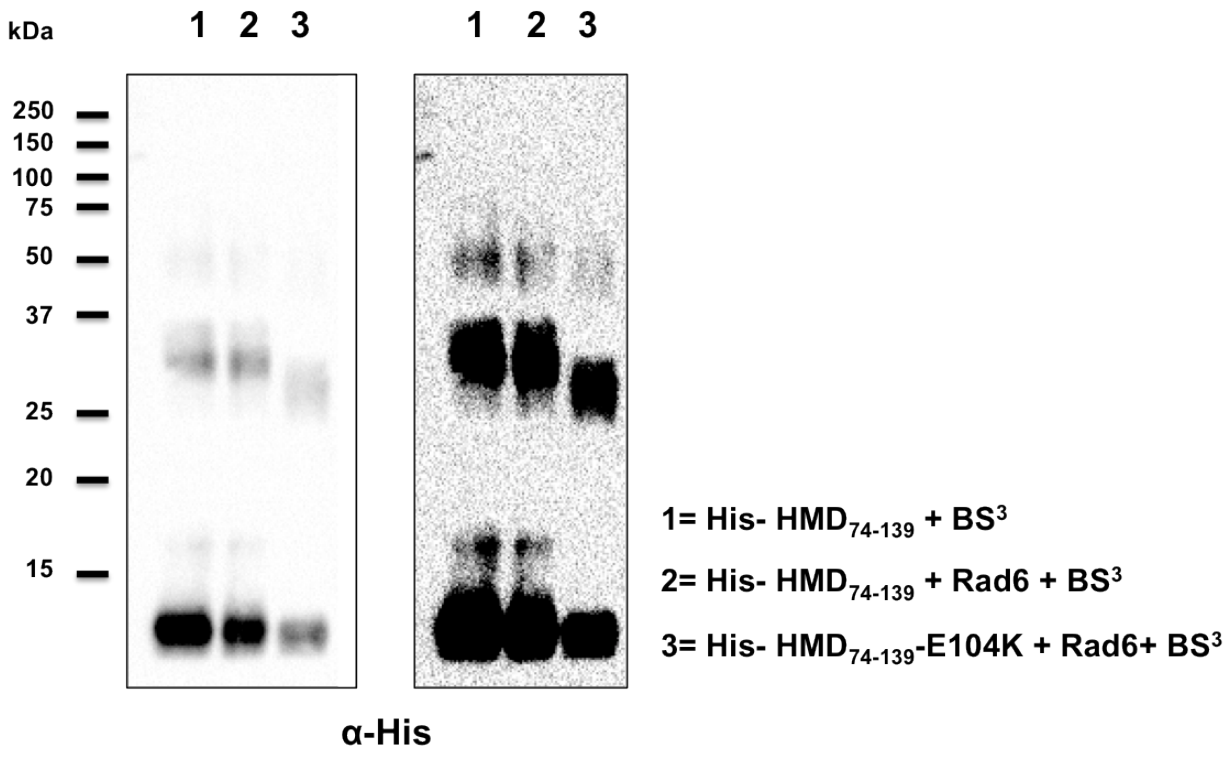

Figure 18: The HMD-Rad6 interaction cannot be detected by *in vitro* crosslinking.

The indicated proteins were mixed with BS^3 under crosslinking conditions. After crosslinking was quenched, HMD-containing species were detected by anti-His western blot.

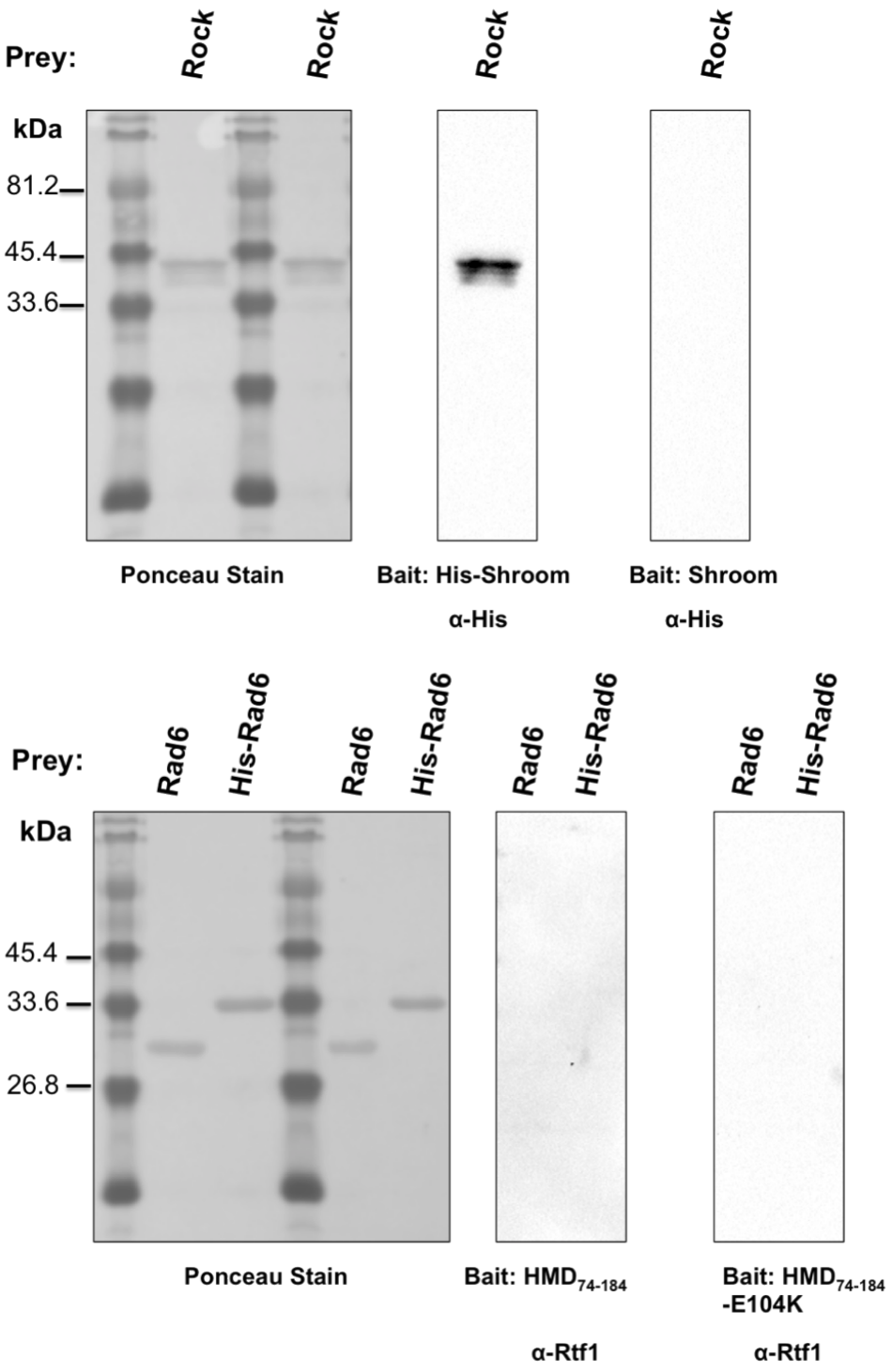

Figure 19: The HMD-Rad6 interaction cannot be detected by far western blotting.

Far western analysis was performed using the indicated proteins and antibodies. The Rock-Shroom interaction is a well-characterized, high affinity interaction (Mohan, et al. 2012) and serves as a positive control.

.

2.4 DISCUSSION

Previous studies demonstrated a conserved requirement for Paf1C in promoting H2Bub *in vivo*, but the mechanism underlying this requirement has remained largely unexplored. Several data in this chapter suggest that Paf1C regulation of H2Bub occurs primarily through the HMD. First, Rtf1 is the only subunit strictly required for the detection of H2B K123ub in *Saccharomyces cerevisiae* (Figure 5). Furthermore, when overexpressed, the HMD is capable of restoring wild-type levels of H2Bub even when all Paf1C subunits are deleted (Figure 12B). Finally, the direct interaction between the HMD and Rad6 detected in Dr. Shirra's BPA experiments (Figure 16) is suggestive of a direct role in promoting the deposition of the mark.

Nevertheless, evidence presented in this chapter also suggests that other Paf1C subunits, namely Paf1 and Ctr9, have a role in promoting H2Bub beyond stabilization of Rtf1 at the protein level. Though *paf1Δ* and *ctr9Δ* strains have very little H2Bub, Rtf1 levels are only partially reduced (Figure 5). Furthermore, even when overexpressed, full-length Rtf1 only weakly restores H2Bub in a strain where all Paf1C subunits are deleted, while the HMD restores wild-type levels of the mark in this context. These results speak to the possibility of an intrinsically inhibitory domain within Rtf1, housed outside of the HMD, that is normally counteracted by Paf1 and/or Ctr9. Consistent with this, I identified a domain within Ctr9, consisting of residues 871-974, that is required for H2Bub but is largely dispensable for Rtf1 stability (Figure 6A). Finally, although I did not identify a role for the Cdc73 and Leo1 in promoting H2Bub, others have shown a dramatic reduction in the mark upon deletion or depletion of these subunits. This suggests that, as has been found for other Paf1C-related phenotypes (see Chapter 1), the specific mechanisms of Paf1C regulation of H2Bub may be

dependent on genetic and/or physiological context, despite the conserved requirement for the HMD

Using BPA crosslinking, Dr. Shirra detected a direct interaction between Rad6 and a conserved, surface-exposed region of the HMD that contains residues essential for HMD function *in vivo* (Figures 8 and 9). Importantly, this interaction is dependent on the Rtf1 E104 residue, an amino acid that is essential for Rtf1's role in promoting H2B K123ub and is invariant across 73 fungal species (Figure 7). My inability to reproducibly detect an HMD-Rad6 interaction with unbiased affinity purification-mass spectrometry methods (Tables 3 and 4), or by a directed coimmunoprecipitation (Figure 17), suggests that this interaction is dynamic and/or low-affinity. Consistent with this, only a very small proportion of endogenously expressed Rad6 crosslinks to the HMD (Figures 16A and 16B).

I was also unable to detect the HMD-Rad6 interaction by *in vitro* crosslinking with purified components or by far western analysis. In these experiments, one might conjecture that the high concentrations of both proteins would overcome the hypothesized low affinity of the HMD-Rad6 interaction. Crosslinking of the HMD to itself, however, suggests that the HMD more readily forms self multimers than HMD-Rad6 heterodimers under these conditions. Consistent with this, Dr. Shirra has detected Rtf1-Rtf1 interactions in her *in vivo* BPA crosslinking experiments. Additionally, recently obtained, unpublished data from our lab suggests that a stable HMD-Rad6 interaction may require the presence of other factors, such as the nucleosome and/or other components of the ubiquitylation reaction. *In vivo* BPA experiments conducted by Christine Cucinotta show that Rtf1 directly interacts with the nucleosome acidic patch. Furthermore, preliminary data from experiments conducted by Donya Shodja and Brendan McShane appears to show *in vitro* BPA crosslinking of Rad6 to the HMD

when all components of the ubiquitylation reaction are present, and not when only Rad6 and the HMD are present.

Of the HMD mutants identified in my genetic analysis as being critical for H2Bub and telomeric silencing, E104, F108, and R110 are all housed within a conserved surface that represents the putative interface between the HMD and Rad6 (Van Oss, et al. 2016). However, H2Bub and telomeric silencing are also greatly diminished in the D91A and R126A mutants, which fall outside of this interface (Figures 8 and 10). Given that the D91A substitution nearly abolishes HMD expression when made in the context of HMD_{63-152}, this residue may be critical for promoting or maintaining proper folding of the HMD. Though an attempt to counteract this substitution with a compensatory mutation in R110 did not restore H2Bub (Figure 8B), discussions following previous presentation of this work suggested that such mutations do not always restore salt bridges. In contrast, the R126A mutation has no apparent effect on Rtf1 stability or fold. It may be that this residue mediates contacts with the nucleosome acidic patch, as Christine Cucinotta has shown that the region of Rtf1 containing R126 is required for the Rtf1-H2A interaction, or that it is involved in DNA binding (see Section 3.3.4).

Finally, my affinity purifications of HMD_{63-152} identified HMD-associated proteins that have not previously been connected to Paf1C function. Although these proteins are unlikely to be involved in HMD-mediated H2Bub, it is possible that they interact with the HMD to perform distinct functions. Consistent with this, a second conserved, surface-exposed region of the HMD, containing the highly conserved E83 and K95 residues, was not implicated in promoting H2Bub (Figure 8). Sub2 is a member of the transcription-export (TREX) complex, which regulates both RNA processing and nuclear export (Katahira 2015). Rtf1 has known RNA-binding activity (Dermody and Buratowski 2010), and its *in vivo* association with various

factors including Sub2 appears to be at least partially RNA-dependent (Table 4). In recent years, the connections between transcription elongation, and RNA processing/export have come to be more fully appreciated (Bentley 2014). H2Bub regulates nuclear export indirectly via crosstalk with members of the CPF complex (Vitaliano-Prunier, et al. 2012), and high levels of Pol II-associated Paf1C were recently shown to correspond with the nuclear export of the associated nascent transcripts (Fischl, et al. 2017). Kap123 is a member of the nuclear pore complex (NPC), which in addition to its role in importing ribosomal proteins is required for the import of histones H3 and H4 (Mosammaparast, et al. 2002; Blackwell, et al. 2007). Interestingly, many other NPC members show high ERC with Paf1C subunits (Dr. Nathan Clark, personal communication). Thus, it remains an intriguing possibility that the HMD "moonlights" to regulate other nuclear processes in addition to its role in promoting H2Bub.

3.0 BIOCHEMICAL ANALYSIS OF RTF1 HISTONE MODIFICATION DOMAIN-MEDIATED H2B MONOUBIQUITYLATION

3.1 INTRODUCTION

Although a requirement for the HMD in promoting H2Bub *in vivo* is well established (see Section 1.6), it is unclear whether the HMD promotes deposition of the mark directly, and/or whether it requires factors other than Rad6 to exert its effect. The most straightforward way to test this is to develop an *in vitro* assay for HMD activity. However, previous attempts by other groups to examine the ability of the full Paf1C to promote H2Bub *in vitro* have yielded complicated results.

Though H2Bub is undetectable *in vivo* in the absence of Rtf1 (Figure 5), H2B can be ubiquitylated *in vitro* in an ATP-dependent reaction containing recombinantly expressed enzymes (human E1 (UBE1; hE1) and yeast Rad6 and Bre1 (yRad6 and yBre1)), HeLa nucleosomes, and a source of ubiquitin (Kim and Roeder 2009). However, when added to this minimal system, purified yPaf1C failed to stimulate H2Bub and instead was somewhat inhibitory (Kim and Roeder 2009). A similar result was seen when human factors were used (Kim, et al. 2009). In contrast, a strong requirement for hPaf1C was observed in a transcription-coupled system that included general transcription factors and Mediator (Kim, et al. 2009).

It is not fully clear whether H2Bub stimulates active transcription, and/or whether the process of transcription itself is required for deposition of the mark *in vivo*. In support of the latter, an earlier report using a similar transcription-coupled system found that H2Bub was dependent on both Paf1C and nucleoside triphosphates (Pavri, et al. 2006). Paf1C and H2Bub stimulated transcription in this system in conjunction with FACT, and Paf1C stimulation occurred post-initiation (Pavri, et al. 2006). Subsequent work, however, called into question whether the E2 used in this study, UbcH6, is actually a functional Rad6 ortholog (Kim, et al. 2009); and as H2Bub was measured by Pavri et al. with an antibody that generically recognizes ubiquitin, it is possible that the activity of UbcH6 in this assay is non-specific. In reactions using hRad6A and an antibody that recognizes the modification directly, while detection of H2Bub in a transcription-coupled system was dependent on the addition of NTPs, addition of ubiquitylation factors to the transcription reaction actually diminished transcriptional output slightly, though this was not an effect of ubiquitylation per se as the same result was observed in an H2B K120R mutant (Kim, et al. 2009). Studies in live human cells indicate that the global patterning of H2Bub is strongly linked to active Pol II transcription elongation (Fuchs, et al. 2014). Nevertheless, the fact that H2Bub can be detected in a minimal system absent both Paf1C and transcription indicates that neither are strictly required for catalysis, raising the question of what cellular conditions impose a requirement for these factors.

In contrast to the inhibitory effect of hPaf1C on H2Bub in a transcription-free system using HeLa oligonucleosomes as a substrate, a more recent report found that hPaf1C was weakly stimulatory in a similar system that utilized a recombinant chromatin template (Yao, et al. 2015). This suggests that the effect of Paf1C on H2Bub may be dependent on the presence or absence of other histone modifications. Interestingly, this study found that Paf1C stimulation of

H2Bub in this system was synergistic with the Mediator complex, largely through the activity of the MED23 subunit (Yao, et al. 2015).

While MED23 alone is able to weakly stimulate H2Bub on a histone octamer substrate lacking DNA, it is insufficient to stimulate H2Bub on recombinant oligonucleosomes unless Paf1C is added to the reaction (Yao, et al. 2015). This suggests that the role of Paf1C in promoting H2Bub may be mediated in part by interactions with nucleosomal DNA, perhaps through the HMD. Rtf1 was previously shown to bind RNA *in vitro* (Dermody and Buratowski 2010), and the HMD was found to co-immunoprecipitate with H2B (Piro, et al. 2012). While this association was dependent on the E104 residue critical for H2Bub (Piro, et al. 2012), this may be due to the fact that E104 is critical for the HMD-Rad6 interaction and for the overall association of the HMD with chromatin (Van Oss, et al. 2016), rather than any specific role of this residue in mediating a possible interaction between the HMD and nucleosomes. To date, no direct interaction between the HMD and either DNA or nucleosomes has been reported.

While Dr. Shirra's BPA experiments identified a conserved surface on the HMD that is required for the HMD-Rad6 interaction (Figure 16) (Van Oss, et al. 2016), the region of Rad6 that mediates this interaction is unknown. The acidic C-terminus of Rad6 has long been known to be important for its intrinsic ability to nonspecifically ubiquitylate histones (Sung, et al. 1988) and was more recently shown to be required for optimal Bre1-mediated ubiquitylation of H2B K120, though it is not required for binding of Bre1 to Rad6 (Kim and Roeder 2009). However, the fact that the Rad6 acidic tail is unique to budding yeast and closely related species (Koken, et al. 1991), while HMD function is conserved from yeast to humans (Cao, et al. 2015), argues against a role for this region in mediating the HMD-Rad6 interaction. In contrast, the N-terminus of Rad6 is well conserved among Rad6 orthologs but is relatively unique among other

ubiquitin-conjugating enzymes, which generally display a high degree of sequence similarity (Watkins, et al. 1993). Modeling performed by Dr. Andrew VanDemark using the HADDOCK protein-protein docking program (Dominguez, et al. 2003) also suggested the possibility of interactions between the HMD and the Rad6 N-terminus; the N-terminus thus represents an intriguing candidate for the Rad6 HMD-interaction domain.

In this chapter, I make use of purified components and a minimal *in vitro* ubiquitylation assay to address some of these questions. I also characterize the *in vitro* activity of an HMD-Rad6 fusion protein. Finally, I examine the ability of the HMD to bind DNA and nucleosomes directly *in vitro*.

3.2 MATERIALS AND METHODS

3.2.1 Yeast strains and plasmids used

All plasmids used in this chapter and their construction are described in Table 5. For *in vivo* analysis of Rad6Δ1-9, plasmids pRS314, KB1167, and KB1386 were transformed into the yeast strain KY1468, which has the following genotype: *MATα rad6Δ::URA3 his4-912δ leu2Δ1 ura3-52 trp1Δ63*.

3.2.2 Protein purification

Expression of all wild-type and mutant Rad6 and HMD proteins, as well as the HMD_{74-139}-Rad6ΔC fusion protein, was performed in *E.coli* Codon+ (RIPL) or (RIL) cells (Stratagene).

Cells expressing HMD proteins and the HMD_{74-139}-Rad6ΔC fusion protein were grown in ZY auto-induction media (Studier 2005) at room temperature for 16-24 hr; cells expressing Rad6 were grown in LB media to an OD of 0.6, induced with 100 μM IPTG, and grown overnight at 18 °C.

Cells were harvested by centrifugation, resuspended in lysis buffer (25 mM Tris-Cl pH 8.0, 500 mM NaCl, 10% glycerol, 5 mM imidazole, 1 mM β-mercaptoethanol, and 1X protease inhibitors (167μg/mL PMSF, 0.7μg/mL pepstatin, 0.5μg/mL leupeptin; 0.5μg/mL aprotinin was also included in most preps)), and lysed with an EmulsiFlex-C3 homogenizer. Lysates were cleared by centrifugation at 30,000 x g. All proteins were purified by nickel affinity chromatography (Ni-NTA agarose; Qiagen) at 4°C followed by digestion with TEV protease, during dialysis into TEV cleavage buffer (20mM Tris-Cl pH 8.0, 400mM NaCl, 8% glycerol, 1 mM β-mercaptoethanol), for 90 minutes at room temperature and then overnight at 4°C. The amount of TEV protease added was based on the amount of protein present as determined by Coomassie staining but was generally 1.5-3mg. Uncleaved protein and His-tagged TEV protease were removed by a second round of nickel affinity chromatography followed by ion exchange chromatography using HiTrap-SP and/or HiTrap-Q FF columns; proteins were kept at 4°C throughout the purification process. Following binding to the HiTrap columns, protein was washed in low-salt buffer (8% glycerol, 20mM Tris-Cl pH 8.0, 1 mM β-mercaptoethanol, 60-100mM NaCl) and then eluted with an increasing salt gradient. Protein used in biochemical experiments was then dialyzed into storage buffer and concentrated when necessary using a Vivaspin concentrator (Millipore). HMD_{74-139}-Rad6ΔC fusion protein used for crystallization was further purified by gel filtration using a HiPrep 16/60 Sephacryl S-200 HR column (GE Healthcare) and concentrated as needed prior to setting up crystallization screens. Dr. Joel

Rosenbaum assisted with the ion exchange and sizing column steps, and conducted the crystallization trials.

Purification of His-pK-HA-Ubiquitin was carried out by Dr. Margaret Shirra. Expression was performed in *E.coli* Codon+ (RIPL) cells using LB media. Cells were grown to an OD of 0.6, induced with 500 μM IPTG, and grown for 3.5 hr at 37 °C. Cells were then harvested by centrifugation and lysed with an EmulsiFlex-C3 homogenizer in 20 mM Tris-Cl pH 7.9, 500 mM NaCl, 10% glycerol, 5 mM imidazole, 0.1% NP-40, and 1 mM PMSF. Lysates were cleared by centrifugation at 30,000 x g. The protein was purified by nickel affinity chromatography through 3 hr of batch binding at 4 °C. The resin was washed with lysis buffer containing 30 mM imidazole, and then incubated in lysis buffer containing 400 mM imidazole. Protein was collected from the supernatant following centrifugation, and then dialyzed into storage buffer. FLAG-yBre1 and FLAG-hE1 were generous gifts from Dr. Jaehoon Kim (Korea Advanced Institute of Science and Technology). Both proteins were purified from *S. frugiperda* (SF9) cells infected with baculoviruses, using M2 agarose as described previously (Ito, et al. 1999; Kim, et al. 2009). Recombinant *X. laevis* nucleosomes were a generous gift from Dr. Song Tan (Penn State University). Nhp6 protein was a generous gift from the lab of Dr. Timothy Formosa (University of Utah).

3.2.3 Western blot analysis

For whole cell extracts used in Figure 22A, SUTEB extracts were prepared as described in Chapter 2. All samples were resolved on SDS-PAGE gels, blotted to a nitrocellulose membrane, and probed with the indicated antibodies. The antibodies used in this chapter were α-H2Bub (Cell Signaling #5546; 1:1000 dilution), α-H2A (Active Motif #39235; 1:5000), α-H2B (Active

Motif #39237; 1:3000), α-G6PDH (Sigma #A9521; 1:20000), and α-c-Myc (9E10) (Covance #MMS-150P; 1:1000). Blots were then probed with a 1:5000 dilution of the appropriate horseradish peroxidase-conjugated secondary antibody (either donkey anti-rabbit, or sheep anti-mouse; GE Healthcare), and visualized via enhanced chemiluminescence. For α-H2Bub, α-H2B, and α-c-Myc blots in Figure 22A, milk was added to the secondary antibody in order to increase specificity, at a concentration of 3%, 5%, and 2%, respectively. Blots were visualized on either a Kodak Image Station (440CF) or a Bio-Rad ChemiDoc XRS+ imager. Signal was quantitated using the ImageJ (NIH) and Image Gauge (Fujifilm) software packages.

3.2.4 *In vitro* H2Bub assay

Reactions were carried out in 1X Reaction Buffer (50 mM Tris-Cl pH 7.9, 5 mM $MgCl_2$, 4 mM ATP, 2mM NaF, and 0.4 mM DTT). The indicated purified proteins were added on ice; Rad6 and, when applicable, HMD or HMD_{74-139}-Rad6ΔC were added last. Following gentle mixing, reactions were incubated at 30 °C and stopped by boiling for 3 minutes in 1X SDS loading buffer, and samples were then examined by western blotting.

3.2.5 Electrophoretic mobility shift assay

The DNA substrate used in these experiments is a 309bp, double-stranded DNA fragment described in Section A.2.2. This DNA was radiolabeled via end-labeling with γ-ATP using T4 polynucleotide kinase. Nucleosomes incorporating radiolabeled DNA were reconstituted and purified as described in Sections 5.2.5 and 5.2.6. Ten fmol of DNA and/or nucleosomes (i.e. nucleosomes with 10fmol of DNA content) were used in each binding reaction. Reactions were

carried out essentially as described previously (Hepp, et al. 2014) in a volume of 15µL for DNA-binding reactions or 16.5µL for nucleosome-binding reactions by incubating the labeled substrate, diluted to 3.0µL (DNA) or 4.5µL (nucleosomes) in FCR buffer (100mM NaCl, 10mM Tris-Cl pH 7.4, 1mM EDTA pH 8.0, 5mM DTT, 0.5mM PMSF, 0.05% NP-40, 10% glycerol and 100µg/mL BSA), with proteins diluted in 1X EMSA buffer (49.4mM KCl, 12.9mM HEPES-KOH pH 7.9, 1.6mM DTT, 0.5mM PMSF, 9.9% glycerol, 0.1% NP-40, 6.4mM $MgCl_2$, 68.7 µg/mL BSA, 39.1mM NaCl, 2.6mM Tris-Cl pH 8.0, 0.3mM MgOAc, 0.3mM imidazole, 0.5mM EGTA, 0.4mM HEPES-KOH pH 7.4, 0.4mM $ZnCl_2$) for 30 minutes at 30°C. Note that EMSA buffer is derived by combining remodeling, CRC, and Gal4 buffers described in Hepp et al. and can be simplified for future experiments). Dye-free TBE loading buffer was added to samples at a final concentration of 10% sucrose and 0.75X TBE. Samples were loaded to a 5%, 0.3X TBE native polyacrylamide gel that had been pre-run at 180V for a minimum of 1 hour. TBE loading buffer containing bromophenol blue dye was run in outside, empty lanes in order to estimate the migration of samples. For initial experiments, migration of samples was checked by measuring radioactivity until an appropriate time for resolving samples was determined. For the experiments described here, gels were run at 180V for ~6.5 hours in the cold room (~4°C). Gels were then dried and imaged on a Typhoon FLA 7000 instrument.

Table 5. Plasmids used in Chapter 3

Plasmid	Construction	Promoter	Gene Product	Markers
pAV882	HMD_{74-139}, a cleavable thrombin linker, and $Rad6_{1-154}$ were inserted into pKA8 by Gibson assembly	T7	8XHis-TEV-HMD_{74-139}-Thrombin-$Rad6_{1-154}$	Amp^R
pET-15b-His-pK-HA-Ub	(Tan, et al. 1999)	T7	His-Thrombin-pK-HA-Ubiquitin	Amp^R
pFASTBAC1-hE1	(Kim, et al. 2009)	PH	FLAG-hE1	Amp^R
pFASTBAC1-yBre1	(Kim and Roeder 2009)	PH	FLAG-yBre1	Amp^R
pKB993	(Van Oss, et al. 2016)	T7	6XHis-V5-TEV-HMD_{74-184}-E104K	Amp^R
pKB1157	Residues 171-254 of the 710 amino acid variant of human Rtf1 were amplified and cloned into the pQlink H vector using BamHI and NotI sites	tac	7XHis-TEV-$hRtf1_{171-254}$-	Amp^R
pKB1158	Residues 171-304 of the 710 amino acid variant of human Rtf1 were amplified and cloned into the pQlink H vector using BamHI and NotI sites	tac	7XHis-TEV-$hRtf1_{171-304}$-	Amp^R
pKB1167	Rad6-13XMyc was amplified from KY1026 and cloned into pRS314 using Pst1 and KpnI sites	*RAD6*	Rad6-13XMyc	*TRP1*; Amp^R
pKB1386	PCR stitching was used to delete sequence encoding the first nine residues of Rad6 from pKB1167	*RAD6*	rad6Δ1-9-13XMyc	*TRP1*; Amp^R
pKB1408	rad6Δ1-9 sequence was amplified from pKB1386 and cloned into the KMKB5 vector using NheI and HindIII sites	T7	6XHis-MBP-TEV-rad6Δ1-9	Kan^R
pKB1418	PCR stitching was used to introduce the E104K mutation into the HMD portion of pAV882	T7	8XHis-TEV-HMD_{74-139}-E104K-Thrombin-$Rad6_{1-154}$	Amp^R
pKMK4	(Van Oss, et al. 2016)	T7	6XHis-MBP-TEV-Rad6	Kan^R

pRS314	(Sikorski and Hieter 1989)	n/a	n/a	*TRP1*; Amp^R
pTOPO-yHMD $_{57-152}$	(Van Oss, et al. 2016)	T7	6XHis-V5-TEV-HMD $_{57-152}$	Amp^R
pTOPO-yHMD $_{74-139}$	(Van Oss, et al. 2016)	T7	6XHis-V5-TEV-HMD $_{74-139}$	Amp^R
pTOPO-yHMD $_{74-184}$	(Van Oss, et al. 2016)	T7	6XHis-V5-TEV-HMD $_{74-184}$	Amp^R

3.3 RESULTS

3.3.1 The Rtf1 HMD stimulates Bre1-dependent H2Bub in a minimal *in vitro* system

Given the ability of the HMD to promote H2B K123ub *in vivo* in the absence of Paf1C (Figure 12), I examined the effect of adding purified HMD to a minimal *in vitro* system similar to that previously described (Kim and Roeder 2009), except that instead of using HeLa nuucleosomes as a substrate, I made use of "naked" nucleosomes (containing no modifications) reconstituted from recombinant *X. laevis* histones. Addition of either recombinant HMD_{74-139} or HMD_{57-152} to the reaction had no effect on the amount of H2Bub detected (Figure 20A). Because an initial bioinformatic analysis performed by Dr. Adam Wier (Van Oss, et al. 2016) identified a larger HMD-containing domain, which included Rtf1 residues 74-184, I examined the effect of adding HMD_{74-184} to the reconstituted H2B ubiquitylation reaction. Interestingly, the larger Rtf1 fragment stimulated H2Bub by approximately 4-fold in a manner that depended on E104 (Figure 20B), a residue essential for stimulation of H2B K123ub *in vivo* (Figure 8).

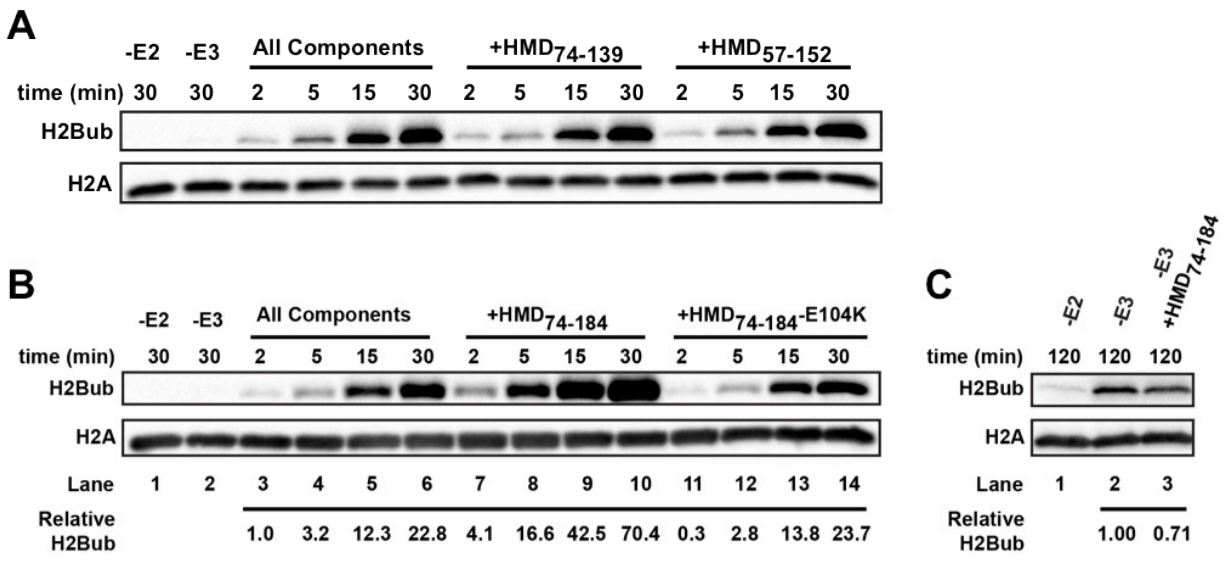

Figure 20: HMD_{74-184} stimulates Bre1-dependent H2Bub.

(A-C) Unless otherwise indicated, *in vitro* ubiquitylation reactions contained: recombinant *X. laevis* nucleosomes, FLAG-yBre1 (E3), FLAG-hE1, His-HA-pK-Ubiquitin, and yRad6 (E2). HMD proteins, or an equivalent volume of storage buffer, were added to the indicated reactions. Reactions were incubated at 30°C for the indicated times and analyzed by Western blotting. H2A levels function as a loading control. Relative H2Bub was determined by setting the signal for lane 3 (Panel B) or lane 2 (Panel C) to one. Though all experiments were conducted at least twice, quantitations are from the replicate shown.

Rad6 has been shown to promiscuously ubiquitylate histones *in vitro*, including H2B, without Bre1 or any other E3 present (Haas, et al. 1988; Sung, et al. 1988; Kim and Roeder 2009). In this minimal system, I observe robust H2Bub after 2 hours in the absence of the E3 (Figure 20C). I found that the ability of the HMD to stimulate H2Bub was dependent on the presence of Bre1 (Figure 6B). In fact, addition of $HMD_{74\text{-}184}$ to a reaction lacking Bre1 had a modest inhibitory effect on Bre1-independent H2Bub by Rad6 (Figure 20C).

Previously, our lab showed that expression of HMD orthologs in yeast, including human HMD, effected partial rescue of H3 K4 and K79 Me^2/Me^3, but not of H2B K123ub (Piro, et al. 2012). However, it remained unclear whether this is due to a fundamental inability of the human HMD to fully stimulate catalysis, perhaps because of a weakened interaction with yRad6, or due to secondary genetic factors. Thus, I purified HMD-containing fragments of human Rtf1 in order to test them in our minimal *in vitro* system. The two proteins tested are roughly equivalent to the yeast $HMD_{74\text{-}139}$ and $HMD_{74\text{-}184}$ boundaries, as determined by multiple sequence alignment (Figure 7). When added to an *in vitro* ubiquitylation reaction containing yRad6 and yBre1, both proteins had a very weak stimulatory effect on H2Bub (Figure 21). While it remains possible that these proteins are largely inactive for technical reasons, this is consistent with what was seen *in vivo* and suggests that *in vitro* stimulation by hHMD requires human E2 and/or E3 proteins.

3.3.2 Analysis of a Rad6 N-terminal deletion mutant

In order to ask whether the N-terminus of Rad6 is responsible for mediating the HMD-Rad6 interaction, I first sought to reproduce the previously published observation that deletion of the

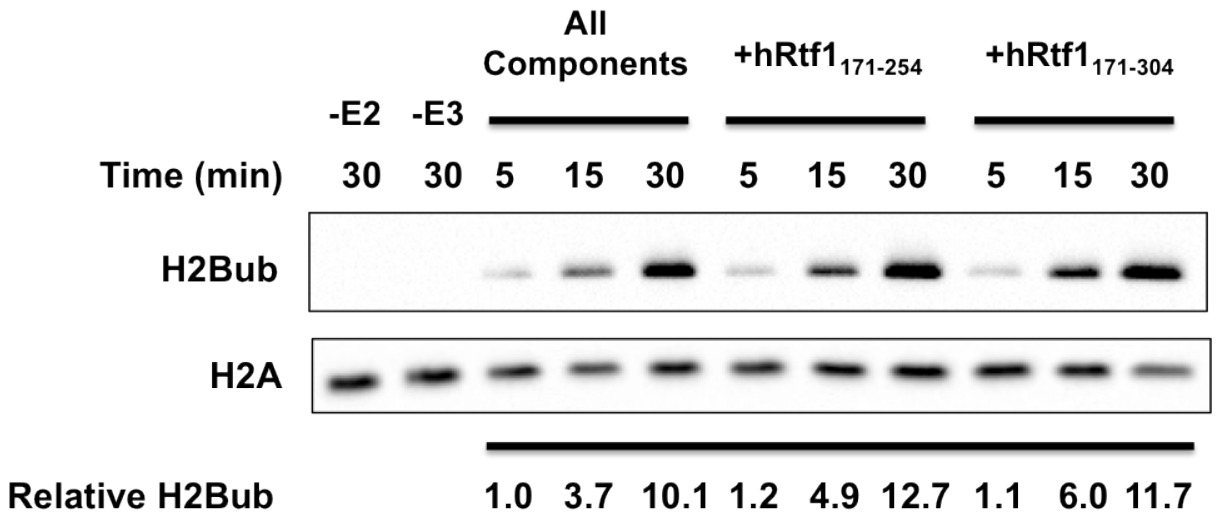

Figure 21: Human HMD constructs show minimal activity with yRad6 and yBre1.

Unless otherwise indicated, all reactions contained recombinant *X. laevis* nucleosomes, FLAG-yBre1 (E3), FLAG-hE1, His-HA-pK-Ubiquitin, and yRad6 (E2). hRtf1 fragments, or an equivalent volume of storage buffer, were added to the indicated reactions. Reactions were incubated at 30°C for the indicated times and analyzed by Western blotting. H2A levels function as a loading control. Relative H2Bub was determined by setting the signal for lane 3 to one.

first nine Rad6 residues abolishes detectable H2Bub *in vivo* (Sun and Allis 2002). Indeed, H2B K123ub was undetectable in a *rad6Δ1-9* strain (Figure 22A). Rad6 protein levels were substantially reduced, though not abolished, in the mutant (Figure 22A), partially explaining the reduced activity. Consistent with what was observed in other H2Bub-deficient mutants (e.g. Figures 5, 6A, 8D, and 11) and with the observation that H2Bub promotes nucleosome stability (Batta, et al. 2011), total H2B levels were also diminished.

To test directly whether Rad6Δ1-9 is able to respond to HMD stimulation, I purified the mutant protein from *E. coli* and tested it in our minimal *in vitro* ubiquitylation system. Both Bre1-dependent H2Bub (lanes 9 and 10) and Bre1-independent H2Bub (lane 3) were undetectable when Rad6Δ1-9 was added to the reactions (Figure 22B). Addition of HMD_{74-184} allowed for detection of H2Bub in Rad6Δ1-9-containing reactions, although levels were much lower than those seen with wild-type Rad6 (Figure 22B; compare lanes 7 and 8 to lanes 11 and 12). This result indicates both that the N-terminus of Rad6 is important for its intrinsic catalytic ability beyond its role in promoting Rad6 stability *in vivo*, and that this region of Rad6 is not essential for its interaction with the HMD.

3.3.3 Analysis of an HMD_{74-139}-Rad6ΔC fusion protein

My inability to detect the HMD-Rad6 interaction by standard affinity purification techniques suggests that the interaction is low affinity. Furthermore, HMD_{74-139}, while fully functional *in vivo* (Figure 12), fails to stimulate H2Bub *in vitro* (Figure 20A), possibly because it fails to functionally interact with Rad6 in an *in vitro* setting. In order to facilitate structural studies with the goal of obtaining an HMD-Rad6 co-crystal structure, our collaborator Dr. Joel Rosenbaum in Dr. Andrew VanDemark's lab sought to address these challenges by constructing a plasmid

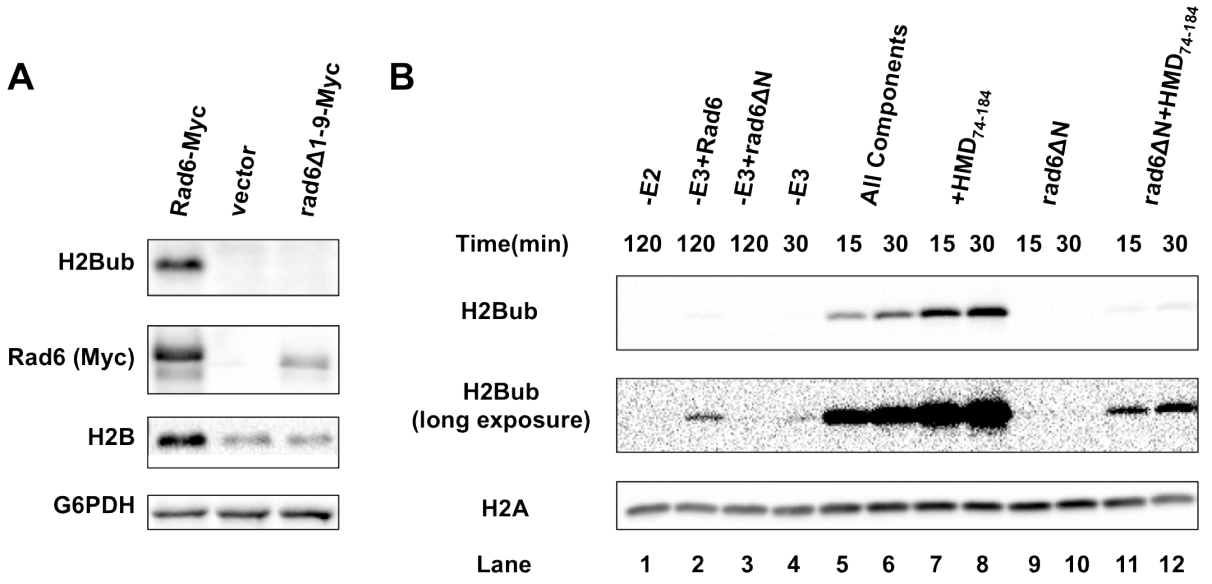

Figure 22: A Rad6 N-terminal deletion mutant responds to HMD stimulation.

A) The indicated plasmids were transformed into a *rad6Δ* strain (KY1468), and whole cell extracts were probed by western blotting. This experiment was conducted using biological triplicates derived from independent transformants. (B) Unless otherwise indicated, all reactions contained recombinant *X. laevis* nucleosomes, FLAG-yBre1 (E3), FLAG-hE1, His-HA-pK-Ubiquitin, and wild-type or mutant yRad6 (E2). HMD_{74-194}, or an equivalent volume of storage buffer, was added to the indicated reactions. Reactions were incubated at 30°C for the indicated times and analyzed by Western blotting. H2A levels function as a loading control.

expressing a fusion of HMD_{74-139} to the first 154 residues of Rad6 with a linker containing a thrombin cleavage site, excluding the Rad6 C-terminal acidic tail because it is disordered and would likely not be amenable to crystallization. I then made a derivative of this construct in which HMD_{74-139} contains the inactivating E104K mutation, and purified both proteins in order to examine their activity in our minimal *in vitro* system. In a separate purification, I used thrombin to cleave the fusion protein and then purified the HMD_{74-139} and Rad6ΔC components separately to compare the activity of the fusion protein to the effect of adding its separate components "in trans."

In reactions with no HMD present, the Rad6ΔC protein displays diminished activity when compared to wild-type Rad6 (Figure 23; compare lane 3 to lane 6), as has been reported previously (Kim and Roeder 2009). Remarkably, addition of the fusion protein to the ubiquitylation reaction stimulates H2Bub to the same extent as when HMD_{74-184} is added to a reaction containing wild-type, full-length Rad6 (compare lane 5 to lane 9), and this stimulation is dependent on E104 (lane 10). Addition of HMD_{74-184} to a reaction containing Rad6ΔC also stimulates H2Bub to the same levels as when wild-type Rad6 is used (compare lane 5 to lane 8), seemingly bypassing the requirement for the Rad6 C-terminus. In contrast, addition of HMD_{74-139} and Rad6ΔC "in trans" results in the same low levels of H2Bub seen with Rad6ΔC when no HMD is present (compare lane 6 to lane 7). As was seen with $HMD_{74-184,}$ addition of the fusion protein to a reaction lacking Bre1 is modestly inhibitory (compare lanes 1 and 2, long exposure).

Following biochemical characterization of the fusion protein, I performed a large-scale purification for use by Dr. Rosenbaum in crystallization trials (Figure 24). After scanning a large number of crystallization conditions, Dr. Rosenbaum successfully generated crystal

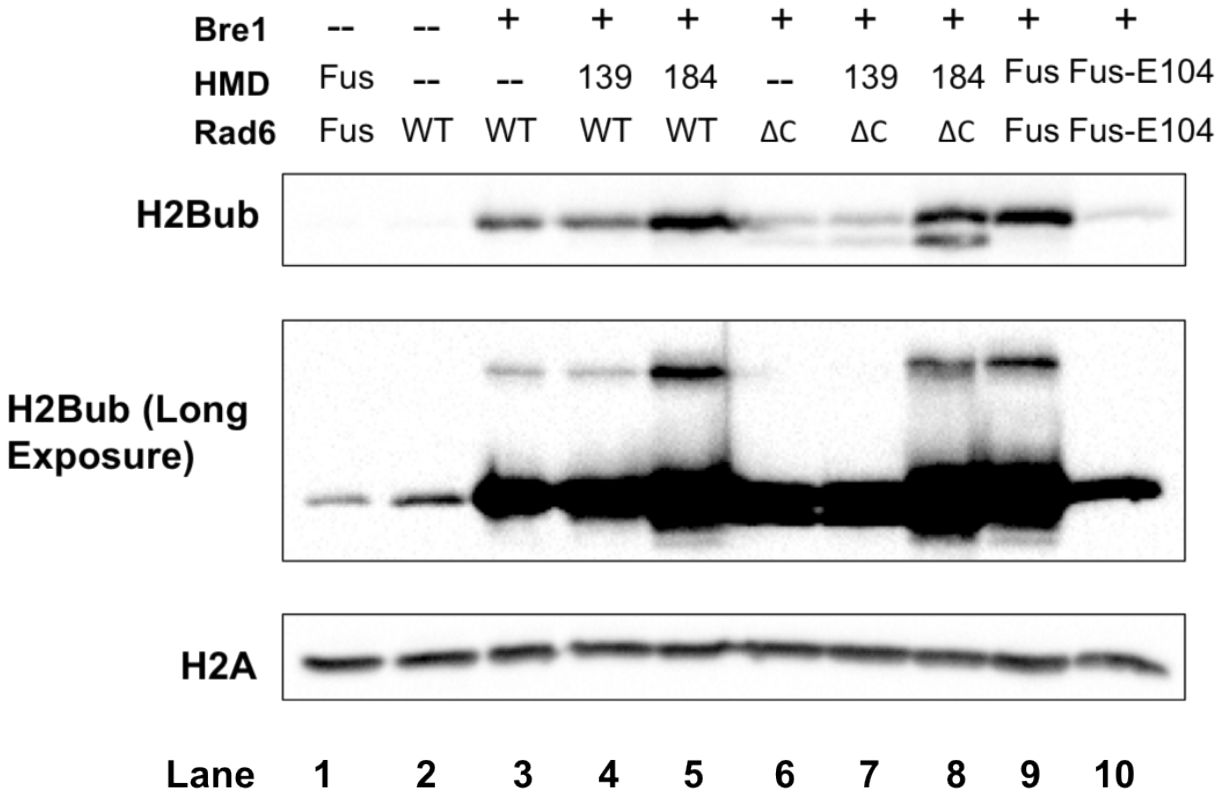

Figure 23: An HMD_{74-139}-Rad6ΔC fusion protein bypasses requirements for Rtf1 residues 140-184 and the Rad6 C-terminus

All reactions contained recombinant *X. laevis* nucleosomes, FLAG-hE1, and His-HA-pK-Ubiquitin. FLAG-yBre1 was added where indicated. Rad6 and HMD proteins, or an equivalent volume of HMD storage buffer, were added as indicated, either as separate proteins (139=HMD_{74-139}; 184=HMD_{74-184}; WT=wild-type; ΔC=$Rad6_{1-154}$) or as an HMD_{74-139}-Rad6ΔC fusion containing either a wild-type HMD_{74-139} portion (Fus) or a derivative containing the E104K mutation (Fus-E104). Reactions were incubated at 30°C for 30 minutes and analyzed by Western blotting. H2A levels function as a loading control. This experiment was conducted twice with the exception of samples in lanes one and two.

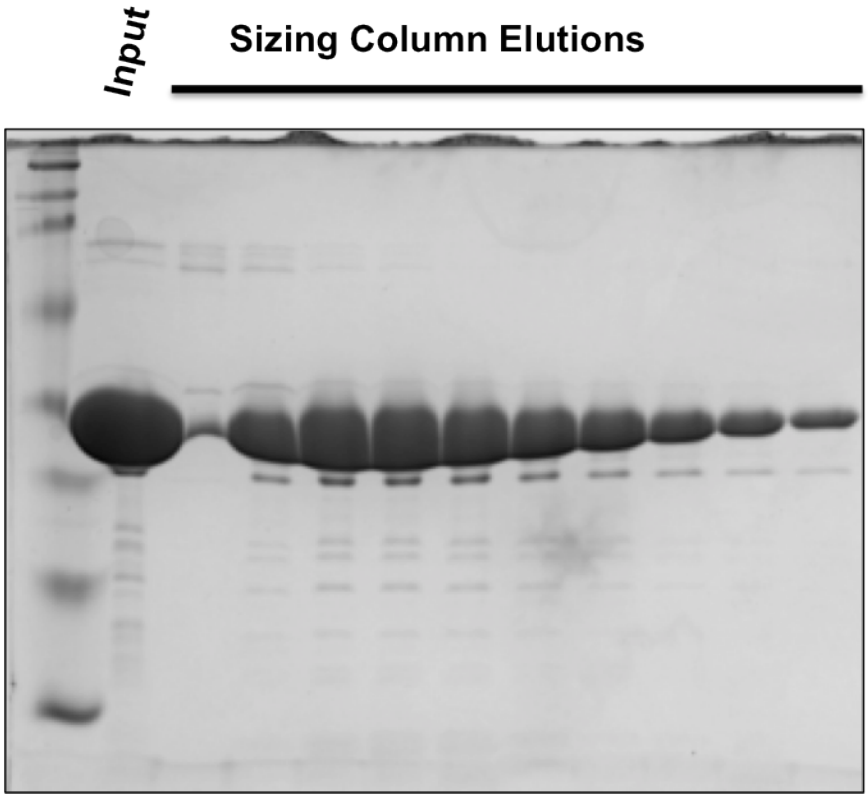

Figure 24: Purification of $HMD_{74\text{-}139}$-Rad6ΔC for crystallization trials.

Coomassie-stained SDS-PAGE gel showing elution fractions following purification by size exclusion on a HiPrep 16/60 Sephacryl S-200 HR column. Dr. Joel Rosenbaum assisted with use of the FPLC during ion exchange and sizing column steps of the purification.

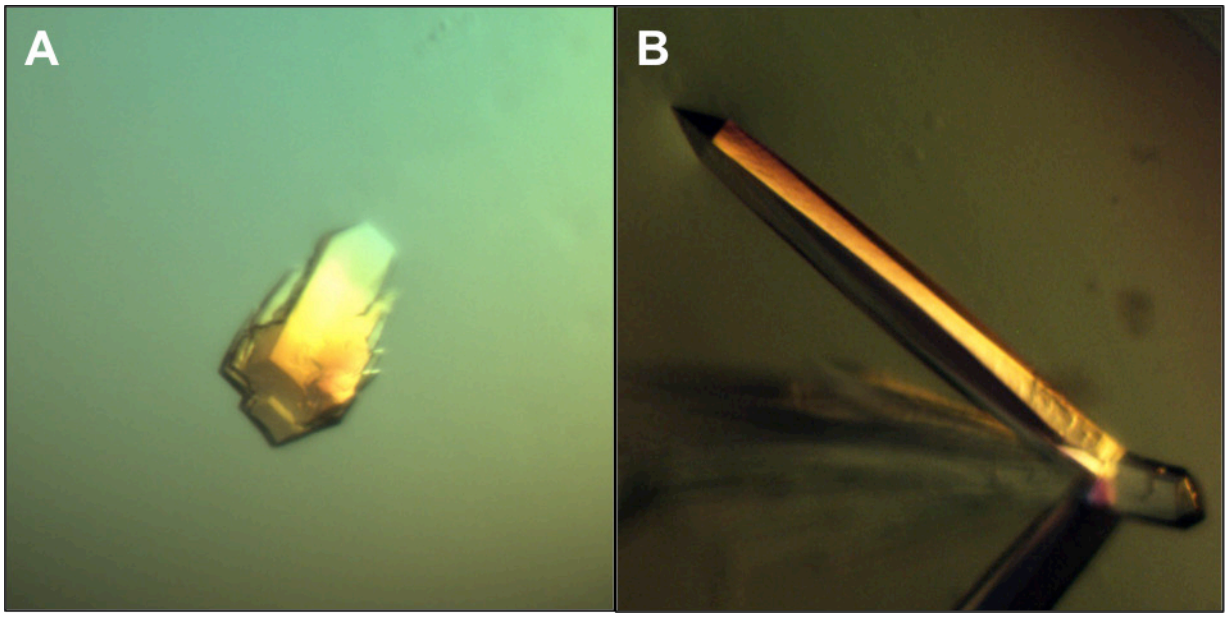

Figure 25: Images of HMD_{74-139}-rad6ΔC crystal lattices.

Crystallization trials were conducted, and images were taken by, Dr. Joel Rosenbaum. The buffers used are (A) 100 mM Tris-Cl pH 8.5, 29% PEG 3350 and (B) 100mM Tris-Cl pH 8.5, 100mM NaCl, 16% PEG 3350, 7% 2-Methyl-2,4-pentanediol (MPD).

lattices (Figure 25). Initial attempts at data collection yielded low-resolution data, and attempts to generate high-quality x-ray crystallography data are ongoing.

3.3.4 An HMD-containing Rtf1 fragment binds DNA

Given the known RNA-binding activity of Rtf1 (Dermody and Buratowski 2010) and the ability of the HMD to associate with chromatin independently of Paf1C (Piro, et al. 2012; Van Oss, et al. 2016), I used the electrophoretic mobility shift assay to ask whether HMD_{57-152} was able to bind DNA. A radiolabeled, 309 bp double-stranded DNA fragment was used as the substrate (see Section A.2.2). Nhp6, a protein known to bind DNA with high affinity (Hepp, et al. 2014),

was used a positive control. While Nhp6 forms complexes with DNA at concentrations as low as 5nM, no shift indicative of an HMD_{57-152}-DNA complex was observed even when HMD_{57-152} was added to concentrations as high as 1.8μM (Figures 26A-B). In sharp contrast, addition of the larger HMD_{74-184} fragment showed evidence of DNA binding at concentrations as low as 30nM, binding with an apparent K_D of ~75nM (Figure 26B).

I next tested the ability of HMD_{74-184} to bind to purified, recombinant nucleosomes containing yeast histones and the same DNA template used in the DNA-binding assays. Addition of HMD_{74-184} shifted the mobility of the nucleosome species in a concentration-dependent manner, indicating the formation of an HMD-nucleosome complex (Figure 26C). This shift was evident at HMD_{74-184} concentrations as low as 130nM. As these nucleosomes contain ~120bp of extranucleosomal "linker" DNA, it is not clear whether HMD_{74-184} is capable of binding nucleosomal DNA, linker DNA, or both; thus, further experimentation is warranted (see Section 4.2). It should also be noted that, although nucleosomes were gel extracted, it remains possible that some of the Nap1 protein used in nucleosome reconstitutions (see Section A.2.5) is still present. However, it is interesting to observe that the mobility of the HMD_{74-184}-nucleosome complex is strongly dependent on HMD_{74-184} concentration, which may be indicative of the binding of multiple HMD molecules.

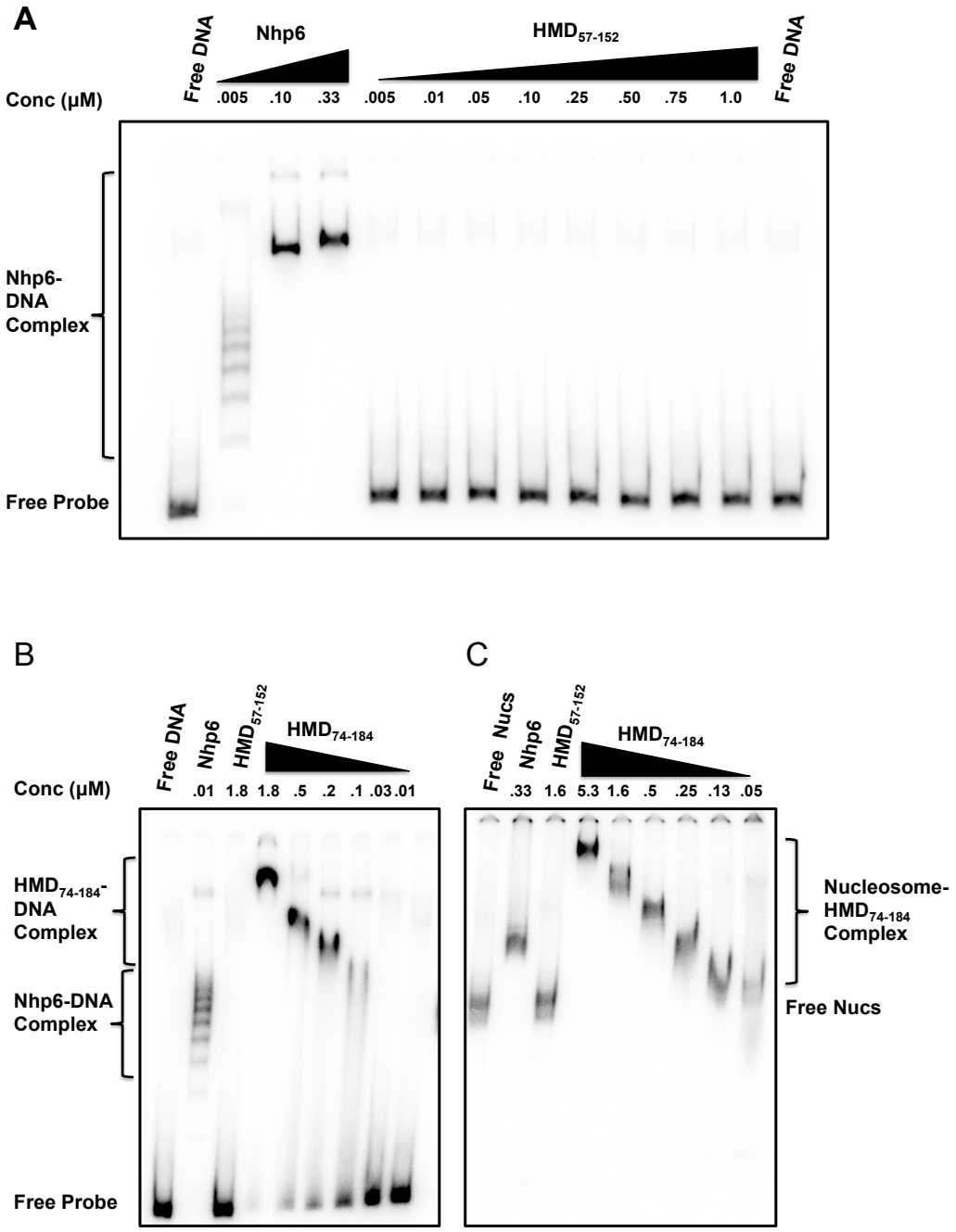

Figure 26: HMD_{74-184} binds double-stranded DNA

Ten fmol of radiolabeled, double-stranded DNA probe (A-B) or radiolabeled nucleosomes with 10fmol of DNA content were mixed with (A) HMD_{57-152} or (B and C) HMD_{74-184} added to the indicated concentrations in 1X EMSA buffer, and samples were resolved by native PAGE. Nhp6 serves as a positive control for both DNA and

nucleosome binding. The positive result observed in panels B and C was observed in two (DNA probe) or three (nucleosome probe) independent experiments.

3.4 DISCUSSION

In a minimal, transcription-free *in vitro* ubiquitylation assay, I observe approximately 4-fold stimulation of H2Bub upon addition of HMD_{74-184} to the reaction (Figure 20B). This activity is dependent on the Rtf1/HMD residue E104, a residue required both for deposition of H2Bub (Figure 8) and a physical interaction with the ubiquitin conjugase Rad6 (Figure 16) *in vivo*. This demonstrates that the role of the HMD in promoting H2Bub is direct. HMD-dependent stimulation of H2Bub is likely mediated at least in part by its direct interaction with Rad6, as the same residue required to maintain the HMD-Rad6 interaction *in vivo* (Figure 16A) is required for HMD activity *in vitro* (Figures 20B and 23).

One striking difference between the *in vivo* and *in vitro* activity of the HMD is the *in vitro* requirement for Rtf1 residues 140-184. Though HMD_{74-139} is sufficient to promote H2Bub *in vivo* even in the absence of all Paf1C subunits (Figure 12), addition of HMD_{74-139} or HMD_{57-152} to an *in vitro* ubiquitylation reaction does not affect H2Bub levels (Figure 20A). It is not immediately clear why this is the case, but it is interesting to note that an HMD_{74-139}-Rad6ΔC fusion protein bypasses this requirement (Figure 23). This suggests that residues 140-184 may stabilize a low-affinity HMD-Rad6 interaction, a function that may be performed by some other factor *in vivo* in an *rtf1Δ* context. One possible candidate is the histone chaperone Spt16, which is required for normal levels of H2Bub *in vivo* (Fleming, et al. 2008) and associates with both HMD_{63-152} (Tables 3 and 4) and full-length Rtf1 (Mayekar, et al. 2013).

Interestingly, unpublished data from Christine Cucinotta in our lab indicates that both Rtf1 and Spt16 interact directly with the nucleosome acidic patch. In the case of Rtf1, residues 111-152, housed within the HMD, appear to be required for this interaction. The association of Rtf1 with the nucleosome may involve binding of nucleosomal DNA. Here, I show that HMD_{74-184}, but not HMD_{57-152}, binds both double-stranded DNA and nucleosomes *in vitro* (Figure 26), with the caveat that binding to the nucleosomal substrate may be mediated entirely by linker DNA. Again, the role of residues 153-184 in the DNA binding capability of the HMD is unclear. The basic R173 residue is extraordinarily well-conserved in fungi (Figure 7). Substitution of R173 with alanine did not affect global H2Bub levels *in vivo* as measured by western blot (data not shown); however, this does not necessarily exclude a role for this residue in mediating DNA binding or in affecting the specific localization of H2Bub across the genome.

The HMD_{74-139}-Rad6ΔC fusion protein also stimulates H2Bub to the same extent as seen with wild-type Rad6 upon addition of HMD_{74-184}, seemingly bypassing the requirement for the Rad6 C-terminal acidic tail (Figure 23). It may be interesting to examine whether fusion of HMD_{74-139} to full-length Rad6 results in even greater levels of H2Bub, or whether the activity of the fusion protein represents the maximum specific activity of Rad6 under these reaction conditions. Previous studies have shown that the Rad6 C-terminus is important both for its specific and non-specific ability to ubiquitylate histones *in vitro* (Sung, et al. 1988; Kim and Roeder 2009). Although the fusion protein retains a few residues of the acidic tail not found in the mutants previously examined, the inability of Rad6ΔC to fully stimulate H2Bub in reactions lacking the HMD suggests that these additional residues are not of themselves able to substitute for the full-length tail. Furthermore, the Rad6 acidic tail is also required for full *in vivo* activity (Sun and Allis 2002), yet HMD_{74-184} still fully stimulates Bre1-dependent H2Bub in reactions

with Rad6ΔC, indicating both that the acidic tail is not essential for the HMD-Rad6 interaction and that the *in vivo* HMD-Rad6 interaction is not sufficient to bypass the requirement for the acidic tail. It is possible that either Rtf1 residues 140 to 184 or artificial fusion of $HMD_{74\text{-}139}$ to Rad6ΔC act to stabilize the HMD-Rad6ΔC interaction and/or maintain Rad6 in its active conformation *in vitro*. The fact that Rtf1 residues 140-184 are insufficient to bypass the requirement for the Rad6 C-terminus *in vivo* may speak to the possible presence of intrinsically inhibitory regions of Rtf1 that lie outside of the HMD, a hypothesis supported by the reduced *in vivo* activity of full-length Rtf1 in the absence of an intact Paf1C (Figure 12). In any event, the ability of $HMD_{74\text{-}139}$ to stimulate H2Bub in the context of the fusion protein remains Bre1-dependent, as was observed for $HMD_{74\text{-}184}$ (Figure 20C).

In vitro ubiquitylation assays conducted in a transcription-free system that used nucleosomes purified from HeLa cells as a substrate found that addition of either yPaf1C or hPaf1C to the reaction was mildly inhibitory (Kim, et al. 2009; Kim and Roeder 2009), while hPaf1C stimulated H2Bub on nucleosomes made with recombinantly expressed histones, both in transcription-coupled (Kim, et al. 2009) and transcription-free (Yao, et al. 2015) systems. Here I observe HMD stimulation of H2Bub in the absence of transcription. The role of the HMD in stimulating H2Bub therefore appears to be at least partially independent of Pol II transcription, and may also be dependent on the absence of other histone marks. Previously, I had collaborated with Dr. Brian Strahl's lab (University of North Carolina) to examine whether $HMD_{74\text{-}139}$ *preferentially* interacted with peptides containing a range of common modifications, obtaining a negative result. To my knowledge, although there are no known modifications that have been shown to *inhibit* H2Bub *in vivo* or *in vitro*, the combined results of the various *in vitro* studies that have been conducted suggest this interesting possibility.

The conserved N-terminus of Rad6 mediates the interaction between Rad6 and Ubr1, an E3 client unrelated to H2Bub (Watkins, et al. 1993). Mutational analysis of Rad6 coupled with binding assays showed that the Rad6 N-terminus was not sufficient to maintain binding to Bre1, although whether or not it is required for such binding remains an open question (Kim and Roeder 2009). My studies indicate that a Rad6 N-terminal deletion mutant is severely deficient in both Bre1-independent and Bre1-dependent H2Bub, yet is capable of responding to HMD stimulation (Figure 22B). This suggests a role for the Rad6 N-terminus that is independent of both Bre1 and the HMD, perhaps by interfacing with the nucleosome or otherwise maintaining Rad6 in an active conformation. Mutations to "non-canonical" residues in the Rad6 backside impair the ability of Rad6 to both mono- and polyubiquitylate H2B in a Bre1-independent manner (Kumar, et al. 2015). Interestingly, addition of either HMD_{74-184} or the HMD_{74-139}-rad6ΔC fusion protein inhibits Bre1-independent H2Bub (Figures 20C and 23), while in the presence of Bre1 both proteins stimulates both mono- and polyubiquitylation of H2B (Figure 23; polyubiquitylation of H2B is seen as a higher molecular weight species on the long exposure). While the region of Rad6 that mediates its interaction with the HMD remains unknown, this question would be answered directly by an HMD-Rad6 co-crystal structure, which we have made promising progress towards obtaining (Figures 24 and 25).

4.0 CONCLUSIONS AND FUTURE DIRECTIONS

The monoubiquitylation of histone H2B governs chromatin structure and is implicated in the regulation of gene expression and other transcription-linked processes (see Section 1.3). Interest in this modification has continued to grow as it has become clear that H2Bub regulates development and differentiation in higher eukaryotes, and that mutations to genes involved in the H2Bub pathway are linked to human diseases, including cancer (see Section 1.7). My studies and the work of my colleagues have advanced our understanding of the molecular mechanism underpinning HMD-dependent H2B ubiquitylation. Still, several fundamental questions remain unanswered.

4.1 IS HMD STIMULATION OF RAD6 SPECIFIC OR GENERAL?

One fundamental mechanistic question yet to be addressed is whether the HMD stimulates Rad6 catalysis per se, or whether it acts as an E3 cofactor by enhancing the ability of Bre1 to direct Rad6 to its canonical target on H2B (or, relatedly, whether HMD stimulation of Rad6 activity takes place only at H2B K123/K120, or also at non-specific targets). To test the first hypothesis, I have conducted a preliminary experiment examining the ubiquitin discharge rate of pre-charged Rad6 in the absence or presence of both Bre1 and the HMD. While these data are inconclusive, optimization of the protocol in order to address technical issues should provide a

rather straightforward assay for probing this question. An alternative approach would be to carry out ubiquitylation reactions under conditions of limited ubiquitin, measuring by western blot whether the addition of the HMD to the reaction accelerates the disappearance of free ubiquitin from the sample.

A technique suited to testing both hypotheses is to use mass spectrometry to identify all sites of ubiquitylation from minimal *in vitro* reactions carried out in the presence or absence of the HMD. I recently conducted such an experiment in collaboration with Dr. Amber Mosley at Indiana University. Samples from reactions containing or lacking the HMD both yielded very few peptides corresponding to ubiquitylated histones, precluding statistical analysis. It may be that the reactions simply need to be scaled up to increase signal, or there may be more fundamental technical considerations.

One alternative method to address the question of whether the HMD stimulates Rad6 catalysis specifically (i.e. exclusively at the canonical lysine on H2B) or non-specifically is to examine other sites of *in vitro* H2B ubiquitylation by western blot, utilizing a collection of mutant H2B proteins. An interesting study employing a ubiquitin species containing a substitution that inhibits removal by deubiquitylating enzymes found evidence of both mono- and polyubiquitylation of histone H2B in yeast, both at the canonical K123 location and at several additional lysines (Geng and Tansey 2008). These experiments made use of various H2B mutant proteins in which some or most lysines within H2B have been substituted with arginines. For example, one such H2B derivative retained only the lysines found on the N-terminal tail of the protein, while another retained only those lysines found in the globular core and others retained only a single, non-canonical lysine (i.e. not K123) (Geng and Tansey 2008).

Examination of the effect of the HMD on Rad6 and Bre1-dependent *in vitro* ubiquitylation of such mutants should provide evidence as to whether HMD stimulation of H2Bub is general, or is limited to a particular substrate. A pilot study along these lines could make use of the recently developed antibody against H2B K34ub (Wu, et al. 2014), one caveat being that the antibody was raised against the human form of the modification. Such an approach would have the advantage of avoiding potential off-target effects of substitutions within H2B. The study conducted by Geng and Tansey states that "most of the lysine residues" within H2B can serve as ubiquitylation substrates, but does not specifically address the status of K34. Thus, should no H2B K34ub be detected in an assay using yeast enzymes, one could consider making use of the human orthologs (it is possible that human nucleosomes would be required as well). Detection of H2Bub at other sites (or other regions within H2B, depending on the specific substitutions made) would best be accomplished by epitope-tagging of H2B in combination with lysine to arginine substitutions within H2B. While such a study would be more labor-intensive than a mass spectrometry approach, it would avoid the associated technical challenges.

4.2 DOES DNA BINDING BY THE HMD PROMOTE H2BUB?

I have observed binding of $HMD_{74\text{-}184}$ to a substrate containing reconstituted yeast nucleosomes (Figure 26C); however, because the binding assays I conducted used nucleosomes with a substantial amount (~120bp) of "linker" DNA, the data do not conclusively indicate whether or not the HMD binds nucleosomes per se. In order to test this more systematically, binding assays can be conducted with nucleosomes containing variable amounts of linker DNA, including

nucleosomes with essentially no linker DNA. This can be accomplished either by making use of restriction sites available within my current G-less cassette/601 NPS template (see Section A.2.2), or by reconstituting nucleosomes using DNA fragments containing various amounts of linker DNA. To determine the specificity of the DNA-binding activity, HMD binding to free dsDNA substrates of different lengths and sequence composition, as well as ssDNA and RNA substrates, can be tested. The latter would be of particular interest, given the known RNA-binding activity of full-length Rtf1 (Dermody and Buratowski 2010), the *in vivo* association of the HMD with RNA and RNA processing factors that I observed (Tables 3 and 4), and a recent genome-wide survey showing extensive *in vivo* crosslinking of mRNAs to elongation factors, including Rtf1 (Battaglia, et al. 2017).

An important question yet to be addressed is whether the DNA-binding activity of the HMD that I identified is relevant to the mechanism by which it promotes H2Bub. The HMD R126 residue is required for normal H2Bub *in vivo* (Figures 8B-D), yet lies outside of the likely Rad6 interaction surface (Van Oss, et al. 2016). An $HMD_{74\text{-}184}$-R126A derivative can be tested in DNA and nucleosome binding assays to determine the extent to which this residue contributes to that function. Furthermore, the $HMD_{74\text{-}139}$-Rad6ΔC fusion protein is functional for *in vitro* ubiquitylation, while $HMD_{74\text{-}139}$, added "in trans," is not (Figure 23). It would therefore be interesting to see if the fusion protein is capable of binding DNA, bypassing the requirement for Rtf1 residues 140-184 as is seen in the ubiquitylation assay. Finally, to directly examine whether HMD stimulation of H2Bub is DNA-dependent, *in vitro* ubiquitylation assays can be carried out using histone octamers, as well as H2A-H2B dimers, as a substrate, to determine if Rad6 still responds to HMD stimulation in this context.

4.3 WHAT IS THE ROLE OF PAF1C, TRANSCRIPTION, AND OTHER CELLULAR FACTORS IN HMD-DEPENDENT H2BUB?

Though overexpression of the HMD is sufficient to support global H2Bub in the absence of Paf1C (Figure 12), Paf1 and Ctr9 are required for normal levels of the modification and appear to have roles beyond promoting Rtf1 stability (Figures 5 and 6A). Furthermore, reduced activity of full-length Rtf1 in the absence of other Paf1C subunits (Figure 12B) suggests the possibility of an inhibitory domain within Rtf1. An attempt to purify full-length Rtf1 bearing an N-terminal GST tag and C-terminal His tag for use in ubiquitylation assays was unsuccessful due the fact that the full-length protein is unstable and could not be separated from breakdown products. Other purification strategies might be explored, as it would be interesting to see whether full-length Rtf1 is hypofunctional *in vitro* as *in vivo*. Intact Paf1C can be purified from yeast cells via TAP-tagging of the endogenous subunits (Krogan, Kim, et al. 2002; Squazzo, et al. 2002; Dermody and Buratowski 2010). Personal conversations with Dr. Joseph Reese at Penn State University indicated that complex purified from strains expressing Paf1-TAP was deficient in Pol II binding in *in vitro* assays, whereas complex purified from strains expressing Leo1-TAP was fully functional. It would be interesting to compare the activity of the full Paf1C to that of the HMD, both in our minimal *in vitro* system as well as in the context of active transcription (see below), where the role of the full human complex has been previously characterized (Kim, et al. 2009).

Our studies indicate that the role of the HMD in promoting H2Bub is direct and at least partially independent of transcription. Nevertheless, the minimal system used in my *in vitro* experiments differs from what is seen in the cell in that, in the *in vitro* system, the HMD is not essential for the detection of H2Bub. This may be due to requirements imposed by the cellular

environment that are not present in an *in vitro* setting; alternatively, it may be that H2Bub in an *rtf1Δ* strain remains below the level of detection due to the activity of the deubiquitylating enzymes Ubp8 and Ubp10 (and possibly, Ubp7 as well). Although H2Bub remains undetectable by the FLAG-H2B method in an *rtf1Δ ubp8Δ* strain (Piro, et al. 2012), it may be informative to examine global H2Bub levels with the α-H2Bub antibody in an *rtf1Δ ubp8Δ ubp10Δ ubp7Δ* strain.

If H2Bub remains undetectable in this context, it may be because the act of transcription renders Rad6 and Bre1 insufficient to catalyze H2Bub in the absence of the HMD. The transcription-coupled assay that observed an absolute requirement for hPaf1C included a number of additional factors, including TFIIS, Mediator, and general transcription factors (Kim, et al. 2009). I have purified the components of a more minimal transcription-coupled *in vitro* system, described in the Appendix. It will be interesting to see whether this system recapitulates the requirement for Paf1C, and if so, whether the HMD can also independently promote H2Bub in this context. This system is also suited for addressing the question of whether H2Bub exerts an effect on Pol II transcription, stimulatory or otherwise (see Section A.3).

Once the activity of the HMD and Paf1C have been more fully characterized in these minimal systems, additional factors can be added to reactions to examine their contributions and interplay with the HMD/Paf1C. Given that both TFIIS and Mediator stimulate H2Bub *in vitro* in assays using human enzymes (Kim, et al. 2009; Yao, et al. 2015), it would be interesting to observe the effect of adding the orthologous yeast factors to transcription-free and transcription-coupled *in vitro* reactions. As a strain lacking the TFIIS ortholog Dst1 does not have an *in vivo* H2Bub defect (Figure 14A), it is possible that the *in vitro* effect of TFIIS on H2Bub is an indirect consequence of transcription; however, TFIIS/Dst1 may stimulate H2Bub directly in a

manner that is redundant with another factor *in vivo*. Mediator stimulates H2Bub in a transcription-free assay, largely through the activity of the MED23 subunit (Yao, et al. 2015). While no MED23 ortholog has been identified in *S. cerevisiae*, this may be a function of relatively weak sequence conservation between the yeast and human complexes (Allen and Taatjes 2015). Rtf1 shows high ERC with several Mediator subunits (data not shown), and deletion of *RTF1* in yeast in combination with the deletion of *SRB5*, which encodes a Mediator subunit, results in synthetic phenotypes (Costa and Arndt 2000). It would therefore be interesting to examine the *in vitro* activity of the yeast Mediator complex in the context of reactions containing or lacking the HMD. Should one seek to carry out reactions using human factors, I have purified human HMD derivatives that can be used for this purpose. Additional factors are known to promote H2Bub *in vivo* and could also be added to reactions, including the FACT complex and Lge1.

Mutant Rad6 proteins lacking the nine most N-terminal residues or the 18 most C-terminal residues are hypofunctional *in vitro* but respond to stimulation by the HMD (Figures 22B and 23), indicating that these regions of Rad6 are not essential for the HMD-Rad6 interaction. If successful, solving the structure of the HMD-Rad6 fusion protein will directly identify the Rad6 surface mediating the interaction. This will allow for validation through the use substitutions within Rad6 predicted to disrupt the HMD-Rad6 interaction, the effects of which can be assessed both *in vivo* and *in vitro*. As a complementary approach, Brendan McShane is generating random mutations within *RAD6* and looking for suppression of phenotypes associated with mutations to the HMD. Beyond identifying the HMD-Rad6 interaction surface, a co-crystal structure may provide clues as to the mechanism of HMD stimulation. This may be assisted by the use of molecular modeling tools. Given that structures

already exist for the individual essential components of HMD-mediated H2Bub (Luger, et al. 1997; Kumar, et al. 2015; Kumar and Wolberger 2015), it is possible that such modeling might be used to suggest possible interactions between the HMD and the nucleosome and/or ubiquitin.

4.4 APPLICATIONS OF THIS WORK TO HUMAN HEALTH

In recent years, researchers have come to more fully appreciate the many connections between H2Bub and human health (see Section 1.7). Although my studies of HMD-mediated H2Bub are focused on budding yeast, it is possible to imagine therapeutic applications of this work. While the underlying cause of H2Bub loss observed in many types of cancer is unknown (Dickson, et al. 2016), the absence of the mark in parathyroid tumors is associated with mutations to *CDC73* (Hahn, et al. 2012). If the human HMD proves capable of stimulating H2Bub in the absence of Paf1C as I observed in yeast, it may be a candidate for gene therapy approaches to treating such tumors. Thus far, stimulation of H2Bub is the only activity identified for the HMD, meaning that its use as a therapeutic might be less likely to cause off-target effects. Additionally, some have explored the potential use of Rad6 inhibitors (Sanders, et al. 2013). Such inhibitors seek to target the DNA-repair function of Rad6, which is largely a function of Rad18-mediated ubiquitylation of proliferating cell nuclear antigen (PCNA) (Hoege, et al. 2002), although Bre1-mediated H2Bub is also implicated in this pathway (Hung, et al. 2017). Furthermore, studies are underway to explore the potential therapeutic uses of E1 inhibitors for a variety of conditions (Petroski 2008). In cases such as these where inhibition of H2Bub might represent an unwanted side effect, exogenous delivery of the HMD could potentially serve to counteract this by driving residual Rad6 activity towards H2Bub.

In contrast to cancers in which loss of H2Bub is observed, some malignancies, notably those mediated by mixed lineage leukemia (MLL) rearrangements, exhibit abnormally elevated levels of H2Bub (Wang, et al. 2013). Recently developed therapies that impair H2Bub have shown efficacy in extending survival (Castro, et al. 2017) but target the H2Bub pathway indirectly. It is possible that disruption of HMD function, via small molecule inhibitors or other methods, may represent a more targeted approach.

In summary, my studies of the Rtf1 HMD have shown that it has a direct role in promoting H2Bub that is independent of Paf1C and transcription. These studies and the work of my colleagues and collaborators have laid the groundwork for several further lines of investigation, many of which are actively ongoing, to further probe the molecular mechanisms governing this important modification. Moving forward, it will be exciting to apply this knowledge to the broadening understanding of the role that H2Bub plays in regulating fundamental processes in humans.

APPENDIX A: CONSTRUCTION OF A TRANSCRIPTION-COUPLED *IN VITRO* UBIQUITYLATION SYSTEM

A.1 INTRODUCTION

The use of *in vitro* systems with defined components allows for detailed dissection of the molecular mechanisms that govern fundamental biological processes such as the post-translational modification of histone proteins. In this appendix, I describe in detail a protocol for the reconstitution and purification of yeast nucleosomes, and some potential applications of this system to our studies of HMD-mediated H2Bub.

A.2 MATERIALS AND METHODS

The protocols described in Sections A.2.2, A.2.3, A.2.4, A.2.5, and A.2.6 are modified versions of protocols received from the lab of Dr. Joseph Reese. J. Brooks Crickard of the Reese lab provided many helpful suggestions related to these protocols.

A.2.1 Plasmids used

The DNA template is made from a plasmid containing a fragment from the Hsp70 G-less cassette (Zhang, et al. 2004), which was amplified and cloned into a pBluescript KS(+) vector that expresses the 601 nucleosome positioning sequence (NPS) (Thastrom, et al. 1999) and confers resistance to ampicillin (Amp) using *Sac*I and *Sac*II sites. The plasmid was transformed into *E. coli* DH5-α cells and added to the KB collection (KB1223). Note that the *E. coli* cells are extremely sick when carrying this plasmid.

Sequences encoding the yeast genes *HTA1*, *HTB1*, *HHT1*, and *HHF*1 were amplified and cloned into the pET11a vector using *Nde*I and *Bam*HI sites (Saha, et al. 2002). Genes are under control of the T7 promoter, and the pET11a vector contains the *lac* repressor and confers resistance to Amp. Plasmids were transformed into *E. coli* and added to the KB collection, both in DH5-α cells (KB1198-KB1201) and in BL21 Codon Plus (DE3) RIL cells (KB1202-KB1205). Note that chloramphenicol (Chl) is needed to maintain selection for rare tRNAs expressed in RIL cells. An H2BK123R derivative was also made by site-directed mutagenesis of wild-type *HTB1*, and was also transformed into both DH5-α cells and BL21 Codon Plus (DE3) RIL cells and added to the KB collection (KB1206-KB1207).

Sequence encoding the yeast gene *NAP1* was amplified and cloned into the pET28 vector. *NAP1* is under the control of the T7 promoter and has an N-terminal 6XHis tag, and the pET28 vector contains the *lac* repressor and confers resistance to kanamycin (Kan). The plasmid was transformed into *E. coli* and added to the KB collection, both in DH5-α cells (KB1208) and in BL21 (DE3) pLysS cells (KB1209). All plasmids used in this chapter except for the plasmid encoding the H2BK123R derivative were generous gifts from the lab of Dr. Joseph Reese.

A.2.2 Purification of template

Primers BVO58 and BVO59 and *Pfu* DNA polymerase were used to amplify a 309bp double-stranded DNA fragment from pKB1223. To generate template with a 5' biotin label, BVO70 was used instead of BVO59. The PCR products were then subjected phenol-chloroform isoamyl alcohol/chloroform isoamyl alcohol (PCI/CI) extraction, followed by an EtOH precipitation and resuspension in 0.1X TE. DNA was then gel extracted using the Wizard kit (Promega) (note that this final gel extraction step is imperative). This "tailless" DNA (with and without the biotin moiety) was used in nucleosome reconstitution trials.

To make "tailed template", PCI/CI treated material was subjected to an overnight digest with *Bgl*II, then treated with calf intestinal alkaline phosphatase (CIP) for 3 hours at 37°C and again subjected to PCI/CI extraction followed by an EtOH precipitation and resuspension in 0.1X TE. The tail (BVO57) was ligated using T4 DNA ligase (NEB). Note that the tail should be added in great molar excess; the ratio of tail:template in ng should be ~0.9:1.0. Tailed template was then gel extracted using the Wizard kit.

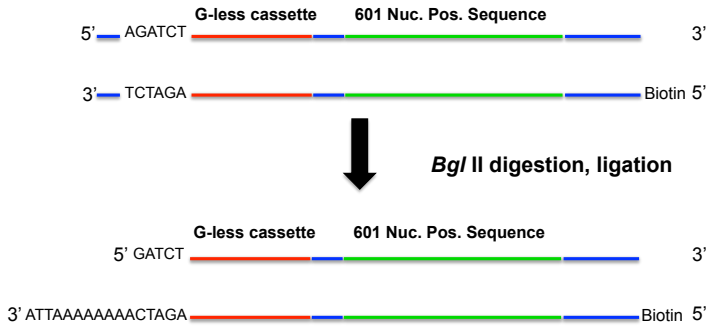

Figure 27: Generation of a biotinylated, tailed template.

Schematic showing the template used in reconstitution of yeast nucleosomes. The double-stranded template is 309bp in length prior to digestion and ligation of the tail. It contains 70bp of a G-less cassette, amplified from a previously described plasmid (Missra and Gilmour 2010), upstream of a 147bp nucleosome positioning sequence derived from a SELEX experiment (Lowary and Widom 1998). The diagram is to scale with the exception of bases/base pairs shown as letters.

A.2.3 Purification of His-Nap1 and histones

For purification of H2A, H2B, H2BK123R, and H4, histone expression plasmids were transformed into BL21 Codon Plus (DE3) RIL cells. Fresh transformants were used to inoculate LB-Amp-Chl media, and cells were grown to an OD_{600} of ~0.4-0.5, followed by induction with 1mM IPTG. Cells were harvested at ~3.5 hours post-induction, and pellets were flash frozen and stored at -70°C. Histone H3 expressed poorly in RIL cells and was instead purified from Rosetta (DE3) pLysS cells. An IPTG induction time course indicated that the optimal time for harvesting cells expressing H3 is 2 hours post-induction.

Pellets were resuspended in 25mL of TW buffer (50 mM Tris-HCl, pH 7.5, 100 mM NaCl, 1 mM Na-EDTA, 5 mM β-mercaptoethanol, 1% Triton X-100, and 1X protease inhibitors

(167μg/mL PMSF, 0.7μg/mL pepstatin, 0.5μg/mL leupeptin, 0.5μg/mL aprotinin)) per liter of culture and lysed with an EmulsiFlex-C3 homogenizer. Samples were then sonicated ("standard" tip, 2X20 seconds on setting 2, 7X20 seconds on setting 3, with one minute on ice in between), and inclusion bodies were pelleted by spinning for 20 minutes at 20,000xg and 4°C in SA-600 tubes. Samples were resuspended in 25mL TW buffer plus 1X protease inhibitors per liter of culture by using a PipetAid, and then pelleted again. Samples were then washed twice by resuspending in 25mL wash buffer (TW buffer minus Triton X-100) plus 1X protease inhibitors with 20 minute, 20,000 x g, 4°C spins in between. Following the final spin, inclusion bodies were flash frozen and stored at -70°C.

Inclusion body pellets from one liter of culture were thawed on ice for ~10 minutes and were then soaked in 200 μL of dimethyl sulfoxide for ~30 minutes at room temperature. Samples were minced well with a spatula, and the volume was then brought up with 6.5mL of freshly made unfolding buffer (7M guanidine HCl, 20mM Tris-Cl pH 7.5, 10mM DTT), and samples were incubated on a tabletop shaker with gentle shaking for one hour at room temperature. Samples were then collected by spinning for 20 minutes at 20,0000 x g and 4°C in SA-600 tubes. Supernatent was set aside, and pellets were minced again in an additional 1.5mL of unfolding buffer, followed by incubation on a tabletop shaker with gentle shaking for 20 minutes at room temperature. Samples were then collected again by spinning for 20 minutes at 20,0000 x g and 4°C in SA-600 tubes. Supernatents were combined and dialyzed against 2L of urea dialysis buffer (10mM Tris-Cl pH 8.0, 100mM NaCl, 7M deionized urea, 1mM EDTA pH 8.0, 5mM β-mercaptoethanol) for 4 hours at room temperature, followed by a buffer change and overnight dialysis at 4°C. Urea dialysis buffer is made using a freshly made 8M urea stock that is deionized by stirring with 25g/L of AG501-X8 resin for 30 minutes at room temperature.

Stirring must be gentle enough not to crush the beads but vigorous enough that they are evenly distributed throughout the solution.

Histones were then purified by ion exchange, using the fast protein liquid chromatography (FPLC) machine with assistance from Dr. Adam Wier and Christopher Amrich from Dr. Andrew VanDemark's lab. HiTrap Q and SP ion exchange columns (5mL) were set up in tandem, with the Q column first. Columns were washed with 50mL buffer A (10mM Tris-Cl pH 8.0, 7M urea, 1mM EDTA pH 8.0, 1mM DTT), then with 50mL buffer B (same as buffer A, plus 1M NaCl), then equilibrated in 10% buffer B/90% buffer A. Buffers were made using a freshly made 10M urea stock that is deionized as described above. Samples were filtered with a syringe filter prior to loading onto the ion exchange columns; note that histone H4 tends to form precipitates during dialysis. The columns were then washed with several column volumes of 10% buffer B/90% buffer A (until the UV trace has returned to baseline). The Q column was then removed. Elution was performed as a 10% buffer B/90% buffer A to 40% buffer B/ 60% buffer A gradient for histones H2A and H2B, and as a 20% buffer B/80% buffer A to 50% buffer B/ 50% buffer A gradient for histones H3 and H4, over 20 column volumes (100mL) at a flow rate of 4mL/minute. Following the gradient elutions, the Q column was washed with 100% buffer B.

Elution fractions were examined on a Coomassie-stained SDS-PAGE mini gel, and fractions containing histones were pooled and dialyzed into lyophilization buffer (10mM Tris-Cl pH 8.0, 5mM β-mercaptoethanol) overnight at 4°C, with 1X PMSF (167μg/mL) added to the dialysis bag. Dialysis buffer was changed twice, at 3 hours and at 6 hours. Following dialysis, samples were divided into 2mg aliquots, as determined by adjusted A280 readings, which were confirmed by comparing proteins to a lysozyme standard on a Coomasssie-stained SDS-PAGE

mini gel. Aliquots were then lyophilized at the Peptide Synthesis facility of the Pitt Genomics and Proteomics Core Laboratory, and kept in long-term storage at -20°C.

For purification of His-Nap1, pKB1208 was transformed into BL21 (DE3) pLysS cells. Fresh transformants were used to inoculate 50mL LB-Kan-Chl media, and cells were grown at 37°C to an OD_{600} of ~1.0. These cells were used to inoculate 1L of LB-Kan-Chl. Cells were grown at 37°C to an OD_{600} of ~0.4-0.5, then shifted to 30°C and grown for an additional 20 minutes. Nap1 expression was then induced with 0.4mM IPTG. Cells were harvested at 2.5-3 hours post-induction, and pellets were flash frozen and stored at -70°C.

The pellet was resuspended in 25mL lysis buffer (50mM Tris-Cl pH 8.0, 100mM KCl, 10mM imidazole, 5mM β-mercaptoethanol) plus 1X protease inhibitors (167μg/mL PMSF, 0.7μg/mL pepstatin, 0.5μg/mL leupeptin, 0.5μg/mL aprotinin) and lysed with an EmulsiFlex-C3 homogenizer. Sample was then sonicated (9X20 seconds on setting 7 with 1.5 minutes on ice in between). Lysate was then spun in SA-600 tubes for 20 minutes at 20,000 x g and 4°C.

Fresh protease inhibitors were added to the supernatant, which was incubated with 2.5mL (see note below) of pre-equilibrated (in lysis buffer) Ni-NTA resin in a 50mL Falcon tube with gentle mixing for 2 hours at 4°C. Resin was collected by low-speed centrifugation (1 minute, 500rpm, 4°C) and then washed three times by gentle mixing with lysis buffer plus 1X protease inhibitors. Resin was then transferred to a disposable column and washed with 10 volumes of buffer A (20mM Tris-Cl pH 8.0, 100mM KCl, 20mM imidazole, 10% glycerol, 5mM β-mercaptoethanol) plus 1X protease inhibitors, then with 5 volumes of buffer B (same as buffer A but with 1M KCl) plus 1X protease inhibitors, then with 10 additional volumes of buffer A plus 1X protease inhibitors. Sample was eluted with 25mL elution buffer (20mM Tris-Cl pH 8.0, 100mM KCl, 150mM imidazole, 10% glycerol, 5mM β-mercaptoethanol) and

collected in 1.0-1.5mL fractions. Fractions were then examined by SDS-PAGE/Coomassie staining and pooled. The presence of a considerable amount of His-Nap1 in the unbound fraction indicates that more Ni-NTA resin should be used for future purifications.

Next, the sample was purified by ion exchange. A HiTrap Q column (5mL) was equilibrated in 0.1M Q buffer (20mM Tris-Cl pH 8.0, 100mM KCl, 0.5mM EDTA pH 8.0, 20mM imidazole, 10% glycerol, 5mM β-mercaptoethanol). Sample was loaded by hand and a "step" elution was performed by adding 15mL of 200mM KCl Q buffer (same as above with respect to other components), then 15mL of 300mM KCl Q buffer, then 15mL of 400mM KCl Q buffer, then 15mL of 600mM KCl Q buffer, followed by a final wash with 10mL 1M KCl Q buffer. Elution fractions were examined by SDS-PAGE/Coomassie staining, pooled, and dialyzed into storage buffer (20mM HEPES-OH pH 7.9, 100mM KCl, 0.2mM EDTA pH 8.0, 20mM imidazole, 10% glycerol, 1mM β-mercaptoethanol). Sample was then concentrated with a Vivaspin concentrator, flash frozen, and stored at -70°C.

A.2.4 Purification of H2A-H2B dimers and H3-H4 tetramers

Lyophilized, 2mg aliquots of each core histone were incubated in 750μL of freshly made unfolding buffer with rotation at room temperature for 75 minutes. H2A sample was then combined with H2B, and H3 sample was combined with H4. Samples were then dialyzed into 2L of freshly made refolding buffer at 4°C (2M NaCl, 10mM Tris-Cl pH 7.5, 0.5mM EDTA pH 8.0, 5mM β-mercaptoethanol). It is imperative that refolding buffer be pre-chilled to 4°C prior to beginning dialysis. Buffer was changed at 2 hours, 4 hours, and 6 hours, and then dialysis proceeded overnight.

On the same day that histones are unfolded and refolded, one should equilibrate the Bio-Rex 70 (Bio-Rad) resin that is used to purify dimers and tetramers. In a 50mL Falcon tube, 8.33g of resin was mixed with 20mL of low-salt "refolding buffer" (500mM NaCl, 10mM Tris-Cl pH 7.5, 0.5mM EDTA pH 8.0, 5mM β-mercaptoethanol) for 30 minutes at 4°C, then collected by spinning at low speed (500rpm) for 2 minutes at 4°C. An additional 20mL of low-salt refolding buffer was added and incubated with the resin for an additional 30 minutes at 4°C, then collected as described. The conductivity of the supernatant was compared to that of the buffer to confirm that they were the same; if the two values are different, an additional buffer exchange should be performed. The resin was resuspended in low-salt refolding buffer and the pH was measured. The pH was adjusted with HCl until the pH of the resuspended resin matched that of the low-salt refolding buffer. Resin was collected as described, then resuspended in 20mL low-salt refolding buffer and incubated overnight at 4°C.

Following overnight dialysis into 2M NaCl refolding buffer, the salt concentration of each sample was diluted to 500mM NaCl by adding no-salt "refolding buffer" (10mM Tris-Cl pH 7.5, 0.5mM EDTA pH 8.0, 5mM β-mercaptoethanol). Each sample (H2A/H2B; H3/H4) was then added to ~1mL bed volume of equilibrated Bio-Rex 70 resin and incubated with rotation for six hours at 4°C. Resin was then packed into a disposable column and washed with 15mL of wash buffer (H2A/H2B: 500mM NaCl, 10mM Tris-Cl pH 8.0, 0.5mM EDTA pH 8.0; H3/H4: 750mM NaCl, 10mM Tris-Cl pH 8.0, 0.5mM EDTA pH 8.0). Samples were then eluted with 6mL elution buffer (H2A/H2B: 1M NaCl, 10mM Tris-Cl pH 8.0, 0.5mM EDTA pH 8.0; H3/H4: 2M NaCl, 10mM Tris-Cl pH 8.0, 0.5mM EDTA pH 8.0) and collected in seven ~850μL fractions. Flowthrough, wash and elution fractions were then examined by SDS-PAGE/Coomassie staining. Elution fractions were pooled (see below) and concentrated to a

final concentration of 0.5-2.0 mg/mL, then mixed with 100% glycerol to a final concentration of 50% and stored at 4°C. Accurate concentrations of dimer and tetramer can be difficult to obtain by A280, and it is advisable to quantitate these preps against a standard such as lysozyme or BSA before proceeding to nucleosome reconstitutions.

Per communication with Dr. Joesph Reese's lab, the Bio-Rex 70 resin should bind to histone dimers and tetramers, and not histone monomers. The protocol received from Dr. Joseph Reese's lab states that fractions in which the H2A:H2B or H3:H4 ratios are 1:1 as determined by SDS-PAGE/Coomassie staining should be pooled, while other elution fractions should be excluded. My experience was that all elution fractions from H2A/H2B samples displayed an H2A:H2B ratio of ~1:1, while the elution fractions from most H3/H4 samples contained a substantial excess of H4. Probing of H3/H4 elution fractions for H3 and H4 by western blot revealed that H3 preferentially failed to fully resolve in the gel, likely leading to an artificially low H3:H4 ratio by Coomassie. Therefore all H3/H4 elution fractions were pooled, concentrated and stored as described irrespective of apparent H3:H4 ratio.

A.2.5 Nucleosome reconstitutions

Two attempts were made to reconstitute nucleosomes using an unlabeled template and ethidium bromide for visualization. Weak staining made it extremely difficult to assess the results. All subsequent reconstitutions were performed with template that was radiolabeled with γ-ATP. Note that radiolabeling of template is for purposes of titrating nucleosome reconstitutions and obtaining substrates for binding assays, and should not be performed when making nucleosomes for the transcription-coupled assays described in Section A.3.

Following preparation of "tailless" template as described in Section A.2.2 (note that template can be biotinylated or not depending on downstream applications), template was end-labeled using T4 Polynucleotide Kinase (NEB). Approximately 1.25μg of template was labeled in a 20μL reaction carried out in 1X PNK buffer (NEB) using 10U (1μL) of enzyme. Approximately 25μCi of γ-ATP was used in each labeling reaction. Reactions were incubated at 37°C for a minimum of 30 minutes, and labeled DNA was then purified using a G-50 spin column. The column was drained of buffer for 10 minutes, and excess buffer was removed by gentle tapping. The column was then spun for 2 minutes at 2500 rpm in a tabletop centrifuge, and excess buffer was again removed by gentle tapping. Following transfer of the column to a fresh collection tube, the labeling reaction was added to the center of the membrane, and the column was then spun for 5 minutes at 2500 rpm in a tabletop centrifuge. The success of the labeling reaction was confirmed by checking 1μL of sample with a scintillation counter.

For purposes of calculating DNA input in nucleosome reconstitutions, 100% recovery from the G-50 column was assumed. Initial reconstitutions were performed with 1μg of DNA, of which 270ng was labeled and 730ng was unlabeled. Later reconstitutions were scaled down to ~650ng of total DNA, keeping the ratio of "hot" to "cold" DNA the same.

Reconstitutions were carried out in 1X assembly buffer (10mM HEPES-KOH pH 7.6, 50mM KCl, 5mM $MgCl_2$, 10% glycerol, 2mg/mL BSA) which was made by adding a from a 4X stock to a final 1X concentration. Reaction volumes are partially determined by protein concentrations (usually tetramer concentrations) but should not exceed 50μL. Reaction components are added in the following order: 4X assembly buffer and ddH_2O, then His-Nap1, then dimer, then tetramer. Following gentle mixing, reactions are incubated for 30 minutes on ice. Hot and cold DNA are then added, along with additional 4X assembly buffer to keep the

concentration at 1X, and reactions were then incubated at 30°C for 4 hours. Reactions are then spun for minutes at 13,500rpm in a 4°C microfuge to remove aggregates. Samples were transferred to a fresh Eppendorf tube and stored at 4°C.

The amount of proteins added to the reactions is determined by performing titrations. For each titration experiment performed, three reactions were carried out, keeping DNA amount constant and varying the amount of the protein components added. A reaction containing only DNA was carried out as a control. As a starting point, the Reese lab protocol suggests that the molar ratio of tetramer:DNA should be 0.8-1.1:1, that the ratio of dimer:tetramer should be 2.2-2.5:1, and that the ratio of His-Nap:dimer should be 2:1. My experience was that a successful reconstitution, i.e. one in which all of the template DNA was incorporated into nucleosomes, fell well outside these ratios (see Figures 26B and 26C for molar ratios of individual reactions), possibly indicating inaccurate quantitation of one or more reaction components.

To determine the success of the reconstitutions, dye-free TBE loading buffer was added to samples at a final concentration of 10% sucrose and 0.75X TBE. Samples were loaded to a 4%, 0.5X TBE native polyacrylamide gel that had been pre-run at 100V for a minimum of 1 hour, and the gel was run at 100V for ~4 hours in the cold room (~4°C). TBE loading buffer containing bromophenol blue dye was run in outside, empty lanes in order to estimate the migration of samples. Gels were dried and imaged on a Typhoon FLA 7000 instrument.

A.2.6 Gel purification of labeled nucleosomes

A nucleosome reconstitution was performed as described in Section A.2.5 using 700ng of labeled template. Ratios of other components were determined by titration as shown in Figures 28B and 28C. The sample was loaded to a 5%, 0.3X TBE native polyacrylamide gel that had

been pre-run at 180V for a minimum of 1 hour, and the gel was run at 180V for ~4 hours in the cold room (~4°C). A free DNA sample was loaded for purposes of comparison to the nucleosome reconstitution sample, and TBE loading buffer containing bromophenol blue dye was run in outside, empty lanes in order to estimate the migration of samples.

The glass plates containing the gel were then separated, and the gel was covered with saran wrap. A radioactive Sharpie was used to create landmarks near the gel for purposes of orientation. The gel was covered with a radiation-sensitive screen for 5 minutes, and an image was taken on a Typhoon FLA 7000 instrument. With assistance from Roni Lahr and Daniel Totten in Dr. Andrea Berman's lab, this image was used to create a transparency, which was aligned to the landmarks so that the positions of free DNA and nucleosomes could be identified. Nucleosomes were excised from the gel. A second image was taken to confirm that nucleosomes had been removed and that any free DNA in the sample remained in the gel. The excised gel slice was transferred to an Eppendorf tube, crushed with a closed P200 tip, and then incubated overnight with rotation at 4°C in 200µL gel elution buffer (10mM Tris-Cl pH 7.4, 100mM NaCl, 1mM EDTA pH 8.0, 5mM DTT, 0.5mM PMSF, 0.1 mg/mL BSA).

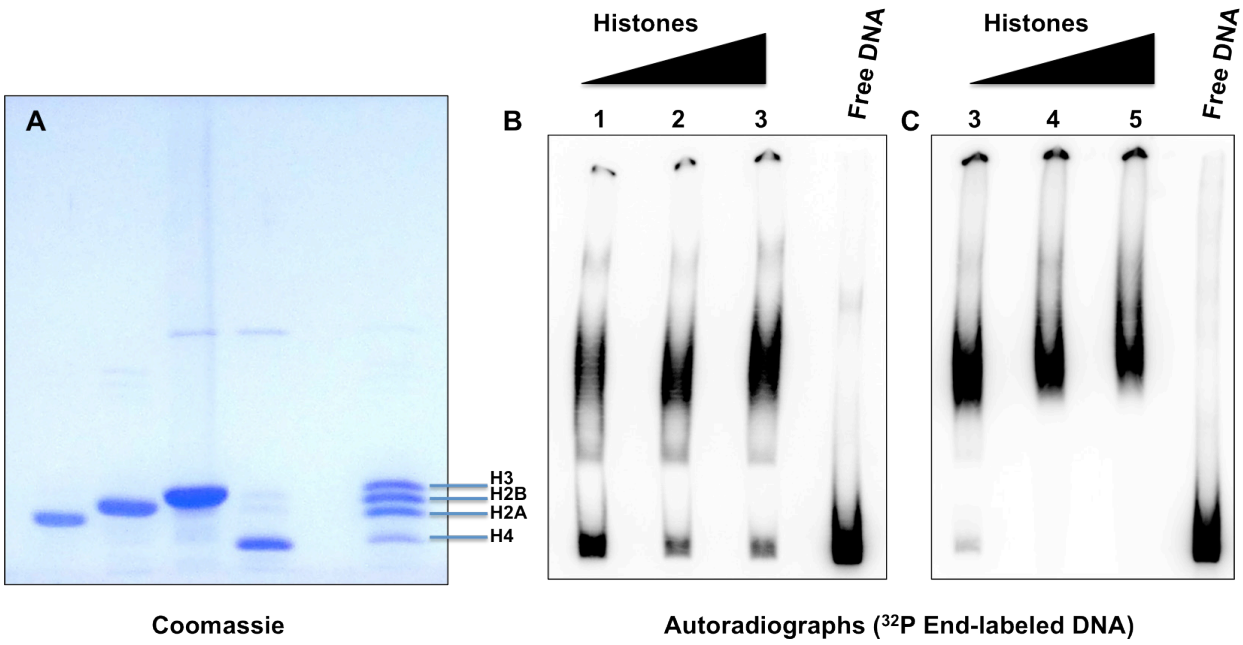

Figure 28: Reconstitution of yeast nucleosomes

(A) Coomassie stained gel showing the successful purification of the 4 core histones prior to lyophilization. (B and C) Nucleosome reconstitutions were performed by titrating dimer, tetramer, and His-Nap1 in order to determine the amount required for full incorporation of radiolabeled DNA into the nucleosome. The approximate molar ratios of each component, relative to the DNA, are: (1) Tetramer: 3.8:1; Dimer: 14.4:1; His-Nap1: 28.3:1 (2) Tetramer: 6.6:1; Dimer: 14.4:1; His-Nap1: 28.3:1 (3) Tetramer: 6.6:1; Dimer: 20.1:1; His-Nap1: 39.6:1 (4) Tetramer: 11.6:1; Dimer: 35.2:1; His-Nap1: 69.3:1 (5) Tetramer: 16.6:1; Dimer: 50.3:1; His-Nap1: 99.0:1. Reaction 4 indicates the optimal molar ratios for a reconstitution using these reagents. Note that a titration must be performed with each new batch of reaction components.

Samples were then centrifuged for 5 minutes at 21,000 x g and 4°C, and a barrier tip was used to transfer the liquid to a fresh Eppendorf tube. 5X gel final buffer (10mM Tris-Cl pH 7.4, 100mM NaCl, 1mM EDTA pH 8.0, 5mM DTT, 0.5mM PMSF, 0.1 mg/mL BSA, 50% glycerol, 0.25% NP-40) was added to a final concentration of 1X. An aliquot of the sample was checked with a scintillation counter. To estimate the DNA content of the purified nucleosomes, I assumed 90% recovery of DNA from the end-labeling reaction. The reading from the scintillation counter at the time of the end-labeling reaction was adjusted for decay, and compared to the reading from the purified nucleosome sample to determine the percent recovery.

A.3 APPLICATIONS OF THIS SYSTEM

The role of transcription in HMD-mediated H2Bub, and the effect of H2Bub on transcription, remain open questions. The DNA template described in this chapter can be used to carry out transcription-coupled, *in vitro* ubiquitylation reactions. Unlike previous transcription-coupled systems that have examined H2Bub, which make use of a host of initiation factors (Kim, et al. 2009), transcription from a tailed template can be initiated by simple addition of the dinucleotide UpG (Zhang, Fu, et al. 2005; Kruk, et al. 2011). Pol II can be preincubated with radioactive [α-^{32}P] UTP, followed by addition of a "cold" nucleotide mix lacking GTP. Pol II will then transcribe through the G-less cassette portion of the transcript, upstream of the nucleosome, and arrest when it encounters a guanine. At this point, GTP and cold UTP are added to the reaction, plus or minus factors of interest (Kruk, et al. 2011), such as ubiquitylation factors including the HMD. H2Bub can then be measured by western blot to determine the role

of the HMD in the context of active transcription. Furthermore, assuming that ubiquitylation takes place under these conditions, the amount of labeled "run-off" RNA products can be assessed to determine the effect of ubiquitylation on transcriptional output. Such reactions can be carried out on nucleosomes purified as described above, or using biotinylated nucleosomes that have been immobilized on streptavidin beads, as has been described (Yun, et al. 2012). The latter method has the advantage of confidently removing the His-Nap1 used in reconstitutions from the reactions.

As described in Section 3.2.5, radiolabeled nucleosomes can be purified and used as substrates in binding assays. The binding assays I conducted used nucleosomes devoid of any histone modifications. In the cell, however, catalysis of H2Bub occurs in the context of nucleosomes that are copiously and dynamically modified at other sites. The cumulative evidence of *in vitro* studies of H2Bub suggests the possibility of modifications that are inhibitory to HMD stimulation of H2Bub (see Section 3.4). If one wishes to make nucleosomes containing specific modifications, in vitro reactions with the required histone modification factors can be carried out as described on immobilized nucleosomes (Yun, et al. 2012), which can subsequently be released from beads via restriction enzymes and gel purified for use in binding assays. Finally, this system is readily adaptable to the study of histone mutants and the effects that they have on ubiquitylation. Mutant nucleosomes can be constructed to examine, for example, the effect of the HMD in the context of mutations to the H2A repression domain (see Section 1.5.2), or to examine the effect of the HMD on Rad6-dependent ubiquitylation of other sites on H2B, as described in Section 4.1.

BIBLIOGRAPHY

Adelman K, Lis JT. 2012. Promoter-proximal pausing of RNA polymerase II: emerging roles in metazoans. Nat Rev Genet 13:720-731.

Adelman K, Wei W, Ardehali MB, Werner J, Zhu B, Reinberg D, Lis JT. 2006. Drosophila Paf1 modulates chromatin structure at actively transcribed genes. Mol Cell Biol 26:250-260.

Ahn SH, Kim M, Buratowski S. 2004. Phosphorylation of serine 2 within the RNA polymerase II C-terminal domain couples transcription and 3' end processing. Mol Cell 13:67-76.

Akanuma T, Koshida S, Kawamura A, Kishimoto Y, Takada S. 2007. Paf1 complex homologues are required for Notch-regulated transcription during somite segmentation. EMBO Rep 8:858-863.

Albert TK, Antrecht C, Kremmer E, Meisterernst M. 2016. The Establishment of a Hyperactive Structure Allows the Tumour Suppressor Protein p53 to Function through P-TEFb during Limited CDK9 Kinase Inhibition. PLoS One 11:e0146648.

Allen BL, Taatjes DJ. 2015. The Mediator complex: a central integrator of transcription. Nat Rev Mol Cell Biol 16:155-166.

Alpert T, Herzel L, Neugebauer KM. 2017. Perfect timing: splicing and transcription rates in living cells. Wiley Interdiscip Rev RNA 8.

Bahrampour S, Thor S. 2016. Ctr9, a Key Component of the Paf1 Complex Affects Proliferation and Terminal Differentiation in the Developing Drosophila Nervous System. G3 (Bethesda).

Bartkowiak B, Liu P, Phatnani HP, Fuda NJ, Cooper JJ, Price DH, Adelman K, Lis JT, Greenleaf AL. 2010. CDK12 is a transcription elongation-associated CTD kinase, the metazoan ortholog of yeast Ctk1. Genes Dev 24:2303-2316.

Basnet H, Su XB, Tan Y, Meisenhelder J, Merkurjev D, Ohgi KA, Hunter T, Pillus L, Rosenfeld MG. 2014. Tyrosine phosphorylation of histone H2A by CK2 regulates transcriptional elongation. Nature 516:267-271.

Batta K, Zhang Z, Yen K, Goffman DB, Pugh BF. 2011. Genome-wide function of H2B ubiquitylation in promoter and genic regions. Genes Dev 25:2254-2265.

Battaglia S, Lidschreiber M, Baejen C, Torkler P, Vos SM, Cramer P. 2017. RNA-dependent chromatin association of transcription elongation factors and Pol II CTD kinases. Elife 6.

Bedard LG, Dronamraju R, Kerschner JL, Hunter GO, Axley ED, Boyd AK, Strahl BD, Mosley AL. 2016. Quantitative Analysis of Dynamic Protein Interactions during Transcription Reveals a Role for Casein Kinase II in Polymerase-associated Factor (PAF) Complex Phosphorylation and Regulation of Histone H2B Monoubiquitylation. J Biol Chem 291:13410-13420.

Bentley DL. 2014. Coupling mRNA processing with transcription in time and space. Nat Rev Genet 15:163-175.

Betz JL, Chang M, Washburn TM, Porter SE, Mueller CL, Jaehning JA. 2002. Phenotypic analysis of Paf1/RNA polymerase II complex mutations reveals connections to cell cycle regulation, protein synthesis, and lipid and nucleic acid metabolism. Mol Genet Genomics 268:272-285.

Blackwell JS, Jr., Wilkinson ST, Mosammaparast N, Pemberton LF. 2007. Mutational analysis of H3 and H4 N termini reveals distinct roles in nuclear import. J Biol Chem 282:20142-20150.

Bohm S, Szakal B, Herken BW, Sullivan MR, Mihalevic MJ, Kabbinavar FF, Branzei D, Clark NL, Bernstein KA. 2016. The Budding Yeast Ubiquitin Protease Ubp7 Is a Novel Component Involved in S Phase Progression. J Biol Chem 291:4442-4452.

Bowman EA, Kelly WG. 2014. RNA polymerase II transcription elongation and Pol II CTD Ser2 phosphorylation: A tail of two kinases. Nucleus 5:224-236.

Bray S, Musisi H, Bienz M. 2005. Bre1 is required for Notch signaling and histone modification. Dev Cell 8:279-286.

Buratowski S. 2009. Progression through the RNA polymerase II CTD cycle. Mol Cell 36:541-546.

Cao QF, Yamamoto J, Isobe T, Tateno S, Murase Y, Chen Y, Handa H, Yamaguchi Y. 2015. Characterization of the Human Transcription Elongation Factor Rtf1: Evidence for Nonoverlapping Functions of Rtf1 and the Paf1 Complex. Mol Cell Biol 35:3459-3470.

Castro PG, van Roon EHJ, Pinhancos SSM, Trentin L, Schneider P, Kerstjens M, Te Kronnie G, Heidenreich O, Pieters R, Stam RW. 2017. The HDAC inhibitor Panobinostat (LBH589) exerts in vivo anti-leukaemic activity against MLL-rearranged acute lymphoblastic leukaemia and involves the RNF20/RNF40/WAC-H2B ubiquitination axis. Leukemia.

Chandrasekharan MB, Huang F, Sun ZW. 2009. Ubiquitination of histone H2B regulates chromatin dynamics by enhancing nucleosome stability. Proc. Natl. Acad. Sci. USA 106:16686-16691.

Chen FX, Woodfin AR, Gardini A, Rickels RA, Marshall SA, Smith ER, Shiekhattar R, Shilatifard A. 2015. PAF1, a Molecular Regulator of Promoter-Proximal Pausing by RNA Polymerase II. Cell 162:1003-1015.

Chen Y, Yamaguchi Y, Tsugeno Y, Yamamoto J, Yamada T, Nakamura M, Hisatake K, Handa H. 2009. DSIF, the Paf1 complex, and Tat-SF1 have nonredundant, cooperative roles in RNA polymerase II elongation. Genes Dev 23:2765-2777.

Cheung AC, Cramer P. 2011. Structural basis of RNA polymerase II backtracking, arrest and reactivation. Nature 471:249-253.

Cheung V, Chua G, Batada NN, Landry CR, Michnick SW, Hughes TR, Winston F. 2008. Chromatin- and transcription-related factors repress transcription from within coding regions throughout the Saccharomyces cerevisiae genome. PLoS Biol 6:e277.

Chin JW, Cropp TA, Anderson JC, Mukherji M, Zhang Z, Schultz PG. 2003. An expanded eukaryotic genetic code. Science 301:964-967.

Chu X, Qin X, Xu H, Li L, Wang Z, Li F, Xie X, Zhou H, Shen Y, Long J. 2013. Structural insights into Paf1 complex assembly and histone binding. Nucleic Acids Res 41:10619-10629.

Chu Y, Simic R, Warner MH, Arndt KM, Prelich G. 2007. Regulation of histone modification and cryptic transcription by the Bur1 and Paf1 complexes. EMBO J 26:4646-4656.

Churchman LS, Weissman JS. 2011. Nascent transcript sequencing visualizes transcription at nucleotide resolution. Nature 469:368-373.

Clark NL, Alani E, Aquadro CF. 2012. Evolutionary rate covariation reveals shared functionality and coexpression of genes. Genome Res 22:714-720.

Conaway RC, Conaway JW. 2013. The Mediator complex and transcription elongation. Biochim Biophys Acta 1829:69-75.

Costa PJ, Arndt KM. 2000. Synthetic lethal interactions suggest a role for the Saccharomyces cerevisiae Rtf1 protein in transcription elongation. Genetics 156:535-547.

Cox JS, Chapman RE, Walter P. 1997. The unfolded protein response coordinates the production of endoplasmic reticulum protein and endoplasmic reticulum membrane. Mol. Biol. Cell 8:1805-1814.

Cucinotta CE, Young AN, Klucevsek KM, Arndt KM. 2015. The nucleosome acidic patch regulates the H2B K123 monoubiquitylation cascade and transcription elongation in Saccharomyces cerevisiae. PLoS Genet. 11:e1005420.

Cui P, Jin H, Vutukuru MR, Kaplan CD. 2016. Relationships Between RNA Polymerase II Activity and Spt Elongation Factors to Spt- Phenotype and Growth in Saccharomyces cerevisiae. G3 (Bethesda) 6:2489-2504.

Dermody JL, Buratowski S. 2010. Leo1 subunit of the yeast paf1 complex binds RNA and contributes to complex recruitment. J Biol Chem 285:33671-33679.

Dickson KA, Cole AJ, Gill AJ, Clarkson A, Gard GB, Chou A, Kennedy CJ, Henderson BR, Australian Ovarian Cancer S, Fereday S, et al. 2016. The RING finger domain E3 ubiquitin ligases BRCA1 and the RNF20/RNF40 complex in global loss of the chromatin mark histone H2B monoubiquitination (H2Bub1) in cell line models and primary high-grade serous ovarian cancer. Hum Mol Genet 25:5460-5471.

Ding L, Paszkowski-Rogacz M, Nitzsche A, Slabicki MM, Heninger AK, de Vries I, Kittler R, Junqueira M, Shevchenko A, Schulz H, et al. 2009. A genome-scale RNAi screen for Oct4 modulators defines a role of the Paf1 complex for embryonic stem cell identity. Cell Stem Cell 4:403-415.

Dominguez C, Boelens R, Bonvin AM. 2003. HADDOCK: a protein-protein docking approach based on biochemical or biophysical information. J Am Chem Soc 125:1731-1737.

Dormán G, Prestwich GD. 1994. Benzophenone photophores in biochemistry. Biochemistry 33:5661-5673.

Dronamraju R, Strahl BD. 2014. A feed forward circuit comprising Spt6, Ctk1 and PAF regulates Pol II CTD phosphorylation and transcription elongation. Nucleic Acids Res 42:870-881.

Eckschlager T, Plch J, Stiborova M, Hrabeta J. 2017. Histone Deacetylase Inhibitors as Anticancer Drugs. Int J Mol Sci 18.

Fierz B, Chatterjee C, McGinty RK, Bar-Dagan M, Raleigh DP, Muir TW. 2011. Histone H2B ubiquitylation disrupts local and higher-order chromatin compaction. Nat Chem Biol 7:113-119.

Fischl H, Howe FS, Furger A, Mellor J. 2017. Paf1 Has Distinct Roles in Transcription Elongation and Differential Transcript Fate. Mol Cell 65:685-698 e688.

Flanagan JF, Mi LZ, Chruszcz M, Cymborowski M, Clines KL, Kim Y, Minor W, Rastinejad F, Khorasanizadeh S. 2005. Double chromodomains cooperate to recognize the methylated histone H3 tail. Nature 438:1181-1185.

Fleming AB, Kao CF, Hillyer C, Pikaart M, Osley MA. 2008. H2B ubiquitylation plays a role in nucleosome dynamics during transcription elongation. Mol Cell 31:57-66.

Fong N, Saldi T, Sheridan RM, Cortazar MA, Bentley DL. 2017. RNA Pol II Dynamics Modulate Co-transcriptional Chromatin Modification, CTD Phosphorylation, and Transcriptional Direction. Mol Cell 66:546-557 e543.

Fonseca GJ, Cohen MJ, Mymryk JS. 2014. Adenovirus E1A recruits the human Paf1 complex to enhance transcriptional elongation. J Virol 88:5630-5637.

Fonseca GJ, Cohen MJ, Nichols AC, Barrett JW, Mymryk JS. 2013. Viral retasking of hBre1/RNF20 to recruit hPaf1 for transcriptional activation. PLoS Pathog 9:e1003411.

Formosa T. 2012. The role of FACT in making and breaking nucleosomes. Biochim Biophys Acta 1819:247-255.

Fuchs G, Hollander D, Voichek Y, Ast G, Oren M. 2014. Cotranscriptional histone H2B monoubiquitylation is tightly coupled with RNA polymerase II elongation rate. Genome Res 24:1572-1583.

Fuchs G, Shema E, Vesterman R, Kotler E, Wolchinsky Z, Wilder S, Golomb L, Pribluda A, Zhang F, Haj-Yahya M, et al. 2012. RNF20 and USP44 regulate stem cell differentiation by modulating H2B monoubiquitylation. Mol. Cell 46:662-673.

Gallego LD, Ghodgaonkar Steger M, Polyansky AA, Schubert T, Zagrovic B, Zheng N, Clausen T, Herzog F, Kohler A. 2016. Structural mechanism for the recognition and ubiquitination of a single nucleosome residue by Rad6-Bre1. Proc Natl Acad Sci U S A 113:10553-10558.

Geng F, Tansey WP. 2008. Polyubiquitylation of histone H2B. Mol Biol Cell 19:3616-3624.

Giannattasio M, Lazzaro F, Plevani P, Muzi-Falconi M. 2005. The DNA damage checkpoint response requires histone H2B ubiquitination by Rad6-Bre1 and H3 methylation by Dot1. J Biol Chem 280:9879-9886.

Gupta K, Sari-Ak D, Haffke M, Trowitzsch S, Berger I. 2016. Zooming in on Transcription Preinitiation. J Mol Biol 428:2581-2591.

Haas AL, Bright PM, Jackson VE. 1988. Functional diversity among putative E2 isozymes in the mechanism of ubiquitin-histone ligation. J. Biol. Chem. 263:13268-13275.

Hahn MA, Dickson KA, Jackson S, Clarkson A, Gill AJ, Marsh DJ. 2012. The tumor suppressor CDC73 interacts with the ring finger proteins RNF20 and RNF40 and is required for the maintenance of histone 2B monoubiquitination. Hum Mol Genet 21:559-568.

Hanks S, Perdeaux ER, Seal S, Ruark E, Mahamdallie SS, Murray A, Ramsay E, Del Vecchio Duarte S, Zachariou A, de Souza B, et al. 2014. Germline mutations in the PAF1 complex gene CTR9 predispose to Wilms tumour. Nat Commun 5:4398.

He N, Chan CK, Sobhian B, Chou S, Xue Y, Liu M, Alber T, Benkirane M, Zhou Q. 2011. Human Polymerase-Associated Factor complex (PAFc) connects the Super Elongation Complex (SEC) to RNA polymerase II on chromatin. Proc Natl Acad Sci U S A 108:E636-645.

Henry KW, Berger SL. 2002. Trans-tail histone modifications: wedge or bridge? Nat Struct Biol 9:565-566.

Henry KW, Wyce A, Lo WS, Duggan LJ, Emre NC, Kao CF, Pillus L, Shilatifard A, Osley MA, Berger SL. 2003. Transcriptional activation via sequential histone H2B ubiquitylation and deubiquitylation, mediated by SAGA-associated Ubp8. Genes Dev. 17:2648-2663.

Hepp MI, Alarcon V, Dutta A, Workman JL, Gutierrez JL. 2014. Nucleosome remodeling by the SWI/SNF complex is enhanced by yeast high mobility group box (HMGB) proteins. Biochim Biophys Acta 1839:764-772.

Herissant L, Moehle EA, Bertaccini D, Van Dorsselaer A, Schaeffer-Reiss C, Guthrie C, Dargemont C. 2014. H2B ubiquitylation modulates spliceosome assembly and function in budding yeast. Biol Cell 106:126-138.

Hibbert RG, Huang A, Boelens R, Sixma TK. 2011. E3 ligase Rad18 promotes monoubiquitination rather than ubiquitin chain formation by E2 enzyme Rad6. Proc Natl Acad Sci U S A 108:5590-5595.

Hoege C, Pfander B, Moldovan GL, Pyrowolakis G, Jentsch S. 2002. RAD6-dependent DNA repair is linked to modification of PCNA by ubiquitin and SUMO. Nature 419:135-141.

Holt LJ, Tuch BB, Villen J, Johnson AD, Gygi SP, Morgan DO. 2009. Global analysis of Cdk1 substrate phosphorylation sites provides insights into evolution. Science 325:1682-1686.

Hung SH, Wong RP, Ulrich HD, Kao CF. 2017. Monoubiquitylation of histone H2B contributes to the bypass of DNA damage during and after DNA replication. Proc Natl Acad Sci U S A 114:E2205-E2214.

Hwang WW, Venkatasubrahmanyam S, Ianculescu AG, Tong A, Boone C, Madhani HD. 2003. A conserved RING finger protein required for histone H2B monoubiquitination and cell size control. Mol. Cell 11:261-266.

Ito T, Levenstein ME, Fyodorov DV, Kutach AK, Kobayashi R, Kadonaga JT. 1999. ACF consists of two subunits, Acf1 and ISWI, that function cooperatively in the ATP-dependent catalysis of chromatin assembly. Genes Dev. 13:1529-1539.

Jacquier A. 2009. The complex eukaryotic transcriptome: unexpected pervasive transcription and novel small RNAs. Nat Rev Genet 10:833-844.

Jaenicke LA, von Eyss B, Carstensen A, Wolf E, Xu W, Greifenberg AK, Geyer M, Eilers M, Popov N. 2016. Ubiquitin-Dependent Turnover of MYC Antagonizes MYC/PAF1C Complex Accumulation to Drive Transcriptional Elongation. Mol Cell 61:54-67.

Jiang C, Pugh BF. 2009. A compiled and systematic reference map of nucleosome positions across the Saccharomyces cerevisiae genome. Genome Biol 10:R109.

Jonkers I, Lis JT. 2015. Getting up to speed with transcription elongation by RNA polymerase II. Nat Rev Mol Cell Biol 16:167-177.

Kao CF, Hillyer C, Tsukuda T, Henry K, Berger S, Osley MA. 2004. Rad6 plays a role in transcriptional activation through ubiquitylation of histone H2B. Genes Dev 18:184-195.

Karmakar S, Seshacharyulu P, Lakshmanan I, Vaz AP, Chugh S, Sheinin YM, Mahapatra S, Batra SK, Ponnusamy MP. 2017. hPaf1/PD2 interacts with OCT3/4 to promote self-renewal of ovarian cancer stem cells. Oncotarget 8:14806-14820.

Karpiuk O, Najafova Z, Kramer F, Hennion M, Galonska C, König A, Snaidero N, Vogel T, Shchebet A, Begus-Nahrmann Y, et al. 2012. The histone H2B monoubiquitination regulatory pathway is required for differentiation of multipotent stem cells. Mol. Cell 46:705-713.

Katahira J. 2015. Nuclear export of messenger RNA. Genes (Basel) 6:163-184.

Keogh MC, Kurdistani SK, Morris SA, Ahn SH, Podolny V, Collins SR, Schuldiner M, Chin K, Punna T, Thompson NJ, et al. 2005. Cotranscriptional set2 methylation of histone H3 lysine 36 recruits a repressive Rpd3 complex. Cell 123:593-605.

Kikuchi I, Takahashi-Kanemitsu A, Sakiyama N, Tang C, Tang PJ, Noda S, Nakao K, Kassai H, Sato T, Aiba A, et al. 2016. Dephosphorylated parafibromin is a transcriptional coactivator of the Wnt/Hedgehog/Notch pathways. Nat Commun 7:12887.

Kim J, Guermah M, McGinty RK, Lee JS, Tang Z, Milne TA, Shilatifard A, Muir TW, Roeder RG. 2009. RAD6-Mediated transcription-coupled H2B ubiquitylation directly stimulates H3K4 methylation in human cells. Cell 137:459-471.

Kim J, Guermah M, Roeder RG. 2010. The human PAF1 complex acts in chromatin transcription elongation both independently and cooperatively with SII/TFIIS. Cell 140:491-503.

Kim J, Kim JA, McGinty RK, Nguyen UT, Muir TW, Allis CD, Roeder RG. 2013. The n-SET domain of Set1 regulates H2B ubiquitylation-dependent H3K4 methylation. Mol Cell 49:1121-1133.

Kim J, Roeder RG. 2009. Direct Bre1-Paf1 complex interactions and RING finger-independent Bre1-Rad6 interactions mediate histone H2B ubiquitylation in yeast. J Biol Chem 284:20582-20592.

Kim T, Buratowski S. 2009. Dimethylation of H3K4 by Set1 recruits the Set3 histone deacetylase complex to 5' transcribed regions. Cell 137:259-272.

Koken MH, Reynolds P, Jaspers-Dekker I, Prakash L, Prakash S, Bootsma D, Hoeijmakers JH. 1991. Structural and functional conservation of two human homologs of the yeast DNA repair gene RAD6. Proc Natl Acad Sci U S A 88:8865-8869.

Kowalik KM, Shimada Y, Flury V, Stadler MB, Batki J, Buhler M. 2015. The Paf1 complex represses small-RNA-mediated epigenetic gene silencing. Nature 520:248-252.

Krogan NJ, Dover J, Khorrami S, Greenblatt JF, Schneider J, Johnston M, Shilatifard A. 2002. COMPASS, a histone H3 (Lysine 4) methyltransferase required for telomeric silencing of gene expression. J. Biol. Chem. 277:10753-10755.

Krogan NJ, Dover J, Wood A, Schneider J, Heidt J, Boateng MA, Dean K, Ryan OW, Golshani A, Johnston M, et al. 2003. The Paf1 complex is required for histone H3 methylation by COMPASS and Dot1p: linking transcriptional elongation to histone methylation. Mol Cell 11:721-729.

Krogan NJ, Kim M, Ahn SH, Zhong G, Kobor MS, Cagney G, Emili A, Shilatifard A, Buratowski S, Greenblatt JF. 2002. RNA polymerase II elongation factors of Saccharomyces cerevisiae: a targeted proteomics approach. Mol Cell Biol 22:6979-6992.

Kruk JA, Dutta A, Fu J, Gilmour DS, Reese JC. 2011. The multifunctional Ccr4-Not complex directly promotes transcription elongation. Genes Dev 25:581-593.

Kumar P, Magala P, Geiger-Schuller KR, Majumdar A, Tolman JR, Wolberger C. 2015. Role of a non-canonical surface of Rad6 in ubiquitin conjugating activity. Nucleic Acids Res 43:9039-9050.

Kumar P, Wolberger C. 2015. Structure of the yeast Bre1 RING domain. Proteins 83:1185-1190.

Kuranda K, Leberre V, Sokol S, Palamarczyk G, Francois J. 2006. Investigating the caffeine effects in the yeast Saccharomyces cerevisiae brings new insights into the connection between TOR, PKC and Ras/cAMP signalling pathways. Mol Microbiol 61:1147-1166.

Langenbacher AD, Nguyen CT, Cavanaugh AM, Huang J, Lu F, Chen JN. 2011. The PAF1 complex differentially regulates cardiomyocyte specification. Dev Biol 353:19-28.

Laribee RN, Krogan NJ, Xiao T, Shibata Y, Hughes TR, Greenblatt JF, Strahl BD. 2005. BUR kinase selectively regulates H3 K4 trimethylation and H2B ubiquitylation through recruitment of the PAF elongation complex. Curr Biol 15:1487-1493.

Lee JS, Shukla A, Schneider J, Swanson SK, Washburn MP, Florens L, Bhaumik SR, Shilatifard A. 2007. Histone crosstalk between H2B monoubiquitination and H3 methylation mediated by COMPASS. Cell 131:1084-1096.

Licatalosi DD, Geiger G, Minet M, Schroeder S, Cilli K, McNeil JB, Bentley DL. 2002. Functional interaction of yeast pre-mRNA 3' end processing factors with RNA polymerase II. Mol Cell 9:1101-1111.

Liu X, Bushnell DA, Kornberg RD. 2013. RNA polymerase II transcription: structure and mechanism. Biochim Biophys Acta 1829:2-8.

Liu X, Kraus WL, Bai X. 2015. Ready, pause, go: regulation of RNA polymerase II pausing and release by cellular signaling pathways. Trends Biochem Sci 40:516-525.

Liu Y, Warfield L, Zhang C, Luo J, Allen J, Lang WH, Ranish J, Shokat KM, Hahn S. 2009. Phosphorylation of the transcription elongation factor Spt5 by yeast Bur1 kinase stimulates recruitment of the PAF complex. Mol Cell Biol 29:4852-4863.

Lowary PT, Widom J. 1998. New DNA sequence rules for high affinity binding to histone octamer and sequence-directed nucleosome positioning. J Mol Biol 276:19-42.

Lu X, Zhu X, Li Y, Liu M, Yu B, Wang Y, Rao M, Yang H, Zhou K, Wang Y, et al. 2016. Multiple P-TEFbs cooperatively regulate the release of promoter-proximally paused RNA polymerase II. Nucleic Acids Res 44:6853-6867.

Luger K, Mader AW, Richmond RK, Sargent DF, Richmond TJ. 1997. Crystal structure of the nucleosome core particle at 2.8 A resolution. Nature 389:251-260.

Luse DS. 2013. Promoter clearance by RNA polymerase II. Biochim Biophys Acta 1829:63-68.

Maniatis T, Reed R. 2002. An extensive network of coupling among gene expression machines. Nature 416:499-506.

Marquardt S, Hazelbaker DZ, Buratowski S. 2011. Distinct RNA degradation pathways and 3' extensions of yeast non-coding RNA species. Transcription 2:145-154.

Mayekar MK, Gardner RG, Arndt KM. 2013. The recruitment of the Saccharomyces cerevisiae Paf1 complex to active genes requires a domain of Rtf1 that directly interacts with the Spt4-Spt5 complex. Mol Cell Biol 33:3259-3273.

Mayer A, Landry HM, Churchman LS. 2017. Pause & go: from the discovery of RNA polymerase pausing to its functional implications. Curr Opin Cell Biol 46:72-80.

Mayer A, Lidschreiber M, Siebert M, Leike K, Soding J, Cramer P. 2010. Uniform transitions of the general RNA polymerase II transcription complex. Nat Struct Mol Biol 17:1272-1278.

Mbogning J, Nagy S, Page V, Schwer B, Shuman S, Fisher RP, Tanny JC. 2013. The PAF complex and Prf1/Rtf1 delineate distinct Cdk9-dependent pathways regulating transcription elongation in fission yeast. PLoS Genet 9:e1004029.

McGinty RK, Kim J, Chatterjee C, Roeder RG, Muir TW. 2008. Chemically ubiquitylated histone H2B stimulates hDot1L-mediated intranucleosomal methylation. Nature 453:812-816.

Meas R, Mao P. 2015. Histone ubiquitylation and its roles in transcription and DNA damage response. DNA Repair (Amst) 36:36-42.

Melling N, Grimm N, Simon R, Stahl P, Bokemeyer C, Terracciano L, Sauter G, Izbicki JR, Marx AH. 2016. Loss of H2Bub1 Expression is Linked to Poor Prognosis in Nodal Negative Colorectal Cancers. Pathol Oncol Res 22:95-102.

Mischo HE, Proudfoot NJ. 2013. Disengaging polymerase: terminating RNA polymerase II transcription in budding yeast. Biochim Biophys Acta 1829:174-185.

Missra A, Gilmour DS. 2010. Interactions between DSIF (DRB sensitivity inducing factor), NELF (negative elongation factor), and the Drosophila RNA polymerase II transcription elongation complex. Proc Natl Acad Sci U S A 107:11301-11306.

Mohan S, Rizaldy R, Das D, Bauer RJ, Heroux A, Trakselis MA, Hildebrand JD, VanDemark AP. 2012. Structure of Shroom domain 2 reveals a three-segmented coiled-coil required for dimerization, Rock binding, and apical constriction. Mol Biol Cell 23:2131-2142.

Moniaux N, Nemos C, Schmied BM, Chauhan SC, Deb S, Morikane K, Choudhury A, Vanlith M, Sutherlin M, Sikela JM, et al. 2006. The human homologue of the RNA polymerase II-associated factor 1 (hPaf1), localized on the 19q13 amplicon, is associated with tumorigenesis. Oncogene 25:3247-3257.

Morgan MT, Haj-Yahya M, Ringel AE, Bandi P, Brik A, Wolberger C. 2016. Structural basis for histone H2B deubiquitination by the SAGA DUB module. Science 351:725-728.

Morgan MT, Wolberger C. 2017. Recognition of ubiquitinated nucleosomes. Curr Opin Struct Biol 42:75-82.

Mosammaparast N, Guo Y, Shabanowitz J, Hunt DF, Pemberton LF. 2002. Pathways mediating the nuclear import of histones H3 and H4 in yeast. J Biol Chem 277:862-868.

Mosimann C, Hausmann G, Basler K. 2006. Parafibromin/Hyrax activates Wnt/Wg target gene transcription by direct association with beta-catenin/Armadillo. Cell 125:327-341.

Mueller CL, Jaehning JA. 2002. Ctr9, Rtf1, and Leo1 are components of the Paf1/RNA polymerase II complex. Mol Cell Biol 22:1971-1980.

Mueller CL, Porter SE, Hoffman MG, Jaehning JA. 2004. The Paf1 complex has functions independent of actively transcribing RNA polymerase II. Mol Cell 14:447-456.

Murakami K, Tsai KL, Kalisman N, Bushnell DA, Asturias FJ, Kornberg RD. 2015. Structure of an RNA polymerase II preinitiation complex. Proc Natl Acad Sci U S A 112:13543-13548.

Mutiu AI, Hoke SM, Genereaux J, Liang G, Brandl CJ. 2007. The role of histone ubiquitylation and deubiquitylation in gene expression as determined by the analysis of an HTB1(K123R) Saccharomyces cerevisiae strain. Mol Genet Genomics 277:491-506.

Nagaike T, Logan C, Hotta I, Rozenblatt-Rosen O, Meyerson M, Manley JL. 2011. Transcriptional activators enhance polyadenylation of mRNA precursors. Mol Cell 41:409-418.

Newey PJ, Bowl MR, Thakker RV. 2009. Parafibromin--functional insights. J Intern Med 266:84-98.

Ng HH, Dole S, Struhl K. 2003. The Rtf1 component of the Paf1 transcriptional elongation complex is required for ubiquitination of histone H2B. J Biol Chem 278:33625-33628.

Ng HH, Robert F, Young RA, Struhl K. 2003. Targeted recruitment of Set1 histone methylase by elongating Pol II provides a localized mark and memory of recent transcriptional activity. Mol. Cell 11:709-719.

Nguyen AT, Zhang Y. 2011. The diverse functions of Dot1 and H3K79 methylation. Genes Dev. 25:1345-1358.

Nguyen CT, Langenbacher A, Hsieh M, Chen JN. 2010. The PAF1 complex component Leo1 is essential for cardiac and neural crest development in zebrafish. Dev Biol 341:167-175.

Nordick K, Hoffman MG, Betz JL, Jaehning JA. 2008. Direct interactions between the Paf1 complex and a cleavage and polyadenylation factor are revealed by dissociation of Paf1 from RNA polymerase II. Eukaryot Cell 7:1158-1167.

Orphanides G, Reinberg D. 2000. RNA polymerase II elongation through chromatin. Nature 407:471-475.

Ozonov EA, van Nimwegen E. 2013. Nucleosome free regions in yeast promoters result from competitive binding of transcription factors that interact with chromatin modifiers. PLoS Comput Biol 9:e1003181.

Pavri R, Zhu B, Li G, Trojer P, Mandal S, Shilatifard A, Reinberg D. 2006. Histone H2B monoubiquitination functions cooperatively with FACT to regulate elongation by RNA polymerase II. Cell 125:703-717.

Penheiter KL, Washburn TM, Porter SE, Hoffman MG, Jaehning JA. 2005. A posttranscriptional role for the yeast Paf1-RNA polymerase II complex is revealed by identification of primary targets. Mol Cell 20:213-223.

Peterlin BM, Price DH. 2006. Controlling the elongation phase of transcription with P-TEFb. Mol Cell 23:297-305.

Petroski MD. 2008. The ubiquitin system, disease, and drug discovery. BMC Biochem 9 Suppl 1:S7.

Piro AS, Mayekar MK, Warner MH, Davis CP, Arndt KM. 2012. Small region of Rtf1 protein can substitute for complete Paf1 complex in facilitating global histone H2B ubiquitylation in yeast. Proc Natl Acad Sci U S A 109:10837-10842.

Pokholok DK, Hannett NM, Young RA. 2002. Exchange of RNA polymerase II initiation and elongation factors during gene expression in vivo. Mol Cell 9:799-809.

Ponnusamy MP, Deb S, Dey P, Chakraborty S, Rachagani S, Senapati S, Batra SK. 2009. RNA polymerase II associated factor 1/PD2 maintains self-renewal by its interaction with Oct3/4 in mouse embryonic stem cells. Stem Cells 27:3001-3011.

Porrua O, Libri D. 2015. Transcription termination and the control of the transcriptome: why, where and how to stop. Nat Rev Mol Cell Biol 16:190-202.

Proudfoot NJ, Furger A, Dye MJ. 2002. Integrating mRNA processing with transcription. Cell 108:501-512.

Qiu H, Hu C, Gaur NA, Hinnebusch AG. 2012. Pol II CTD kinases Bur1 and Kin28 promote Spt5 CTR-independent recruitment of Paf1 complex. EMBO J 31:3494-3505.

Rahl PB, Lin CY, Seila AC, Flynn RA, McCuine S, Burge CB, Sharp PA, Young RA. 2010. c-Myc regulates transcriptional pause release. Cell 141:432-445.

Ramachandran S, Haddad D, Li C, Le MX, Ling AK, So CC, Nepal RM, Gommerman JL, Yu K, Ketela T, et al. 2016. The SAGA Deubiquitination Module Promotes DNA Repair and Class Switch Recombination through ATM and DNAPK-Mediated gammaH2AX Formation. Cell Rep 15:1554-1565.

Richard P, Manley JL. 2009. Transcription termination by nuclear RNA polymerases. Genes Dev 23:1247-1269.

Rigbolt KT, Prokhorova TA, Akimov V, Henningsen J, Johansen PT, Kratchmarova I, Kassem M, Mann M, Olsen JV, Blagoev B. 2011. System-wide temporal characterization of the proteome and phosphoproteome of human embryonic stem cell differentiation. Sci Signal 4:rs3.

Robzyk K, Recht J, Osley MA. 2000. Rad6-dependent ubiquitination of histone H2B in yeast. Science 287:501-504.

Rondon AG, Gallardo M, Garcia-Rubio M, Aguilera A. 2004. Molecular evidence indicating that the yeast PAF complex is required for transcription elongation. EMBO Rep 5:47-53.

Rozenblatt-Rosen O, Nagaike T, Francis JM, Kaneko S, Glatt KA, Hughes CM, LaFramboise T, Manley JL, Meyerson M. 2009. The tumor suppressor Cdc73 functionally associates with CPSF and CstF 3' mRNA processing factors. Proc Natl Acad Sci U S A 106:755-760.

Sadeghi L, Prasad P, Ekwall K, Cohen A, Svensson JP. 2015. The Paf1 complex factors Leo1 and Paf1 promote local histone turnover to modulate chromatin states in fission yeast. EMBO Rep 16:1673-1687.

Saha A, Wittmeyer J, Cairns BR. 2002. Chromatin remodeling by RSC involves ATP-dependent DNA translocation. Genes Dev 16:2120-2134.

Sanders MA, Brahemi G, Nangia-Makker P, Balan V, Morelli M, Kothayer H, Westwell AD, Shekhar MP. 2013. Novel inhibitors of Rad6 ubiquitin conjugating enzyme: design, synthesis, identification, and functional characterization. Mol Cancer Ther 12:373-383.

Scheidegger A, Nechaev S. 2016. RNA polymerase II pausing as a context-dependent reader of the genome. Biochem Cell Biol 94:82-92.

Schulze JM, Hentrich T, Nakanishi S, Gupta A, Emberly E, Shilatifard A, Kobor MS. 2011. Splitting the task: Ubp8 and Ubp10 deubiquitinate different cellular pools of H2BK123. Genes Dev. 25:2242-2247.

Sharma N. 2016. Regulation of RNA polymerase II-mediated transcriptional elongation: Implications in human disease. IUBMB Life 68:709-716.

Shaw RJ, Reines D. 2000. Saccharomyces cerevisiae transcription elongation mutants are defective in PUR5 induction in response to nucleotide depletion. Mol Cell Biol 20:7427-7437.

Shema E, Tirosh I, Aylon Y, Huang J, Ye C, Moskovits N, Raver-Shapira N, Minsky N, Pirngruber J, Tarcic G, et al. 2008. The histone H2B-specific ubiquitin ligase RNF20/hBRE1 acts as a putative tumor suppressor through selective regulation of gene expression. Genes Dev 22:2664-2676.

Shi X, Chang M, Wolf AJ, Chang CH, Frazer-Abel AA, Wade PA, Burton ZF, Jaehning JA. 1997. Cdc73p and Paf1p are found in a novel RNA polymerase II-containing complex distinct from the Srbp-containing holoenzyme. Mol Cell Biol 17:1160-1169.

Shi X, Finkelstein A, Wolf AJ, Wade PA, Burton ZF, Jaehning JA. 1996. Paf1p, an RNA polymerase II-associated factor in Saccharomyces cerevisiae, may have both positive and negative roles in transcription. Mol Cell Biol 16:669-676.

Shieh GS, Pan CH, Wu JH, Sun YJ, Wang CC, Hsiao WC, Lin CY, Tung L, Chang TH, Fleming AB, et al. 2011. H2B ubiquitylation is part of chromatin architecture that marks exon-intron structure in budding yeast. BMC Genomics 12:627.

Shirra MK, Rogers SE, Alexander DE, Arndt KM. 2005. The Snf1 protein kinase and Sit4 protein phosphatase have opposing functions in regulating TATA-binding protein association with the Saccharomyces cerevisiae INO1 promoter. Genetics 169:1957-1972.

Sievers F, Wilm A, Dineen D, Gibson TJ, Karplus K, Li W, Lopez R, McWilliam H, Remmert M, Soding J, et al. 2011. Fast, scalable generation of high-quality protein multiple sequence alignments using Clustal Omega. Mol. Syst. Biol. 7:539.

Sikorski RS, Hieter P. 1989. A system of shuttle vectors and yeast host strains designed for efficient manipulation of DNA in Saccharomyces cerevisiae. Genetics 122:19-27.

Sikorski TW, Buratowski S. 2009. The basal initiation machinery: beyond the general transcription factors. Curr Opin Cell Biol 21:344-351.

Singer MS, Kahana A, Wolf AJ, Meisinger LL, Peterson SE, Goggin C, Mahowald M, Gottschling DE. 1998. Identification of high-copy disruptors of telomeric silencing in Saccharomyces cerevisiae. Genetics 150:613-632.

Skalska L, Beltran-Nebot M, Ule J, Jenner RG. 2017. Regulatory feedback from nascent RNA to chromatin and transcription. Nat Rev Mol Cell Biol 18:331-337.

Smolle M, Workman JL. 2013. Transcription-associated histone modifications and cryptic transcription. Biochim Biophys Acta 1829:84-97.

Soares LM, Buratowski S. 2013. Histone Crosstalk: H2Bub and H3K4 Methylation. Mol Cell 49:1019-1020.

Song YH, Ahn SH. 2010. A Bre1-associated protein, large 1 (Lge1), promotes H2B ubiquitylation during the early stages of transcription elongation. J Biol Chem 285:2361-2367.

Squazzo SL, Costa PJ, Lindstrom DL, Kumer KE, Simic R, Jennings JL, Link AJ, Arndt KM, Hartzog GA. 2002. The Paf1 complex physically and functionally associates with transcription elongation factors in vivo. EMBO J 21:1764-1774.

Sridhar VV, Kapoor A, Zhang K, Zhu J, Zhou T, Hasegawa PM, Bressan RA, Zhu JK. 2007. Control of DNA methylation and heterochromatic silencing by histone H2B deubiquitination. Nature 447:735-738.

Stolinski LA, Eisenmann DM, Arndt KM. 1997. Identification of RTF1, a novel gene important for TATA site selection by TATA box-binding protein in Saccharomyces cerevisiae. Mol Cell Biol 17:4490-4500.

Strikoudis A, Lazaris C, Ntziachristos P, Tsirigos A, Aifantis I. 2017. Opposing functions of H2BK120 ubiquitylation and H3K79 methylation in the regulation of pluripotency by the Paf1 complex. Cell Cycle:0.

Strikoudis A, Lazaris C, Trimarchi T, Galvao Neto AL, Yang Y, Ntziachristos P, Rothbart S, Buckley S, Dolgalev I, Stadtfeld M, et al. 2016. Regulation of transcriptional elongation in pluripotency and cell differentiation by the PHD-finger protein Phf5a. Nat Cell Biol 18:1127-1138.

Studier FW. 2005. Protein production by auto-induction in high density shaking cultures. Protein Expr. Purif. 41:207-234.

Sun ZW, Allis CD. 2002. Ubiquitination of histone H2B regulates H3 methylation and gene silencing in yeast. Nature 418:104-108.

Sung P, Prakash S, Prakash L. 1988. The RAD6 protein of Saccharomyces cerevisiae polyubiquitinates histones, and its acidic domain mediates this activity. Genes Dev. 2:1476-1485.

Takahashi A, Tsutsumi R, Kikuchi I, Obuse C, Saito Y, Seidi A, Karisch R, Fernandez M, Cho T, Ohnishi N, et al. 2011. SHP2 tyrosine phosphatase converts parafibromin/Cdc73 from a tumor suppressor to an oncogenic driver. Mol Cell 43:45-56.

Takahashi YH, Schulze JM, Jackson J, Hentrich T, Seidel C, Jaspersen SL, Kobor MS, Shilatifard A. 2011. Dot1 and histone H3K79 methylation in natural telomeric and HM silencing. Mol Cell 42:118-126.

Tan P, Fuchs SY, Chen A, Wu K, Gomez C, Ronai Z, Pan ZQ. 1999. Recruitment of a ROC1-CUL1 ubiquitin ligase by Skp1 and HOS to catalyze the ubiquitination of I kappa B alpha. Mol. Cell 3:527-533.

Tarcic O, Pateras IS, Cooks T, Shema E, Kanterman J, Ashkenazi H, Boocholez H, Hubert A, Rotkopf R, Baniyash M, et al. 2016. RNF20 Links Histone H2B Ubiquitylation with Inflammation and Inflammation-Associated Cancer. Cell Rep 14:1462-1476.

Tenney K, Gerber M, Ilvarsonn A, Schneider J, Gause M, Dorsett D, Eissenberg JC, Shilatifard A. 2006. Drosophila Rtf1 functions in histone methylation, gene expression, and Notch signaling. Proc Natl Acad Sci U S A 103:11970-11974.

Thastrom A, Lowary PT, Widlund HR, Cao H, Kubista M, Widom J. 1999. Sequence motifs and free energies of selected natural and non-natural nucleosome positioning DNA sequences. J Mol Biol 288:213-229.

Thornton JL, Westfield GH, Takahashi YH, Cook M, Gao X, Woodfin AR, Lee JS, Morgan MA, Jackson J, Smith ER, et al. 2014. Context dependency of Set1/COMPASS-mediated histone H3 Lys4 trimethylation. Genes Dev 28:115-120.

Tisseur M, Kwapisz M, Morillon A. 2011. Pervasive transcription - Lessons from yeast. Biochimie 93:1889-1896.

Tomson BN, Davis CP, Warner MH, Arndt KM. 2011. Identification of a role for histone H2B ubiquitylation in noncoding RNA 3'-end formation through mutational analysis of Rtf1 in Saccharomyces cerevisiae. Genetics 188:273-289.

Trappe R, Schulze E, Rzymski T, Frode S, Engel W. 2002. The Caenorhabditis elegans ortholog of human PHF5a shows a muscle-specific expression domain and is essential for C. elegans morphogenetic development. Biochem Biophys Res Commun 297:1049-1057.

Trujillo KM, Osley MA. 2012. A role for H2B ubiquitylation in DNA replication. Mol Cell 48:734-746.

Turco E, Gallego LD, Schneider M, Kohler A. 2015. Monoubiquitination of histone H2B is intrinsic to the Bre1 RING domain-Rad6 interaction and augmented by a second Rad6-binding site on Bre1. J Biol Chem 290:5298-5310.

van Leeuwen F, Gafken PR, Gottschling DE. 2002. Dot1p modulates silencing in yeast by methylation of the nucleosome core. Cell 109:745-756.

Van Oss SB, Shirra MK, Bataille AR, Wier AD, Yen K, Vinayachandran V, Byeon IL, Cucinotta CE, Heroux A, Jeon J, et al. 2016. The Histone Modification Domain of Paf1 Complex Subunit Rtf1 Directly Stimulates H2B Ubiquitylation through an Interaction with Rad6. Mol Cell 64:815-825.

VanDemark AP, Xin H, McCullough L, Rawlins R, Bentley S, Heroux A, Stillman DJ, Hill CP, Formosa T. 2008. Structural and functional analysis of the Spt16p N-terminal domain reveals overlapping roles of yFACT subunits. J Biol Chem 283:5058-5068.

Verrier L, Taglini F, Barrales RR, Webb S, Urano T, Braun S, Bayne EH. 2015. Global regulation of heterochromatin spreading by Leo1. Open Biol 5.

Verzijlbergen KF, Faber AW, Stulemeijer IJ, van Leeuwen F. 2009. Multiple histone modifications in euchromatin promote heterochromatin formation by redundant mechanisms in Saccharomyces cerevisiae. BMC Mol Biol 10:76.

Vitaliano-Prunier A, Babour A, Herissant L, Apponi L, Margaritis T, Holstege FC, Corbett AH, Gwizdek C, Dargemont C. 2012. H2B ubiquitylation controls the formation of export-competent mRNP. Mol Cell 45:132-139.

Vitaliano-Prunier A, Menant A, Hobeika M, Geli V, Gwizdek C, Dargemont C. 2008. Ubiquitylation of the COMPASS component Swd2 links H2B ubiquitylation to H3K4 trimethylation. Nat Cell Biol 10:1365-1371.

Vlaming H, van Welsem T, de Graaf EL, Ontoso D, Altelaar AF, San-Segundo PA, Heck AJ, van Leeuwen F. 2014. Flexibility in crosstalk between H2B ubiquitination and H3 methylation in vivo. EMBO Rep 15:1077-1084.

Wade PA, Werel W, Fentzke RC, Thompson NE, Leykam JF, Burgess RR, Jaehning JA, Burton ZF. 1996. A novel collection of accessory factors associated with yeast RNA polymerase II. Protein Expr Purif 8:85-90.

Walter D, Matter A, Fahrenkrog B. 2010. Bre1p-mediated histone H2B ubiquitylation regulates apoptosis in Saccharomyces cerevisiae. J Cell Sci 123:1931-1939.

Wang E, Kawaoka S, Yu M, Shi J, Ni T, Yang W, Zhu J, Roeder RG, Vakoc CR. 2013. Histone H2B ubiquitin ligase RNF20 is required for MLL-rearranged leukemia. Proc Natl Acad Sci U S A 110:3901-3906.

Wang PF, Tan MH, Zhang C, Morreau H, Teh BT. 2005. HRPT2, a tumor suppressor gene for hyperparathyroidism-jaw tumor syndrome. Horm Metab Res 37:380-383.

Warner MH, Roinick KL, Arndt KM. 2007. Rtf1 is a multifunctional component of the Paf1 complex that regulates gene expression by directing cotranscriptional histone modification. Mol Cell Biol 27:6103-6115.

Waterhouse AM, Procter JB, Martin DM, Clamp M, Barton GJ. 2009. Jalview Version 2--a multiple sequence alignment editor and analysis workbench. Bioinformatics 25:1189-1191.

Watkins JF, Sung P, Prakash S, Prakash L. 1993. The extremely conserved amino terminus of RAD6 ubiquitin-conjugating enzyme is essential for amino-end rule-dependent protein degradation. Genes Dev 7:250-261.

Weake VM, Workman JL. 2008. Histone ubiquitination: triggering gene activity. Mol Cell 29:653-663.

West MH, Bonner WM. 1980. Histone 2B can be modified by the attachment of ubiquitin. Nucleic Acids Res 8:4671-4680.

Wier AD, Mayekar MK, Heroux A, Arndt KM, VanDemark AP. 2013. Structural basis for Spt5-mediated recruitment of the Paf1 complex to chromatin. Proc Natl Acad Sci U S A 110:17290-17295.

Winkler DD, Luger K. 2011. The histone chaperone FACT: structural insights and mechanisms for nucleosome reorganization. J Biol Chem 286:18369-18374.

Winston F, Chaleff DT, Valent B, Fink GR. 1984. Mutations affecting Ty-mediated expression of the HIS4 gene of Saccharomyces cerevisiae. Genetics 107:179-197.

Wolfe NW, Clark NL. 2015. ERC analysis: web-based inference of gene function via evolutionary rate covariation. Bioinformatics 31:3835-3837.

Woo H, Dam Ha S, Lee SB, Buratowski S, Kim T. 2017. Modulation of gene expression dynamics by co-transcriptional histone methylations. Exp Mol Med 49:e326.

Wood A, Krogan NJ, Dover J, Schneider J, Heidt J, Boateng MA, Dean K, Golshani A, Zhang Y, Greenblatt JF, et al. 2003. Bre1, an E3 ubiquitin ligase required for recruitment and substrate selection of Rad6 at a promoter. Mol Cell 11:267-274.

Wood A, Schneider J, Dover J, Johnston M, Shilatifard A. 2005. The Bur1/Bur2 complex is required for histone H2B monoubiquitination by Rad6/Bre1 and histone methylation by COMPASS. Mol Cell 20:589-599.

Wood A, Schneider J, Dover J, Johnston M, Shilatifard A. 2003. The Paf1 complex is essential for histone monoubiquitination by the Rad6-Bre1 complex, which signals for histone methylation by COMPASS and Dot1p. J Biol Chem 278:34739-34742.

Wozniak GG, Strahl BD. 2014. Catalysis-dependent stabilization of Bre1 fine-tunes histone H2B ubiquitylation to regulate gene transcription. Genes Dev 28:1647-1652.

Wright DE, Wang CY, Kao CF. 2011. Flickin' the ubiquitin switch: the role of H2B ubiquitylation in development. Epigenetics 6:1165-1175.

Wu L, Lee SY, Zhou B, Nguyen UT, Muir TW, Tan S, Dou Y. 2013. ASH2L regulates ubiquitylation signaling to MLL: trans-regulation of H3 K4 methylation in higher eukaryotes. Mol Cell 49:1108-1120.

Wu L, Li L, Zhou B, Qin Z, Dou Y. 2014. H2B ubiquitylation promotes RNA Pol II processivity via PAF1 and pTEFb. Mol Cell 54:920-931.

Wu L, Zee BM, Wang Y, Garcia BA, Dou Y. 2011. The RING finger protein MSL2 in the MOF complex is an E3 ubiquitin ligase for H2B K34 and is involved in crosstalk with H3 K4 and K79 methylation. Mol Cell 43:132-144.

Wyce A, Xiao T, Whelan KA, Kosman C, Walter W, Eick D, Hughes TR, Krogan NJ, Strahl BD, Berger SL. 2007. H2B ubiquitylation acts as a barrier to Ctk1 nucleosomal recruitment prior to removal by Ubp8 within a SAGA-related complex. Mol Cell 27:275-288.

Xiao T, Kao CF, Krogan NJ, Sun ZW, Greenblatt JF, Osley MA, Strahl BD. 2005. Histone H2B ubiquitylation is associated with elongating RNA polymerase II. Mol. Cell. Biol. 25:637-651.

Xu Y, Bernecky C, Lee CT, Maier KC, Schwalb B, Tegunov D, Plitzko JM, Urlaub H, Cramer P. 2017. Architecture of the RNA polymerase II-Paf1C-TFIIS transcription elongation complex. Nat Commun 8:15741.

Yang SS, Zhang R, Wang G, Zhang YF. 2017. The development prospection of HDAC inhibitors as a potential therapeutic direction in Alzheimer's disease. Transl Neurodegener 6:19.

Yang Y, Li W, Hoque M, Hou L, Shen S, Tian B, Dynlacht BD. 2016. PAF Complex Plays Novel Subunit-Specific Roles in Alternative Cleavage and Polyadenylation. PLoS Genet 12:e1005794.

Yanisch-Perron C, Vieira J, Messing J. 1985. Improved M13 phage cloning vectors and host strains: nucleotide sequences of the M13mp18 and pUC19 vectors. Gene 33:103-119.

Yao X, Tang Z, Fu X, Yin J, Liang Y, Li C, Li H, Tian Q, Roeder RG, Wang G. 2015. The Mediator subunit MED23 couples H2B mono-ubiquitination to transcriptional control and cell fate determination. EMBO J 34:2885-2902.

Yu M, Yang W, Ni T, Tang Z, Nakadai T, Zhu J, Roeder RG. 2015. RNA polymerase II-associated factor 1 regulates the release and phosphorylation of paused RNA polymerase II. Science 350:1383-1386.

Yun M, Ruan C, Huh JW, Li B. 2012. Reconstitution of modified chromatin templates for in vitro functional assays. Methods Mol Biol 833:237-253.

Zaborowska J, Egloff S, Murphy S. 2016. The pol II CTD: new twists in the tail. Nat Struct Mol Biol 23:771-777.

Zhang X, Kolaczkowska A, Devaux F, Panwar SL, Hallstrom TC, Jacq C, Moye-Rowley WS. 2005. Transcriptional regulation by Lge1p requires a function independent of its role in histone H2B ubiquitination. J Biol Chem 280:2759-2770.

Zhang Z, Fu J, Gilmour DS. 2005. CTD-dependent dismantling of the RNA polymerase II elongation complex by the pre-mRNA 3'-end processing factor, Pcf11. Genes Dev 19:1572-1580.

Zhang Z, Jones A, Joo HY, Zhou D, Cao Y, Chen S, Erdjument-Bromage H, Renfrow M, He H, Tempst P, et al. 2013. USP49 deubiquitinates histone H2B and regulates cotranscriptional pre-mRNA splicing. Genes Dev 27:1581-1595.

Zhang Z, Wu CH, Gilmour DS. 2004. Analysis of polymerase II elongation complexes by native gel electrophoresis. Evidence for a novel carboxyl-terminal domain-mediated termination mechanism. J Biol Chem 279:23223-23228.

Zheng N, Shabek N. 2017. Ubiquitin Ligases: Structure, Function, and Regulation. Annu Rev Biochem 86:129-157.

Zheng S, Wyrick JJ, Reese JC. 2010. Novel trans-tail regulation of H2B ubiquitylation and H3K4 methylation by the N terminus of histone H2A. Mol. Cell. Biol. 30:3635-3645.

Zhi X, Giroux-Leprieur E, Wislez M, Hu M, Zhang Y, Shi H, Du K, Wang L. 2015. Human RNA polymerase II associated factor 1 complex promotes tumorigenesis by activating c-MYC transcription in non-small cell lung cancer. Biochem Biophys Res Commun 465:685-690.

Zhu B, Mandal SS, Pham AD, Zheng Y, Erdjument-Bromage H, Batra SK, Tempst P, Reinberg D. 2005. The human PAF complex coordinates transcription with events downstream of RNA synthesis. Genes Dev 19:1668-1673.